People's Democratic Republic of Algeria

Ministry of Higher Education and Scientific Research

University of Echahid Hamma Lakhdar - El Oued

Faculty of Technology

Department of Process and Petrochemical Engineering

Thesis Submitted in Partial Fulfilment of the Requirement for Degree of

LMD Doctorate

in Process Engineering

Specialty: Pharmaceutical Engineering

Study of the Characteristics and Photocatalytic Application of ZnO Nanoparticles Synthesized by Cold Plasma

Presented by:

MESSAI Ridha

Before the Jury composed of:

LAOUINI Salah Eddin	Professor	University of El Oued	President
FERHAT Med Fouad	MCA	University of El Oued	Supervisor
SEROUTI Abdelghani	MCA	University of El Oued	Co-Supervisor
GHEZZAR Mouffok Redouane	Professor	University of Mostaganem	Examiner
MERZOUGUI Abdelkarim	Professor	University of Bikra	Examiner
HEMMAMI Hadia	MCA	University of El Oued	Examiner

2023/2024

People's Democratic Republic of Algeria

Ministry of Higher Education and Scientific Research

University of Echahid Hamma Lakhdar - El Oued

Faculty of Technology

Department of Process and Petrochemical Engineering

Thesis Submitted in Partial Fulfilment of the Requirement for Degree of

LMD Doctorate

in Process Engineering

Specialty: Pharmaceutical Engineering

Study of the Characteristics and Photocatalytic Application of ZnO Nanoparticles Synthesized by Cold Plasma

Presented by:

MESSAI Ridha

Before the Jury composed of:

LAOUINI Salah Eddin	Professor	University of El Oued	President
FERHAT Med Fouad	MCA	University of El Oued	Supervisor
SEROUTI Abdelghani	MCA	University of El Oued	Co-Supervisor
GHEZZAR Mouffok Redouane	Professor	University of Mostaganem	Examiner
MERZOUGUI Abdelkarim	Professor	University of Bikra	Examiner
HEMMAMI Hadia	MCA	University of El Oued	Examiner

2023/2024

Dedication

First and foremost, I thank Almighty Allah.
I dedicate this modest work with all my love and respect to:
My dear and precious parents, who have always been there for me with their support, sacrifices, and love, and who have provided me with a magnificent example of hard work and perseverance.
My dear brothers and sisters.
My entire family.
My friends, without exception.
To those for whom words cannot express the gratitude and respect I hold:
To my esteemed professors, Dr. Ferhat Mohamed Fouad, Dr. Serouti Abdelghani, Dr. Salah Eddin Laouini, Dr. Allag Nesseiba, and Mr. Ali Tliba ....
I also extend my thanks to Professor Farhati Omar, President of Echahid Hamma Lakhdar University of El Oued, and Professor Ali Chamsa, Dean of the Faculty of Technology, for all the resources they have provided, enabling us to achieve the success we have reached today.
My professors, who have guided me throughout my academic career.
I especially dedicate it to my beloved daughter Chahd, my little son Yahya, and my dear wife.
a special dedication to my friend whom I miss and have not forgotten to this day, Brahmi Saber. May God have mercy on him and forgive him.

Acknowledgments

First and foremost, we thank God, our creator, for giving us the knowledge, strength, will, and courage to complete this modest work. As we conclude this work, we wish to express our sincere thanks and deep gratitude to those who supported us and contributed, directly or indirectly, to the preparation of this research thesis.

My first thanks go to Dr. **FERHAT Mohamed Fouad**, my supervisor, and Dr. **SEROUTI Abdelghani**, my co-supervisor, for all the support, help, guidance, and invaluable advice and encouragement throughout my years of study and during the completion of this thesis.

I am also deeply thankful to the members of my thesis committee, Professor **LAOUINI Salah Eddine**, Professor **GHEZZAR Mouffok Redouane,** Professor **MERZOUGUI Abdelkarim**, and Dr. **HEMMAMI Hadia**, for their thoughtful comments, constructive suggestions, and critical perspectives, which significantly enhanced the quality of this work.

also, I would like to extend my heartfelt thanks to the President of Echahid Hamma Lakhdar University, Professor **FARHATI Omar**, the Dean of the Faculty of Science and Technology, Professor **CHAMSA Ali.**

Additionally, our deepest thanks go to all the faculty members for their efforts during my years of training and to all the members of the Process Engineering team who contributed in their own way, whether directly or simply by showing their support. We are also grateful to the staff of the central laboratory of EPH El-Oued for their kindness and support, especially: Dr. **Djamila Berra**, Dr. **Dia Ouahida**, Dr. **Nousieba Allag**, Mr. **Ali Taliba**, and Mr. **Sadek Nani**. Furthermore, we extend our gratitude to Professor **Mouffok Redouane Ghezzar**, Professor **Mir Waqas Alam**, Professor **Mohamed Bououdina**, Professor **Muhammad Humayun**, Professor **Abdelhalim Zoukel**, Dr **Tedjani Mohammed Laid**, doctoral candidate **Bounedjar Nourelhouda** and **Bilal Belmekki**, and my student **Ammar Said Hammoudi**.

I would also like to thank my parents and my extended family for their unconditional support since our professional project was defined. Thank you for the financial, moral, psychological, and material support. If I am here today, it is thanks to you. Finally, I thank my friends for these years spent together, in the best of times and the worst.

We would also like to express our gratitude to the President and Director General of the National Corporation for Well Works (**ENTP**), as well as all my direct and indirect directors and all my work colleagues, for facilitating my study and providing me with a suitable environment to obtain this certificate.

I also thank my friends **Mahmoud Seboui** and **Abdel Basset Maamara,** as well as their families, for the support they provided. They treated me like a member of their family in el Oued, showering me with their generosity and love without expecting anything in return. Lastly, I will never forget to thank my dear friend **Rachid Achi,** the loyal companion with whom I spent unforgettable days**.**

Abstract

This thesis explores the synthesis, characterization, and photocatalytic applications of zinc oxide nanoparticles (ZnO NPs) produced using a Gliding Arc Discharge (GAD) plasma method. The study primarily investigates the influence of discharge duration on the structural, optical, and photocatalytic properties of ZnO NPs. Characterization techniques such as X-ray diffraction (XRD), scanning electron microscopy (SEM), and UV-visible spectroscopy were employed to evaluate the physical and chemical properties of the nanoparticles. The results show that increasing from 10 min to 60 min the discharge duration leads to a decrease in particle size from 28 nm to 25 nm, higher band gap energies, and improved thermal stability. The ZnO NPs exhibited excellent photocatalytic performance in the degradation of organic pollutants, with degradation efficiencies of 92.9%, 71%, and 88% for Brilliant Cresyl Blue (BCB), Methylene Blue (MB), and Congo Red (CR) dyes, respectively, under UV light. Furthermore, under sunlight, the ZnO NPs achieved up to 97% photodegradation efficiency of CR dye after 150 minutes, with optimal performance at pH 8. The study also demonstrated the effectiveness of combining GAD plasma with ZnO NPs for aspirin degradation, achieving a 96.72% degradation efficiency within 90 minutes. These findings highlight the potential of GAD plasma-synthesized ZnO NPs for practical applications in wastewater treatment, offering a sustainable and efficient solution for organic pollutant degradation. The synthesized ZnO NPs also demonstrated stability and reusability over multiple cycles, showcasing their potential for large-scale environmental applications.

Keywords: ZnO Nanoparticles, Gliding Arc Discharge Plasma, Photocatalysis, Organic Pollutants, Aspirin Degradation, Water Purification, Nanomaterials.

الملخص

تستكشف هذه الأطروحة توليف وتوصيف وتطبيقات التحفيز الضوئي لجسيمات أكسيد الزنك النانوية (ZnO NPs) التي تم إنتاجها باستخدام طريقة تفريغ القوس المنزلق (GAD). تركز الدراسة بشكل رئيسي على تأثير مدة التفريغ على الخصائص الهيكلية والبصرية والتحفيزية الضوئية لجسيمات أكسيد الزنك. تم استخدام تقنيات التوصيف مثل حيود الأشعة السينية (XRD) والمجهر الإلكتروني الماسح (SEM) والمطيافية فوق البنفسجية المرئية لتقييم الخصائص الفيزيائية والكيميائية للجسيمات النانوية. أظهرت النتائج أن زيادة مدة التفريغ من 10 دقائق إلى 60 دقيقة تؤدي إلى تقليل حجم الجسيمات من 28 نانومتر إلى 25 نانومتر وزيادة طاقة فجوة النطاق وتحسن الاستقرار الحراري. أظهرت جسيمات ZnO NPs أداءً ممتازًا في تحفيز التحلل الضوئي للملوثات العضوية، حيث بلغت كفاءة التحلل 92.9٪ و71٪ و88٪ لأصباغ أزرق الكريسيل اللامع والميثيلين الأزرق وأحمر الكونغو على التوالي تحت ضوء الأشعة فوق البنفسجية. علاوة على ذلك، حققت الجسيمات النانوية ZnO كفاءة تصل إلى 97٪ في التحلل الضوئي لصبغة CR تحت أشعة الشمس بعد 150 دقيقة، مع أداء مثالي عند درجة حموضة pH 8. كما أظهرت الدراسة فعالية الجمع بين تفريغ القوس المنزلق وجسيمات ZnO في تحلل الأسبرين، حيث تم تحقيق كفاءة تحلل بلغت 96.72٪ في غضون 90 دقيقة. تُبرز هذه النتائج إمكانيات جسيمات ZnO NPs المُصنّعة باستخدام تفريغ القوس المنزلق في التطبيقات العملية لمعالجة مياه الصرف، مما يوفر حلاً مستدامًا وفعالًا لتحلل الملوثات العضوية. كما أظهرت الجسيمات النانوية المُصنّعة استقرارًا وإمكانية إعادة الاستخدام على مدار دورات متعددة، مما يعزز إمكانياتها في التطبيقات البيئية واسعة النطاق.

الكلمات المفتاحية: جسيمات أكسيد الزنك النانوية، تفريغ القوس المنزلق بالبلازما، التحفيز الضوئي، الملوثات العضوية، تحلل الأسبرين، تنقية المياه، المواد النانوية.

Résumé

Cette thèse explore la synthèse, la caractérisation et les applications photocatalytiques des nanoparticules d'oxyde de zinc (ZnO NPs) produites par une méthode de plasma à décharge d'arc glissant (GAD). L'étude se concentre principalement sur l'influence de la durée de décharge sur les propriétés structurelles, optiques et photocatalytiques des ZnO NPs. Des techniques de caractérisation telles que la diffraction des rayons X (DRX), la microscopie électronique à balayage (MEB) et la spectroscopie UV-visible ont été utilisées pour évaluer les propriétés physiques et chimiques des nanoparticules. Les résultats montrent qu'une augmentation de la durée de décharge, de 10 à 60 minutes, entraîne une diminution de la taille des particules de 28 nm à 25 nm, une énergie de bande interdite plus élevée et une meilleure stabilité thermique. Les ZnO NPs ont montré d'excellentes performances photocatalytiques dans la dégradation des polluants organiques, avec des efficacités de dégradation de 92,9 %, 71 % et 88 % respectivement pour les colorants Brilliant Cresyl Blue (BCB), Bleu de Méthylène (MB) et Rouge Congo (CR), sous lumière UV. De plus, sous la lumière solaire, les ZnO NPs ont atteint une efficacité de photodégradation allant jusqu'à 97 % du colorant CR après 150 minutes, avec une performance optimale à un pH de 8. L'étude a également démontré l'efficacité de la combinaison du plasma GAD avec les ZnO NPs pour la dégradation de l'aspirine, obtenant une efficacité de 96,72 % en 90 minutes. Ces résultats soulignent le potentiel des ZnO NPs synthétisés par plasma GAD pour des applications pratiques dans le traitement des eaux usées, offrant une solution durable et efficace pour la dégradation des polluants organiques. Les ZnO NPs synthétisés ont également montré une stabilité et une réutilisabilité sur plusieurs cycles, démontrant leur potentiel pour des applications environnementales à grande échelle.

Mots-clés : Nanoparticules de ZnO, Plasma à Décharge d'Arc Glissant, Photocatalyse, Polluants Organiques, Dégradation de l'Aspirine, Purification de l'Eau, Nanomatériaux.

TABLE OF CONTENTS

ABSTRACT I
الملخص II
RESUME III
LIST OF TABLES XIII
LIST OF FIGURES XIV
GENERAL INTRODUCTION 1
THESIS PROBLEM 3
CHAPTER I: OVERVIEW OF NANOPARTICLES: SYNTHESIS METHODS, APPLICATIONS AND NANOPARTICLE CHARACTERIZATION TECHNIQUES ... 4
1. NANOPARTICLES SYNTHESIS METHODS: 4
1.1. PHYSICAL METHODS: 6
1.1.1. SPUTTERING: 6
1.1.2. MECHANICAL MILLING: 7
1.2. BIO-ASSISTED METHODS: 7
1.2.1. BIOGENIC SYNTHESIS USING PLANT EXTRACTS: 8
A) SEEDS AS SOURCE FOR NANOPARTICLE SYNTHESIS 8
B) FRUITS AND PEEL AS SOURCE FOR NANOPARTICLE SYNTHESIS 8
C) LEAVES AS SOURCE FOR NANOPARTICLES SYNTHESIS 9
D) ROOT AS SOURCE FOR NANOPARTICLE SYNTHESIS 9
E) FLOWERS AS SOURCE FOR NPS PRODUCTION 10
1.2.2. MICROBIAL-BASED BIOGENIC SYNTHESIS: 10
1.2.3. BIOGENIC SYNTHESIS USING BIOMOLECULES AS TEMPLATES: 10
1.3. CHEMICAL METHODS: 11
1.3.1. CHEMICAL PRECIPITATION 11
1.3.2. SOL-GEL 12
1.3.3. HYDROTHERMAL METHOD 13
1.3.4. COLD PLASMA METHOD 14
1.4. DISADVANTAGES AND ADVANTAGES OF DIFFERENT SYNTHESIS METHODS 14
2. NANOPARTICLES CHARACTERIZATION TECHNIQUES: 16
2.1. OPTICAL PROPERTIES: 16

2.2. Crystalline structures: 17
2.2.1. Fourier Transform Infra-Red Spectroscopy (FTIR) 17
2.2.2. X-ray diffraction (DRX) 17
2.3. Morphological properties: 20
2.3.1. Scanning Electron Microscopy (SEM) and EDAX 20
2.3.2. Transmission Electron Microscopy (TEM) 21
2.4. Thermal properties: 21
3. Various Applications of Nanoparticles 22
3.1. Applications of Nanoparticles in the Industry and Energy 22
3.1.1. Application in petroleum field: 22
3.1.2. Applications in electronics: 23
3.1.3. Uses in pigments: 24
3.1.4. Application in carbon fillers in tires: 24
3.1.5. Uses in solar cells' technology: 24
3.1.6. Uses in batteries: 26
3.2. Applications in the Medical Field: 26
3.3. Nanoparticles Environmental Applications: 27
3.3.1. Application of Nanoparticles in Contaminated Soil Remediation: 27
3.3.2. Application of Nanoparticles in wastewater treatment: 28
a) Nano-sorbents and Adsorption Technology 28
b) Nanotechnology Disinfection 30
c) Photocatalysis 30
REFERENCES OF CHAPTER I 32
CHAPTER II: OVERVIEW OF COLD PLASMA: DEFINITION, CHEMICAL SPECIES GENERATED AND APPLICATIONS 39
1. Definition of Plasma 40
2. Chemical species generated within Cold Plasma: 41
2.1. Hydroxyl radical: 42
2.2. Reactive oxygen species: 43
2.3. Reactive nitrogen species (RNS): 43
2.4. Photon emission: 44

3. APPLICATIONS OF COLD PLASMA 45
3.1. ENVIRONMENTAL PROTECTION: 45
3.1.1. AIR POLLUTANT TREATMENT: 45
3.1.2. WASTE TREATMENT: 46
3.1.3. SOIL TREATMENT: 47
3.2. FOOD INDUSTRY: 48
3.3. AGRICULTURE: 49
3.4. MEDICINE AND HEALTHCARE: 50
3.4.1. WOUND HEALING: 50
3.4.2. CANCER TREATMENT: 50
3.4.3. BLOOD COAGULATION: 50
3.4.4. STERILIZATION: 51
3.4.5. DENTISTRY: 51
3.4.6. COSMETOLOGY: 51
3.4.7. BIOFILM REMOVAL: 52
3.5. ENERGY: 52
3.5.1. PLASMA-ASSISTED COMBUSTION: 52
3.5.2. PLASMA-ASSISTED SOLAR CELL: 52
3.5.3. HYDROGEN PRODUCTION: 53
3.5.4. PLASMA-ASSISTED METHANE CONVERSION: 53
3.6. MATERIAL SCIENCE: 53
3.6.1. SURFACE MODIFICATION: 53
3.6.2. SYNTHESIS OF NANOMATERIAL: 54
D) PLASMA JET: 54
E) DIELECTRIC BARRIER DISCHARGE (DBD) 56
F) MICROWAVE PLASMA: 58
G) GLIDING ARC DISCHARGE PLASMA (GAD) 59
REFERENCES OF CHAPTER II 62
CHAPTER III: SYNTHESIS, CHARACTERIZATION AND PHOTOCATALYTIC APPLICATION OF ZNO NANOPARTICLES PRODUCED USING A GAD PLASMA METHOD ..... **ERROR! BOOKMARK NOT DEFINED.**

1. INTRODUCTION ..... **ERROR! BOOKMARK NOT DEFINED.**
2. MATERIALS AND METHODS ..... **ERROR! BOOKMARK NOT DEFINED.**
2.1. ZINC ACETATE ..... **ERROR! BOOKMARK NOT DEFINED.**
2.2. ORGANIC POLLUTANT: ..... **ERROR! BOOKMARK NOT DEFINED.**
2.2.1. CONGO RED (CR) DYE: ..... **ERROR! BOOKMARK NOT DEFINED.**
2.2.2. BRILLIANT CRESYL BLUE (BCB) DYE: ..... **ERROR! BOOKMARK NOT DEFINED.**
2.2.3. METHYLENE BLUE (MB) DYE: ..... **ERROR! BOOKMARK NOT DEFINED.**
2.2.4. ASPIRIN: ..... **ERROR! BOOKMARK NOT DEFINED.**
2.3. ZNO NANOPARTICLES ..... **ERROR! BOOKMARK NOT DEFINED.**
2.3.1. DEFINITION ..... **ERROR! BOOKMARK NOT DEFINED.**
2.3.2. PROPERTIES OF ZNO NANOPARTICLES: ..... **ERROR! BOOKMARK NOT DEFINED.**
A) STRUCTURAL PROPERTIES: ..... **ERROR! BOOKMARK NOT DEFINED.**
B) OPTICAL PROPERTIES: ..... **ERROR! BOOKMARK NOT DEFINED.**
C) ELECTRONICAL PROPERTIES: ..... **ERROR! BOOKMARK NOT DEFINED.**
D) ELECTRICAL PROPRIETIES ..... **ERROR! BOOKMARK NOT DEFINED.**
E) OPTOELECTRONIC PROPERTIES ..... **ERROR! BOOKMARK NOT DEFINED.**
2.3.3. APPLICATION OF ZNO NANOPARTICLES: ..... **ERROR! BOOKMARK NOT DEFINED.**
A) AGRICULTURE APPLICATION ..... **ERROR! BOOKMARK NOT DEFINED.**
B) OPTOELECTRONIC INDUSTRY ..... **ERROR! BOOKMARK NOT DEFINED.**
C) RUBBER AND CONCRETE INDUSTRIES ..... **ERROR! BOOKMARK NOT DEFINED.**
D) GAS-SENSING ..... **ERROR! BOOKMARK NOT DEFINED.**
E) COSMETIC INDUSTRY ..... **ERROR! BOOKMARK NOT DEFINED.**
F) TEXTILE INDUSTRY ..... **ERROR! BOOKMARK NOT DEFINED.**
G) BIOMEDICAL APPLICATION ..... **ERROR! BOOKMARK NOT DEFINED.**
H) PHOTODEGRADATION ..... **ERROR! BOOKMARK NOT DEFINED.**
3. SYNTHESIZE ZNO NPS BY GAD PLASMA METHOD **ERROR! BOOKMARK NOT DEFINED.**
3.1. SAMPLES PREPARATION ..... **ERROR! BOOKMARK NOT DEFINED.**
A) CASE 1 ..... **ERROR! BOOKMARK NOT DEFINED.**
A) CASE 2 ..... **ERROR! BOOKMARK NOT DEFINED.**
B) CASE 3 ..... **ERROR! BOOKMARK NOT DEFINED.**
3.2. GLIDING ARC DISCHARGE (GAD) APPARATUS: . **ERROR! BOOKMARK NOT DEFINED.**

A(THE KEY COMPONENTS AND THEIR ROLES:..... **ERROR! BOOKMARK NOT DEFINED.**

B) OPTIMIZATION CONSIDERATIONS: ..... **ERROR! BOOKMARK NOT DEFINED.**

3.3. STEPS IN THE SYNTHESIS OF ZNO NANOPARTICLES:**ERROR! BOOKMARK NOT DEFINED.**

A) CASE 1 ..... **ERROR! BOOKMARK NOT DEFINED.**

B) CASE 2..... **ERROR! BOOKMARK NOT DEFINED.**

C) CASE 3..... **ERROR! BOOKMARK NOT DEFINED.**

4. CHARACTERIZATION STUDIES..... **ERROR! BOOKMARK NOT DEFINED.**

5. DEGRADATION ORGANIC POLLUTANTS:..... **ERROR! BOOKMARK NOT DEFINED.**

5.1. PHOTOCATALYTIC TEST..... **ERROR! BOOKMARK NOT DEFINED.**

A) CASE 1 ..... **ERROR! BOOKMARK NOT DEFINED.**

B(CASE 2 ..... **ERROR! BOOKMARK NOT DEFINED.**

C) CASE 3..... **ERROR! BOOKMARK NOT DEFINED.**

5.2. DEGRADATION OF ASA:..... **ERROR! BOOKMARK NOT DEFINED.**

A) USING GAD PLASMA ..... **ERROR! BOOKMARK NOT DEFINED.**

B) POST-DISCHARGE:..... **ERROR! BOOKMARK NOT DEFINED.**

C) USING GAD PLASMA IN COMBINATION WITH ZNO NPS PHOTOCATALYTIC PROCESS: **ERROR! BOOKMARK NOT DEFINED.**

REFERENCES OF CHAPTER III ..... **ERROR! BOOKMARK NOT DEFINED.**

CHAPTER IV: RESULTS AND DISCUSSION ON THE SYNTHESIS, CHARACTERIZATIONS AND PHOTOCATALYTIC: APPLICATIONS OF ZNO NANOPARTICLES..... **ERROR! BOOKMARK NOT DEFINED.**

1. STRUCTURAL, CHEMICAL COMPOSITION, OPTICAL CHARACTERIZATION, AND THERMAL PROPERTIES OF SYNTHESIZED ZNO NPS:..... **ERROR! BOOKMARK NOT DEFINED.**

1.1. X-RAY DIFFRACTION..... **ERROR! BOOKMARK NOT DEFINED.**

A) CASE 1 ..... **ERROR! BOOKMARK NOT DEFINED.**

B) CASE 2..... **ERROR! BOOKMARK NOT DEFINED.**

C) CASE 3..... **ERROR! BOOKMARK NOT DEFINED.**

1.2. SCANNING ELECTRON MICROSCOPY (SEM) AND EDAX**ERROR! BOOKMARK NOT DEFINED.**

A) CASE 1 ..... **ERROR! BOOKMARK NOT DEFINED.**

B) CASE 2..... **ERROR! BOOKMARK NOT DEFINED.**
C) CASE 3..... **ERROR! BOOKMARK NOT DEFINED.**
1.3. UV-VISIBLE SPECTROSCOPY:..... **ERROR! BOOKMARK NOT DEFINED.**
A) CASE 1 ..... **ERROR! BOOKMARK NOT DEFINED.**
B) CASE 2..... **ERROR! BOOKMARK NOT DEFINED.**
C) CASE 3..... **ERROR! BOOKMARK NOT DEFINED.**
1.4. FTIR SPECTROSCOPY: ..... **ERROR! BOOKMARK NOT DEFINED.**
A) CASE 1 ..... **ERROR! BOOKMARK NOT DEFINED.**
B) CASE 2..... **ERROR! BOOKMARK NOT DEFINED.**
1.5. THERMOGRAVIMETRIC ANALYSIS / DIFFERENTIAL SCANNING CALORIMETRY: **ERROR! BOOKMARK NOT DEFINED.**
A) CASE 1 ..... **ERROR! BOOKMARK NOT DEFINED.**
B) CASE 2..... **ERROR! BOOKMARK NOT DEFINED.**
A) CASE 3 ..... **ERROR! BOOKMARK NOT DEFINED.**
2. DEGRADATION ORGANIC POLLUTANTS:..... **ERROR! BOOKMARK NOT DEFINED.**
2.2. PHOTOCATALYTIC TEST:..... **ERROR! BOOKMARK NOT DEFINED.**
A) CASE 1 ..... **ERROR! BOOKMARK NOT DEFINED.**
B) CASE 2..... **ERROR! BOOKMARK NOT DEFINED.**
 EFFECT OF PH SOLUTION ..... **ERROR! BOOKMARK NOT DEFINED.**
 PHOTOCATALYST STABILITY AND REUSABILITY .... **ERROR! BOOKMARK NOT DEFINED.**
C) CASE 3..... **ERROR! BOOKMARK NOT DEFINED.**
 ZNO NPS PHOTOCATALYTIC PROCESS OF ASPIRIN: **ERROR! BOOKMARK NOT DEFINED.**
 DEGRADATION OF ASA USING GAD PLASMA: ..... **ERROR! BOOKMARK NOT DEFINED.**
 DEGRADATION OF ASA BY GAD PLASMA IN COMBINATION WITH ZNO NPS ..... **ERROR! BOOKMARK NOT DEFINED.**
 DEGRADATION OF ASA BY SEQUENTIAL PROCESSES**ERROR! BOOKMARK NOT DEFINED.**
 EFFECT OF POST-DISCHARGE: ..... **ERROR! BOOKMARK NOT DEFINED.**
2.3. PROPOSED PHOTOCATALYTIC MECHANISM:..... **ERROR! BOOKMARK NOT DEFINED.**

2.4. MECHANISTIC INSIGHTS INTO THE SYNERGISTIC EFFECTS BETWEEN THE PLASMA TREATMENT AND PHOTOCATALYSIS FOR ASPIRIN DEGRADATION**ERROR! BOOKMARK NOT DEFINED.**

A) REACTIVE SPECIES GENERATION AND INTERACTIONS:**ERROR! BOOKMARK NOT DEFINED.**

B) SYNERGISTIC EFFECTS AND ADVANTAGES:..... **ERROR! BOOKMARK NOT DEFINED.**

REFERENCES OF CHAPTER IV..... **ERROR! BOOKMARK NOT DEFINED.**

GENERAL CONCLUSION 158

List of abbreviation

Abbreviation	Meaning	Abbreviation	Meaning 2
$[ASA_0]$	Initial Concentration of Aspirin	K	Constant independent on hν
$[ASA_t]$	Concentration of Aspirin at time t	K	Pseudo-First-Order Rate Constant
°C	Degrees Celsius	kHz	Kilohertz
°K	Degrees Kelvin	$KMnO_4$	Potassium Permanganate
µ	Distortion parameter	kΩ	Kilo-ohms
µA	Microamperes	L	Path Length of the sample.
µF	Microfarads	L	Liters
µg	Micrograms	L/mol	Liters per mole
µm	Micrometers	LEDs	Light-Emitting Diodes
µV	Microvolts	Ligand DNPs	Developed Ligand-coated Dense Nanoparticles
µW	Microwatts	LPCP	Low Pressure Cold Plasma
A	Absorbance	m/s	Meters per second
a, b, and c	Lattice parameters	m^2	Square meters
AC	Alternating Current	m^3	Cubic meters
ACP	Atmospheric Cold Plasma	MA	Megestrol Acetate
Ag	Silver	mA	Milliamperes
Ag Cl	silver chloride	mA	milli Amperes
Al_2O_3	Aluminum Oxide	MB	Methylene Blue dye
AOP	Advanced Oxidation Processes	Mbar	Millibars
APGD-t	Atmospheric Pressure Glow Discharge Torch	Mg	Milligrams
APP	Atmospheric Pressure Plasma	MHz	Megahertz
Ar	Argon	Min	Minutes
ASA	Aspirin	Ml	Milliliters
Atm	Atmospheres	Mm	Millimeters
Au	Gold	MnO_2	Manganese Dioxide
AZO	Al-doped ZnO	MNPs	Magnetic NPs
BCB	Brilliant Cresyl Blue dye	MRI	Magnetic Resonance Imaging
C	Carbon	mV	Millivolts
C	Concentration of the absorbing species	mW	Milliwatts
CCD camera	Charge-Coupled Device camera	MΩ	Mega-ohms
CeO_2	Cerium Oxides	N	number of unit cells present
Cm	Centimeters	N_2	Nitrogen
cm/s	Centimeters per second	N_2O	Nitrous Oxide
cm^{-1}	Reciprocal centimeters	NaOH	Sodium Hydroxide
cm^2	Square centimeters	NAPLs	Non-Aqueous Phase Liquids
$cm^2/V.s$	Square centimeters per volt-second	NF	Nanofiltration

cm^3	Cubic centimeters
cm3/mol	Cubic centimeters per mole
CNOs	Carbon Nano-Onions
CNP-based	Carbon Nano Particles-based
CNTs	Carbon Nanotubes
Co	Cobalt
CO	Carbon Monoxide
COD	Chemical Oxygen Demand
C-PSCs	Carbon-Based Perovskite Solar Cells
CR	Congo Red dye
Cu	Copper
CuO	Copper Oxide
D	Grain Size
DBD	Dielectric Barrier Discharge
DC	Direct current
DDT	Dichlorodiphenyl-Trichloroethane
D_{E-E}	Distance between the high voltage and ground electrodes
Deg %	Degradation efficiency
D_{E-O}	Distance between the ground electrode and the orifice
DMSO	Dimethyl Sulfoxide
DNA	Deoxyribonucleic Acid
D_{O-Ts}	Distance from the orifice to the liquid-air interface
DR	Dark room
DRX	X-ray diffraction
DSCs	Dye Solar Cells
DSSCs	Dye-Sensitized Solar Cells
e^-	Electrons
EDX	Energy-Dispersive X-Ray Analysis
E_g	Optical band gap of the NPs
EOR	Enhanced Oil Recovery
eV	Electron volts
$e_{zz}\ 10^{-3}$	Uniform strain
$\varepsilon\ 10^{-3}$	Internal micro-strain
F	Farads
f	Frequencies
FDA	Food and Drug Administration
NiO	Nickel Oxide
Nm	Nanometers
nm^{-1}	Reciprocal nanometers
NPs	Nanoparticles
NTP	Non-Thermal Plasma
nZVI	nanoscale zero-valent iron
O_2	Oxygen
ODS	Oxide Dispersion Strengthened
$ONOO^-$	Peroxynitrite
Or II	Orang II dye
P	Power
Pa	Pascals
PAW	Plasma-Activated Water
PBC	Parthenium Weed Biochar
PbS	Lead Sulfide
PCBs	Polychlorinated Biphenyls
pF	Picofarads
pH	potential of Hydrogen
PLD	Pulsed Laser Deposition
Pls	Plasma
POPs	Persistent Organic Pollutants
Ppm	Parts per million
Pr	Pression
PVD	Physical Vapor Deposition
PVP	Polyvinylpyrrolidone
RF	Radio Frequency
RhB	Rhodamine B dye
RNA	Ribonucleic Acid
RNS	Reactive Nitrogen Species
RONS	Reactive Oxygen-Nitrogen Species
ROS	Reactive Oxygen Species
RR	Reactive Red dye
S/cm	Siemens per centimeter
SEM	Scanning Electron Microscopy
Si	Silicon
SnZVI	sulfide-modified nanoscale zero-valent iron

Fe	Fer
Fe_3O_4	Iron Oxide or Magnetite
FE-DBD	Floating Electrode Dielectric Barrier Discharge
FTIR	Fourier Transform Infra-Red
FTO	Fluorine-Doped Tin Oxide
G	Grams
g/cm3	Grams per cubic centimeter
g/l	Grams per liter
g/mol	Grams per mole
GaAs	Gallium Arsenide
GAD	Gliding Arc Discharge
GaN	Gallium Nitride
GHz	Gigahertz
GZO	Gallium Doped Zinc Oxide
H	Hours
h^+	Positively Charged Holes
H_2	Hydrogen
H_2O	Water
H_2O_2	Hydrogen Peroxide
HEOs	High-Entropy Oxides
HNO_2	Nitrous Acid
HNO_3	Nitric Acid
Hz	Hertz
Hν	Photon energy
IARC	International Agency for Research on Cancer
IR	Infrared
ITO	Indium Tin Oxide
J	Joules
J/s	Joules per second
JP	Jet Plasma
TDP	Time Discharge Plsma
TEM	Transmission Electron Microscopy
TGA	Thermogravimetric analysis
THz	Terahertz
TiO_2	Titanium Dioxide
TOC	Total Organic Carbon
Torr	Torr
UV	Ultraviolet
UV-Vis	Ultra-Violet Visible
V	Volume of the NPs
V	Volts
ViP	Viral Protein
VOCs	Volatile Organic Compounds
VUV	Vacuum Ultraviolet
W	Watts
WO_3	Tungsten Oxide
wt%	Weight %
Y	yttrium
Z10, Z15, Z30, and Z60	ZnO nanoparticles synthesized with discharge plasma times of 10, 15, 30, and 60 minutes, respectively
ZA	Zinc Acetate Dihydrate
$Zn(CH_3COO)_2{\cdot}2H_2O$	Zinc Acetate Dihydrate
$Zn(OH)_2$	zinc hydroxide
ZnO	Zinc Oxide
ZrO_2	Zirconium Dioxide
A	Absorption coefficient
δ	Dislocation density
ε	molar absorptivity (or absorption coefficient)
Θ	Diffraction Angle
λ	Ray Wavelength

List of tables

Table I-1: Comparison of advantages and disadvantages of various NP synthesis methods 15

Table III.1 Comparative study of catalysts synthesized via various plasma methods. ..... **ERROR! BOOKMARK NOT DEFINED.**

Table III.2 Comparative study of key parameters in ZnO NPs synthesis by different physical process. ..... **ERROR! BOOKMARK NOT DEFINED.**

Table. IV .1. Estimation of structural parameters of ZnO NPs**ERROR! BOOKMARK NOT DEFINED.**

Table. IV. 2. Structural parameter calculations from xrd profile of all sample. ....**ERROR! BOOKMARK NOT DEFINED.**

Table. IV. 3. Structural parameter calculations from xrd profile**ERROR! BOOKMARK NOT DEFINED.**

Table. IV. 4. Average particle size, concentration (at%) and weight (w%) of the elements of ZnO NPs prepared at different TDP. ..... **ERROR! BOOKMARK NOT DEFINED.**

Table. IV. 5. Chemical composition and atomic percentage of ZnO NPs prepared using the plasma gad process. ..... **ERROR! BOOKMARK NOT DEFINED.**

Table. IV. 6. Characteristics of synthesized ZnO NPs at different plasma discharge times. ..... **ERROR! BOOKMARK NOT DEFINED.**

Table. IV.7. Quantitative thermogravimetric analysis results of ZnO NPs synthesized via the gad plasma method..... **ERROR! BOOKMARK NOT DEFINED.**

Table.IV.8. Comparative study of the degradation of CR, BCB and MB by photocatalysis of different NPs and ZNO synthetizes by plasma**ERROR! BOOKMARK NOT DEFINED.**

Table.IV.9. Comparison of efficiency, degradation time, and rate constants for the CR dye photodegradation under sunlight utilizing ZnO NPs as catalyst synthesis at varied TDP. ..... **ERROR! BOOKMARK NOT DEFINED.**

Table. IV. 10. Energy consumption and kinetic parameters for aspirin degradation using GAD plasma, photocatalytic and combined processes.**ERROR! BOOKMARK NOT DEFINED.**

List of figures

Figure I-1 Presentation of the diverse methods employed for synthesizing NPs. 5
Figure I.2 : Diagram illustrating X-Ray diffraction in a crystal 18
Figure I.3 Bar chart depicting the effective resolution ranges for two microscopic techniques explored in this chapter, as well as the unaided human eye 21
FIgure I.4 Schematic depiction of the nanofiltration process for water softening..... 29
Figure II.1 Physical description of plasmas 41
Figure II.2. The plasma reactive species generated using different operating gases..... 42
Figure II.3 Illustration depicting the application of cold plasma across various fields. ... 46
Figure II.4 Depiction of the configuration of a plasma jet reactor. 55
Figure II.5 Typical basic configurations of dbd acp reactor. 57
Figure II.6 Schematic representation of the microwave plasma synthesis principle for nps, illustrating two powder collection methods 58
Figure II.7: Configuration of gad plasma reactor used for np synthesis..... 60
Figure III.1 Congo Red (CR) dye chemical structure **ERROR! BOOKMARK NOT DEFINED.**
Figure III.2: Brilliant cresyl blue (BCB) dye chemical structure**ERROR! BOOKMARK NOT DEFINED.**
Figure III.3: Methylene blue (MB) dye chemical structure**ERROR! BOOKMARK NOT DEFINED.**
Figure III.4 Aspirin chemical structure..... **ERROR! BOOKMARK NOT DEFINED.**
Figure. III. 5 hexagonal wurtzite structure model of ZnO**ERROR! BOOKMARK NOT DEFINED.**
Figure. III. 6 Examples of nanostructures de ZnO**ERROR! BOOKMARK NOT DEFINED.**
Figure III.7: Actual photo of the experimental apparatus of the gad plasma reactor used for synthesizing ZnO NPs..... **ERROR! BOOKMARK NOT DEFINED.**
Figure III.8 Schematic depiction of the steps in the synthesis of ZnO NPs via gad plasma method..... **ERROR! BOOKMARK NOT DEFINED.**

Figure.IV.1. X-Ray diffraction pattern of ZnO NPs.**ERROR! BOOKMARK NOT DEFINED.**

Figure.IV.2. X-Ray diffraction spectrum of zno nps prepared by NTP at different discharge times. ..... **ERROR! BOOKMARK NOT DEFINED.**

Figure.IV.3 Variation in particle size and dislocation density..**ERROR! BOOKMARK NOT DEFINED.**

Figure. IV.4. X-Ray diffraction (XRD) pattern of synthetized ZnO NPs.....**ERROR! BOOKMARK NOT DEFINED.**

Figure.IV.5. FIGURE IV.5. Sem image of the ZnO nps plasma synthesized .....**ERROR! BOOKMARK NOT DEFINED.**

Figure.IV.6. Sem images of all synthesized ZnO samples, (a), (b), (c), and (d), correspond to samples Z10, Z15, Z30, and Z60, respectively**ERROR! BOOKMARK NOT DEFINED.**

Figure.IV.7. Particle size distribution histogram and typical EDAX spectra of all synthesized zno samples, (a), (b), (c), and (d), correspond to samples Z10, Z15, Z30, and Z60, respectively..... **ERROR! BOOKMARK NOT DEFINED.**

Figure.IV.8. SEM image of the ZnO NPs GAD plasma synthesized with a magnification of (a) 35.00 kx; (b) 100.00 kx..... **ERROR! BOOKMARK NOT DEFINED.**

Figure.IV.9. Absorbance spectra of initial zinc acetate, zinc acetate after 60 min of plasma discharge, and the final product (ZnO NPs). . **ERROR! BOOKMARK NOT DEFINED.**

Figure.IV.10. Plot Of $(Ahv)^2$ versus photon energy of synthesized ZnO. .....**ERROR! BOOKMARK NOT DEFINED.**

Figure.IV.11. (a) uv–vis absorption spectra, (b) plot of $(\alpha hv)^2$ versus photon energy of synthesized ZnO NPs. ..... **ERROR! BOOKMARK NOT DEFINED.**

Figure.IV.12. Evolution of particles size and Eg of ZnO NPs synthesized by variation of TDP. ..... **ERROR! BOOKMARK NOT DEFINED.**

Figure.IV.13. (a) uv–vis absorption spectra, (b) plot of (αhν)2 versus photon energy of synthesized ZnO NPs. ..... **ERROR! BOOKMARK NOT DEFINED.**

Figure. IV. 14. Ftir spectra of ZnO NPs and inset shows the enlarged spectra in the range < 600 cm-1. ..... **ERROR! BOOKMARK NOT DEFINED.**

Figure. IV. 15. Ftir spectra of ZnO NPs (all samples) (a) all range from 500 to 4000 cm–1, (b) spectra in the range < 700 cm–1..... **ERROR! BOOKMARK NOT DEFINED.**

Figure. IV. 16. TGA/DSC thermogram identifies the transformation of synthesized ZnO NPs. ..... **ERROR! BOOKMARK NOT DEFINED.**

Figure. IV. 17. DSC/TGA thermogram identifies the transformation of the synthesized ZnO NPs by gad plasma. ..... **ERROR! BOOKMARK NOT DEFINED.**

Figure.IV.18. The plot of ln(C0/CT) versus time for (A) BCB, (B) CR (C) and MB dyes. ..... **ERROR! BOOKMARK NOT DEFINED.**

Figure.IV.19. (a) absorbance spectra of dye solution under UV light irradiation, (b) photocatalytic degradation of dye at different times: (1) BCB, (2) CR and (3) MB. ..... **ERROR! BOOKMARK NOT DEFINED.**

Figure.IV.20. Influence of the as-synthesized ZnO NPs on the degradation efficiency of CR dye over specific time intervals in dark room.**ERROR! BOOKMARK NOT DEFINED.**

Figure.IV.21 UV-Vis absorption spectra depicting the photocatalytic degradation of CR. ..... **ERROR! BOOKMARK NOT DEFINED.**

Figure.IV.22. (a) degradation rate, and (b) the pseudo-first-order rate constant k (min^{-1}) ..... **ERROR! BOOKMARK NOT DEFINED.**

Figure.IV.23 Effect of pH on the photocatalytic degradation of CR.....**ERROR! BOOKMARK NOT DEFINED.**

Figure.IV.24. Recyclability test of Z60 sample for photodegradation of CR.....**ERROR! BOOKMARK NOT DEFINED.**

Figure.IV.25 Absorbance spectra of asa solution under UV light**ERROR! BOOKMARK NOT DEFINED.**

Figure.IV.26. Absorbance spectra of asa solution under GAD plasma treatment.**ERROR! BOOKMARK NOT DEFINED.**

Figure. IV. 27. pseudo-first-order rate constant k (min^{-1})**ERROR! BOOKMARK NOT DEFINED.**

Figure IV.28. (a) degradation efficiency (b) energy consumption (kwh) during the degradation of 100 ppm of aspirin according to each process**ERROR! BOOKMARK NOT DEFINED.**

Figure. IV.29. Illustrates the degradation efficiency of 100 ppm aspirin over successive cycles of ZnO photocatalyst exposure to 60 min of UV light**ERROR! BOOKMARK NOT DEFINED.**

Figure IV.30. Proposed mechanism of photocatalytic degradation of organic pollutants by ZnO NPs..... **ERROR! BOOKMARK NOT DEFINED.**

General Introduction

The Znic Oxide nanoparticles (ZnO NPs) have garnered increasing interest in research due to their unique properties and diverse potential applications. The use of cold plasma as a synthesis method offers significant advantages in terms of controlling the size, morphology, and properties of the produced NPs. This work aims to deepen the understanding of the characteristics of ZnO NPs synthesized by cold plasma and to explore their potential as efficient photocatalytic catalysts and highlighter the effect of discharge plasma time on the characterizations and photocatalytic application of ZnO NPs ware synthetized via cold plasma method. This study is part of a research context aiming to develop innovative solutions to address current environmental challenges by harnessing remarkable properties of nanomaterials for sustainable and effective applications. Thus, this research advances knowledge in the nanotechnology area and catalysis, highlighting the crucial role of ZnO NPs synthesized by cold plasma in the field of photocatalysis.

The thesis is divided into four main chapters:

Chapter I: Overview of Nanoparticles: Synthesis methods, Applications and Nanoparticle characterization techniques

This chapter provides an overview of NPs, including their synthesis methods, characterization techniques, and applications. It begins with a brief introduction to nanotechnology and NPs. It then discusses the various methods used to synthesize NPs, including chemical, physical, and biological methods. The chapter also describes the different techniques used to characterize NPs, such as microscopy, spectroscopy, and diffraction. Finally, the chapter discusses the various applications of NPs, including their use in medicine, energy, manufacturing, catalysis, and environmental remediation.

Chapter II: Overview of cold plasma: Definition, Chemical species generated and Applications:

This chapter delves into the concept of cold plasma, its definition, and the chemical species generated within it. It explores the diverse applications of cold plasma in various fields, including environmental protection, agriculture, food industry, medicine and healthcare, energy, and material science.

Chapter III: Synthetize, Characterizations and Photocatalytic application of the ZnO NPs produced using a GAD plasma method

This chapter focuses on the synthesis of ZnO NPs using a GAD plasma method. It describes the materials and methods used for the synthesis, characterization, and photocatalytic application of the produced ZnO NPs.

Chapter IV: Results and discussion on the Synthesis, Characterizations and Photocatalytic Applications of ZnO Nanoparticles

This chapter presents the results and discussion of the structural, optical, and photocatalytic properties of ZnO nanoparticles synthesized using the GAD plasma method. The focus is on the relationship between the synthesis conditions, particularly plasma discharge time, and the resulting nanoparticle properties. Additionally, this chapter examines the performance of ZnO nanoparticles in the photocatalytic degradation of organic pollutants, such as dyes and pharmaceutical compounds, under different conditions. These results are critical for understanding the potential applications of ZnO nanoparticles in environmental remediation.

This research provides valuable insights into the synthesis, characterization, and photocatalytic application of ZnO NPs produced using a GAD plasma method. The findings highlight the effect of time of discharge plasma on the characteristics of ZnO NPs and their potential as efficient photocatalysts for environmental remediation. This research contributes to the advancement of knowledge in the nanotechnology area and catalysis and combining processes for degrading the organic pollutants, paving the way for the development of novel and sustainable solutions for addressing environmental challenges.

Thesis Problem

The toxicity of organic compounds in water following discharge from chemical industries is a global concern due to the threat it poses to aquatic ecosystems. Photo-catalytic processes, utilizing metal oxide NPs as catalysts, are widely recognized as effective solutions to this issue. However, the synthesis of these NPs often involves methods with significant environmental and health impacts. Therefore, it is imperative to explore new synthetic approaches that are both ecologically sustainable and economically viable. In this context, this thesis focuses on the use of cold plasma as an alternative method for synthesizing metal oxide NPs, specifically ZnO. The objective is to evaluate the feasibility and effectiveness of this approach and to explore its application in the treatment of organic compounds found in industrial wastewater, thus contributing to sustainable solutions for industrial effluent treatment. Despite advancements in NP synthesis techniques, a significant research gap exists in plasma-based ZnO NP synthesis, particularly regarding the GAD plasma method. This thesis seeks to fill this gap by examining how GAD discharge time influences the properties and activity of ZnO NPs. Furthermore, the study evaluates the photocatalytic efficacy of these NTP-synthesized NPs in treating wastewater, additionally, the study evaluates the combining of photocatalytic process and GAD plasma process in treating wastewater highlighting their potential in overcoming the limitations of conventional methods and advanced oxidation processes.

Chapter I

Overview of Nanoparticles: Synthesis methods, Applications and Nanoparticle characterization techniques

Chapter I: Overview of Nanoparticles

Synthesis methods, Applications and Nanoparticle characterization techniques

Nanotechnology, a fusion of "nano" and "technology," is dedicated to manipulating matter at the nanoscale, where particles range from one to 100 nanometers [1], involving the engineering of individual atoms and molecules. NPs have ignited widespread interest across various scientific disciplines because of their unique size-dependent characteristics features and versatile applications. This interdisciplinary field holds immense promise for societal advancement across sectors such as medicine [2], energy, the environment, information technology, and aerospace science. In the contemporary era, nanotechnology stands at the forefront of scientific innovation. NPs, with their extraordinary capabilities resulting from large surface area relative to volume and quantum effects [2], have emerged as fundamental components for innovative materials and technologies. They exhibit exceptional physical, chemical, biological, optical, and electronic properties, providing opportunities to enhance existing technologies and explore novel scientific and technological frontiers. Thorough understanding of their synthesis methods, characteristics, and applications is essential for effectively controlling the synthesis parameters and ensuring the production of high-quality NPs [1].

This chapter provides an overview of NP, including characterization techniques, their synthesis methods, and applications. The chapter begins with a brief introduction to nanotechnology and NPs. It then discusses the various methods used to synthesize NPs, including chemical, biological, and physical methods. The chapter also describes the different techniques used to characterize NPs, such as microscopy, spectroscopy, and diffraction. Finally, the chapter discusses the various applications of NPs, including their use in medicine, energy, manufacturing, catalysis, and environmental remediation.

1. Nanoparticles Synthesis Methods:

Various methods have been employed to synthesize the NPs, encompassing biological, chemical, and physical approaches. Vapor deposition involves vaporizing zinc precursor compounds,

followed by their condensation to form NPs [3]. Laser ablation utilizes laser pulses to vaporize the metallic ions, leading to the formation of NPs that are subsequently collected [4]. The sol-gel methodology involves hydrolysis and condensation reactions to convert a precursor solution into a gel, which is then processed to produce NPs [5]. Spray pyrolysis involves atomizing a precursor solution into droplets and rapidly heating them to form solid NPs [6]. In hydrothermal/solvothermal synthesis, a precursor solution and a solvent react in a controlled way at high temperatures and pressures [7, 8].

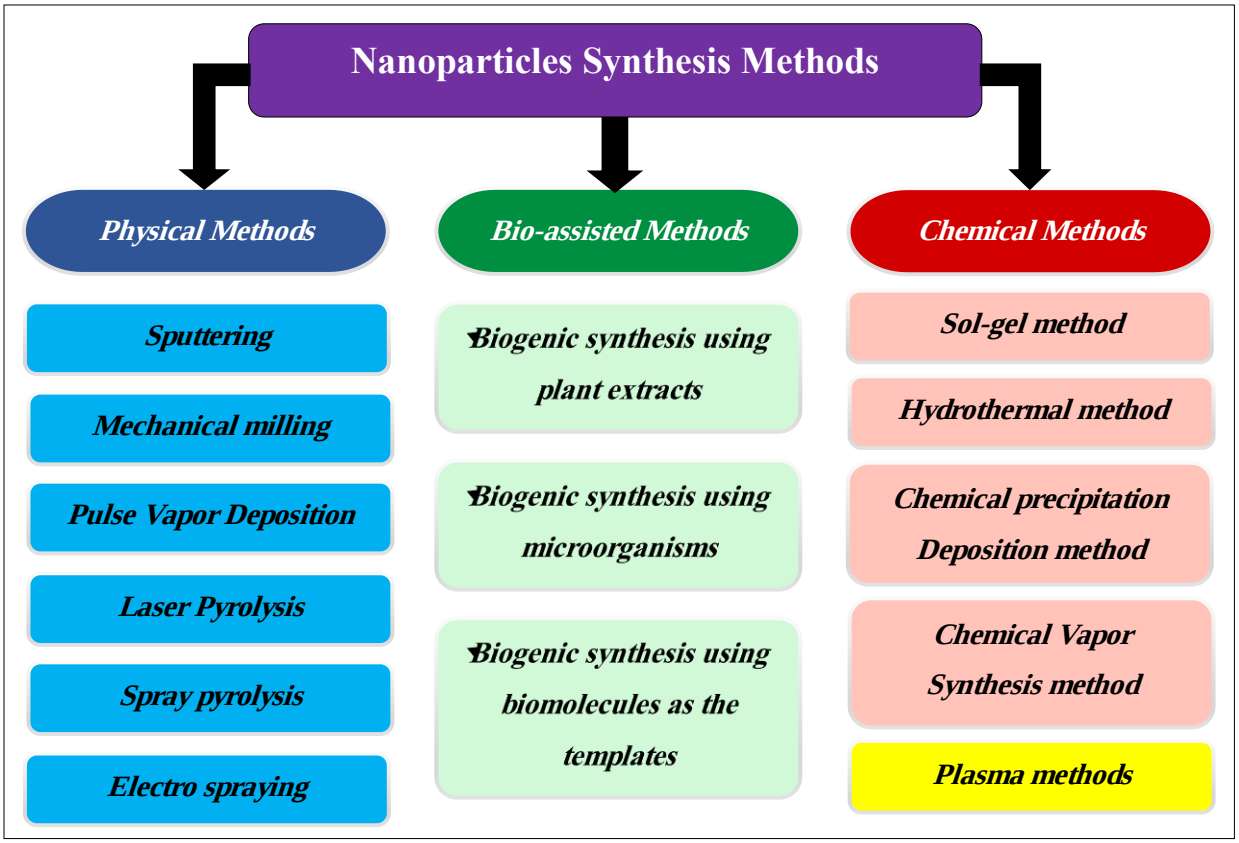

Figure I-1 presentation of the diverse methods employed for synthesizing NPs.

Finally, biosynthesis methods employ bacteria or plant extracts to reduce and stabilize ions, aiding in the formation of NPs with specific characteristics [9-11], enabling the production of NPs from diverse materials, including polymers, metals, semiconductors, and metal oxides. Figure I-1 illustrates the diverse methods employed for synthesizing NPs. Each method has its limitations and advantages, and the choice of synthesis route depends on the desired NPs proprieties and intended applications. Non-thermal plasma (NTP) one of the methods overcome these obstacles and issues, NTP is a source to create reactive species that can oxidize metallic ions. This process enables the

synthesis of NPs without relying on dangerous chemicals or solvents. The plasma-based technique allows for the production of NPs with high purity at low temperatures, making it ideal for temperature-sensitive materials. This method stands out due to its brief synthesis duration compared to other techniques, enhancing its versatility and suitability for industrial applications [12, 13]. Details of some synthesis methods are given below:

1.1. Physical methods:

Physical methods utilize high-energy radiation, electrical energy, mechanical pressure, or thermal energy to induce condensation, melting, evaporation, or material abrasion, thereby producing NPs. These techniques predominantly follow a top-down approach and offer several advantages, including the elimination of solvent contamination and the creation of uniform, monodisperse NPs. However, the significant amount of waste generated during synthesis renders physical processes less economical. Commonly employed physical methods for NP generation include laser ablation, flash spray pyrolysis, high energy ball milling, electro-spraying, inert gas condensation, physical vapor deposition, melt mixing, laser pyrolysis, and sputtering [1, 14]. These are some of the most commonly used physical methods to generate NPs:

1.1.1. Sputtering:

Sputtering, a vacuum-based physical vapor deposition (PVD) technique, is frequently employed for the deposition of thin films and NPs. Operating on the principle of momentum transfer, sputtering involves the ejection of atoms from a target material by ion bombardment. The process can utilize various power sources, including radio frequency (RF), pulsed DC, and direct current (DC) powers [15] . Sputter deposition occurs in multiple stages: Initially, a plasma consisting of neutral gases, typically Ar, is created between two electrodes as electrons collide with gas molecules. Following this, the ions present in the plasma are accelerated towards the target material by applying a voltage difference between the electrodes. These ions, possessing sufficient energy, impact the target, causing material ejection. Finally, the ejected material is transported and deposited onto the substrate, thereby completing the sputtering process [1]. In various sputter deposition processes, NPs of optimal size can be synthesized by carefully selecting appropriate deposition conditions. For instance, Bouchat et al. conducted a study demonstrating the synthesis of a variety of non-metallic and metallic NPs, including yttrium (Y), C, TiO_2, Fe, Au, Ag, and Co

[16]. Veith et al. utilized magnetron sputtering to deposit Au NPs on WO_3 and activated carbon surfaces [17]. Similarly, Hatakeyama and Nishikawa synthesized gold NPs through magnetron sputtering, adjusting the deposition parameters to control particle size and distribution [18].

1.1.2. Mechanical milling:

Mechanical milling stands as a prominent physical synthesis approach, specifically employing high-energy ball milling, recognized as a solid-state processing route for synthesizing a diverse range of non-equilibrium and equilibrium phases as well as phase mixtures. This process entails intense mechanical action on solid surfaces, inducing notable chemical and physical alterations in the near-surface region where solids interface under mechanical forces. Currently utilized for synthesizing inorganic materials, mechanical milling offers several advantages, including reduced sintering temperatures, and can effectively drive various chemical reactions. Equipment utilized in this process includes planetary machines, attritors, and vibrational mills. Mechanical milling has played a crucial role in producing oxide dispersion strengthened (ODS) Ni-base superalloys and other ODS alloys. It has also been key in increasing terminal solid solubilities in commercially important metallic systems. It has demonstrated superiority over fast solidification processing as a non-equilibrium processing tool. However, despite extensive efforts, comprehension of the far-from-equilibrium nature of mechanical milling remains incomplete, presenting ample opportunities for further research in this dynamic domain [14, 19-22]. Simsek et al. documented that wet milling of metallic zinc powder for a duration of 24 hours resulted in a mixture of ZnO, zinc hydroxide ($Zn(OH)_2$), and zinc phases. It was observed that increasing the milling speed from 250 to 400 rpm was necessary to achieve nearly a single phase (98.3% ZnO). Subsequently, a subsequent step of dry milling was implemented to further enhance purity [23]. Similarly, in certain instances, an extended milling duration e.g., 120 hours, as reported by Singh et al. is necessary to attain the nanoscale range [24].

1.2. Bio-assisted methods:

Green synthesis offers an environmentally friendly, non-toxic, economically viable, and effective approach to produce NPs. These methodologies utilize biological entities such plant extracts, yeast, actinomycetes, fungi, as bacteria, viruses, and others to synthesize metal oxide and metal NPs. Bio-assisted synthesis methods can be categorized into three main groups (Biogenic synthesis using

plant extracts, Biogenic synthesis using microorganisms, and Biogenic synthesis using biomolecules as the templates).

1.2.1. Biogenic synthesis using plant extracts:

Green synthesis using plant extracts is a sustainable method that is quickly becoming more popular. Different parts of plants, such as seeds, fruits, leaves, roots, and flowers, can be used to create extracts rich in phytochemicals. These phytochemicals, which include amino acids, tannins, terpenoids, and flavonoids, act as reducing and stabilizing agents, playing a vital role in the synthesis of less toxic NPs compared to conventional methods. This technique has been extensively applied to produce NPs of noble metals, bi-metallic alloys, metal oxides, and other materials. [25] [26].

A) Seeds as source for nanoparticle synthesis

Patil et al. employed fenugreek seed extract, known for its high flavonoid content and other natural bioactive compounds including lignin, saponin, and vitamins, to synthesize Ag NPs. The study aimed to investigate the potential benefits of Ag NPs that were incorporated into tablets along with fenugreek seeds, and were evaluated for their efficacy in reducing blood cholesterol levels, managing diabetes, enhancing breast milk production, aiding digestion, and promoting weight loss [25, 27].

B) Fruits and peel as source for nanoparticle synthesis

Kumar et al., demonstrated the successful synthesis of metallic NPs (Au, Ag, Fe) using extracts from oranges, bananas, and grapes as both reducing and stabilizing agents. The synthesized NPs exhibited a size range of 5 to 50 nanometers and displayed spherical as well as non-uniform shapes. These bio-synthesized NPs were investigated on the potential applications in pomology, particularly focusing on their antimicrobial and antioxidant activities. The NPs exhibited antibacterial and antifungal properties against common plant pathogens, contributing to fruit quality enhancement. Additionally, the NPs demonstrated antioxidant activity, protecting fruit cells from oxidative stress damage. Application of these NPs resulted in extended shelf life and improved sensory properties, including color and taste, of the fruits [28]. As another way, to produce ZnO NPs from zinc acetate dihydrate utilizing botanical sources, Tu Uyen Doan Thi et al.

employed an aqueous extract derived from orange peels as a biological reduction agent. Their investigation revealed that parameters variables, including annealing temperature and pH levels during NP synthesis, exerted significant influence on the size and morphology of the resulting ZnO NPs [29].

C) Leaves as source for nanoparticles synthesis

Ismail, Ahmed et al. investigated how leaf extracts from the Pinus Brutia tree and different pH levels of the green synthesis solution (ranging from 6 to 12) impact the characteristics of ZnO NPs. The study conducted at room temperature demonstrated that varying pH values notably influence the morphology, orientation, shape, and size of the green-synthesized ZnO NPs. These NPs were observed to be spherical in shape and ranged in size from 37.47 to 73.70 nm. Comparative analysis of ZnO NPs produced at different pH levels revealed that those synthesized at pH 8 exhibited favorable quality and notable improvement [30]. Additionally, Messai et al., was conducted a study on the green synthesis of ZnO NPs utilizing the aqueous extract of Phoenix Dactylifera.L leaves as a reducing agent. The method involved the reduction of zinc acetate by the aqueous extract of Phoenix leaves. Through controlling synthesis parameters such as zinc acetate concentration, gelling time, duration, and temperature of heat treatment, the researchers successfully produced ZnO NPs with varying sizes ranging from 14.12 to 22.72 nm [31].

D) Root as source for nanoparticle synthesis

Kobylinska et al., explored the feasibility of utilizing extracts derived from "hairy" root cultures of specific Artemisia plant species (Artemisia tilesii Ledeb. and Artemisia annua L.), as a sustainable and environmentally friendly approach for synthesizing Ag NPs. They also investigated the potential medical applications of these bio-synthesized Ag NPs. Additionally, the study reveals that Ag NPs synthesized from ethanol extracts exhibit a clustered and irregular morphology, with sizes ranging from 10 to 50 nm. In contrast, Ag NPs produced from aqueous extracts at 80°C exhibit smaller and more uniform sizes, ranging from 10 to 30 nm [32]. Furthermore, Al-Radadi successfully synthesized gold (Au) NPs using a straightforward one-step green method, employing licorice root extract as both the reducing and stabilizing agent. Various techniques were employed to confirm the successful formation of spherical AuNPs with an average size ranging from 15 to

20 nm. The antimicrobial and anticancer activities of these synthesized AuNPs were investigated [33].

E) Flowers as source for NPs production

Noruzi et al. investigated an environmentally friendly approach to synthesize Au NPs using rose petals. Similarly, various flowers such as, Clitoria ternatea, Nyctanthes arbortristis and Catharanthus roseus have been employed for synthesizing metallic NPs, each resulting in diverse shapes [34, 35]. Furthermore, Nava et al., investigated a cost-effective and non-toxic method for synthesizing ZnO NPs using Camellia sinensis extract. The research demonstrated the antibacterial efficacy of produced ZnO NPs in the treatment of urinary tract infections [36].

1.2.2. Microbial-Based Biogenic Synthesis:

In recent years, there has been a growing interest in exploring alternative biosynthetic methods involving microorganisms as bionanofactories for the production of NPs. For instance, alkalothermophilic actinomycetes such as Thermomonospora curvata, Thermomonospora fusca, and Thermomonospora chromogena have been employed for the extracellular biosynthesis of Au NPs [37]. Recognizing the safety and economic feasibility of microorganism-mediated NP synthesis, Chauhan et al., investigated the biological synthesis of Au NPs using Candida albicans in their study [38]. Their research demonstrated the potential application of antibody-conjugated gold particles synthesized through this method in the detection of liver cancer, showing successful differentiation between normal and cancerous cells [38]. Additionally, Durán et al. examined the characterization and antimicrobial properties of biogenically synthesized Ag NPs and AgCl NPs. Their review critically evaluated recent studies on the synthesis of these NPs, aiming to establish correlations between NP characterization and antimicrobial effectiveness [39]. Furthermore, Guilger-Casagrande et al. discussed studies involving the use of fungi as reducing agents for synthesizing Ag NPs. They explored the mechanisms, optimization strategies, and applications of Ag NPs synthesis using fungi, highlighting their potential for pathogen control due to their low toxicity and good biocompatibility [40].

1.2.3. Biogenic synthesis using biomolecules as templates:

Biogenic synthesis of NPs utilizes a range of biological entities such as bacteria, fungi, algae, plants, and biomolecules as templates for NPs production. This method presents an eco-friendly and sustainable alternative to chemical synthesis approaches, which often involve the use of hazardous substances. The presence of biological molecules on the NPs surface enhances biocompatibility and can contribute to improved stability. Various natural sources have been investigated for their potential in biogenic NPs synthesis. Goswami et al. presented a successful protein-assisted synthesis method for producing highly crystalline Au NPs within the size range of 3-5 nm, without the use of any reducing agents. Various thermal denaturation techniques were employed to modulate the protein structure, thereby influencing the kinetics, size, and crystallinity of the resulting NPs. The authors suggested that the chemical functionalities of the protein play a critical role in reducing and stabilizing metal ions, thus facilitating NPs formation [41]. Pérez-Page et al explored into template-based synthesis, employing a variety of materials including molecules, polymers, and biological substances to guide nanostructure formation. These templates act as molds or scaffolds, dictating the final shape and size of the resulting nanomaterials. This technique offers several advantages over traditional synthesis methods. Firstly, it allows precise control over NPs shape, enabling the production of diverse geometries such as spheres, rods, and tubes. Secondly, the controlled shape significantly impacts the properties of the nanostructures, customizing them for specific applications. The authors also discussed different template types utilized in this approach, categorizing them as hard templates and soft templates [42].

1.3. Chemical methods:

NPs can be synthesized via a variety of chemical processes, utilizing different intermediates and adjusting parameters such as temperature, reaction time, and concentration. These adjustments yield NPs with variations in dimensions, shape, and geometry. Among the common chemical production methods are the Chemical precipitation method, sol-gel method, and hydrothermal method:

1.3.1. Chemical Precipitation

The chemical precipitation method, a prevalent technique for synthesizing NPs, involves the formation of poorly soluble metal ion salts (typically hydroxide, carbonate, or oxalate salts), followed by filtration or centrifugation and subsequent heat treatment [14, 43]. This method, noted

for its simplicity and cost-effectiveness, has been employed in various studies over the years. In 2009, Zhang et al. utilized a liquid precipitation technique to synthesize megestrol acetate (MA) NPs with a mean size of 208 nm [44]. Similarly, in 2012, Bayal et al. successfully synthesized core-shell CuO–NiO mixed metal oxide NPs using a homogeneous precipitation method [45]. Nazari et al. (2014) synthesized maghemite (γ-Fe_2O_3) NPs with a mean size of 9 nm via chemical precipitation [46]. In 2019, Souza et al. introduced a chemical precipitation method utilizing zinc nitrate hexahydrate and sodium hydroxide (NaOH) for the sonochemical synthesis of ZnO NPs [43, 47]. Subsequently, in 2020, Nayar et al. conducted a comparative study on phase transformation of Al_2O_3 NPs prepared by chemical precipitation and sol-gel auto combustion methods [48]. In 2021, Eskandari and Hasanzadeh synthesized Fe_3O_4 NPs using chemical co-precipitation method via ultrasonic waves and an alternating magnetic field-assisted [49]. Similarly, the chemical precipitation method was employed to synthesize CuO NPs, facilitating the removal of divalent nickel ions from aqueous solutions [50]. Additionally, Thakur et al. reported morphology-controlled chemical synthesis of ZnO nanostructures for water purification in the same year [51].

1.3.2. Sol-gel

The sol-gel method, characterized by its low-temperature chemical synthesis route, facilitates the production of homogeneous and highly pure NPs. This method typically involves five steps: hydrolysis, polycondensation, aging, drying, and heat treatment. Researchers have extensively investigated and utilized the properties of nanodimension metal and alloy particles synthesized through the sol-gel technique. Detailed discussions on the optical properties, characterization techniques, and applications of metal NPs doped oxide and inorganic-organic hybrid films synthesized using the sol-gel method are available in the literature.[52-55]. Experimental conditions, such as the nature and concentration of the metal precursor, solvents, condensation and calcination temperatures, and pH of the reaction medium, profoundly influence the physicochemical properties of the resulting NPs, such as ZnO-NPs [56]. For instance, Ismail et al. (2019) explored the impact of calcination temperature (ranging from 70 to 800 °C) on the structural and antibacterial activity of elongated rod-shaped ZnO-NPs. They observed a significant increase in particle size from 73 to 395 nm as the calcination temperature rose from 70 °C to 800 °C, respectively [57].

1.3.3. Hydrothermal method

Hydrothermal synthesis is a wet-chemical technique, is a widely utilized in NPs research for creating nanostructures, providing versatility in tailoring their properties. This technique involves conducting reactions in sealed environments under high vapor pressure, facilitating the crystallization of substances and the production of NPs with desired characteristics. It is a favored approach for efficiently processing nanostructured particles of various inorganic compounds, enabling the synthesis of NPs with tailored properties. Specifically, heterogeneous chemical reactions, which involve the manipulation of hydrolyzed atomic species in water, can occur within a temperature range of 100–500 ◦C and at high pressures ranging from 0 to 225 bars or higher. Nevertheless, certain researchers also associate the term "hydrothermal" with aqueous systems undergoing reactions below 100 ◦C. Notably, hydrothermal synthesis offers the advantage of continuous operation, enabling the rapid and scalable production of nanomaterials [1, 58]. Over the past two decades, significant endeavors have focused on expediting nucleation kinetics and restraining particle growth, leading to the synthesis of particles exhibiting distinct morphologies and nano-scale dimensions. The subsequent paragraph offers an overview, underscoring the contributions of select published articles [58]. Alam et al. explored an innovative approach to fabricate nanofluids with enhanced thermal insulation properties, employing ZnO nanorods as the insulating material. The synthesis of ZnO nanorods was effectively accomplished at a low temperature of 170 ◦C for 6 hours, with the particle morphology and size controlled by a surfactant agent, polyvinylpyrrolidone (PVP). Heat transfer coefficient measurements were conducted to evaluate the efficiency of the nanofluid, revealing that laminar nanofluids comprising 0.3 vol% of ZnO nanorods and ethylene glycol exhibited favorable heat transfer coefficients [59]. The research conducted by Watanabe et al. aimed to enhance the dispersibility of ZrO_2 NPs in toluene. The study revealed that the organic 6-phenyl hexanoic acid component regulated the growth of NPs through surface modification, with its influence dependent on temperature. When ZrO_2 NPs were present at a concentration of 0.33 wt%, synthesized under subcritical conditions (300 ◦C for 10 min) and dispersed in toluene with 1,4-bis(5-phenyl2-oxazolyl) benzene and 2,5-diphenyl oxazole, the resulting liquid scintillator exhibited the highest X-ray-induced radioluminescence response [60]. In another study, Chen et al. synthesized diverse morphologies of ZnO NPs using $ZnCl_2$ and NaOH in a hydrothermal process, employing various organic templates to control nanostructure size [61]. Baruwati et al. reported the aqueous synthesis of ZnO in an autoclave at 120°C, adjusting the pH

with ammonium hydroxide. However, this method requires overnight drying to obtain the final product, rendering it time-consuming [62].

1.3.4. Cold Plasma method

Various types of cold plasma have been employed for synthesizing the NPs with tailored properties, such as high purity or controlled particle size, the subsequent chapter provides a comprehensive exposition of this method.

1.4. Disadvantages and Advantages of Different Synthesis Methods

In Table I-1, a comparative analysis is provided, outlining the strengths and weaknesses inherent in each synthesis method. While methods such as Ball milling and sputtering demonstrate efficacy in achieving precise size control and high yields, they are constrained by limitations concerning the range of applicable materials and associated processing times and costs. Also, the bio-assisted methods, while laudably sustainable and environmentally friendly, are restricted by a narrow selection of materials and may necessitate additional post-processing steps.

Moreover, hydrothermal and sol-gel methods offer advantages in size and shape control as well as high yields, but are associated with the use of hazardous chemicals and require subsequent processing. Notably, cold plasma synthesis emerges as a promising approach due to its low-temperature operation, energy efficiency, and environmental compatibility. Consequently, this method yields high-quality NPs with a relatively straightforward setup. However, further research is imperative to optimize synthesis conditions and enhance size control [13, 52, 63-70].

Table I-1: Comparison of advantages and disadvantages of various np synthesis methods.

Synthesis Method	**Advantages**	**Disadvantages**	**Ref**
Ball Milling	❖ high yield ❖ precise NP size control ❖ low cost ❖ ligand free NPs	❖ long processing times ❖ limited in materials ❖ difficult to make NPs	[63-65]
Sputtering	• Preservation of material composition • Suitable for refractory metals and intermetallic compounds • Low impurity generation • Enhanced control over alloy composition • Versatility in synthesizing ionic NPs • Precise control over parameters	• Influence on surface morphology • Effect on composition • Impact on texture • Influence on optical properties Slow deposition rates, usually less than 300 nm/min. • Critical substrate surface preparation for adhesion and properties. • High setup costs due to vacuum requirements and low energy efficiency (70% or more of input energy is expended in target heating). • Requires vacuum chamber	[52, 65, 66]
Bio-assisted methods	✓sustainable ✓eco-friendly ✓biocompatible NPs ✓narrow size distribution ✓low cost ✓many species available ✓high reproduction rate	✓ Difficulty in reproducing identical materials across different environmental conditions or time periods. ✓ Limited materials ✓ Limited combinations for NPs synthesis ✓ Require post processing ✓ NPs may not be suitable for catalytic and electronic applications due to ligands	[13, 65, 67]
Hydrothermal	❖ Controlled size and shape ❖ Formation of well-crystallized powder ❖ High crystallinity ❖ Cost-effectiveness ❖ High yield	❖ Lack of process control ❖ Reliability and reproducibility limitations ❖ Extended processing time ❖ High temperature requirements ❖ Use of hazardous chemicals ❖ Post-processing steps	[52, 65, 67, 68]
Sol-gel	• Precise size control • Wide material range • Simple process • Uniform NPs production • Control through reaction monitoring	• Long processing time • Formation of unwanted by-products • Post-processing steps • Use of hazardous chemicals	[52, 65, 67]
Cold plasma	✓Low temperatures ✓Suitable for temperature-sensitive materials. ✓Short synthesis time ✓Highly flexible and scalable ✓Reduced chemical products ✓Utilizes only a salt of metal precursor ✓Minimizing chemical usage. ✓Simple equipment ✓Energy-efficient operation. ✓Operates in ambient air at low pressure ✓Environmental-friendly conditions. ✓High efficiency ✓Yields high-quality NPs effectively.	✓ Optimal parameter determination: Ongoing research to identify the most effective synthesis conditions. ✓ Obtaining NPs of varying sizes.	[13, 69, 70]

2. Nanoparticles characterization techniques:

2.1. Optical properties:

UV-visible spectroscopy: UV-visible spectroscopy is a fundamental technique utilized to characterize the optical properties of NPs within the wavelength range of 200 to 900 nm. In our work, the Shimadzu 3101PC double-beam spectrophotometer was employed to measure UV-Vis absorption. This spectrophotometer disperses transmitted light, which is then analyzed by a CCD camera with a resolution of 1 nm. By assessing the absorption of NPs, valuable insights into their optical characteristics, are obtained based on band gap width and peak positions corresponding to NPs absorption. In our experiments, the absorption data were collected under standardized parameters, including wavelength range, speed, integration time, volume and concentration. The underlying principle of UV-visible spectroscopy lies in the interaction between emitted light and the sample. When a substance absorbs light in this range, it induces disturbances in the electronic structure of atoms, ions, or molecules, as electrons transition from lower to higher energy levels. The absorption spectra obtained from these measurements allow for the determination of the absorption coefficient (ε) using the Beer-Lambert law:

$$A = \varepsilon\, c\, l \qquad (I-16)$$

Also

$$A = \log\left(\frac{I_0}{I}\right) \qquad (I-17)$$

A is the absorbance, ε is the molar absorptivity (or absorption coefficient), c is the concentration of the absorbing species, and l is the path length of the sample.

The following equation (Eq. I-18) calculates the NPs' direct transition optical band gap energy [71]:

$$(\alpha h\upsilon)^2 = \mathrm{K}\left(h\nu - \mathrm{E_g}\right) \qquad (I-18)$$

where :

α is the absorption coefficient,

E_g is the optical band gap of the NPs,

hν is the photon energy,

K is a constant independent on hν.

As a result, Tauc's plot is used in order to compute the optical band gap. This is accomplished by plotting $(hv)^2$ versus (hv), and then extrapolating the linear section in order to determine the energy axis intercept.

2.2. Crystalline structures:

2.2.1. Fourier Transform Infra-Red Spectroscopy (FTIR)

FTIR is a widely used analytical technique that enables the identification and analysis of materials by measuring their infrared absorption or emission. Applicable to solids, liquids, and gases, FTIR works by passing infrared light through a sample, where specific wavelengths are absorbed based on the molecular vibrations within. A mathematical process called Fourier Transform converts raw data into a spectrum that reveals molecular structures and functional groups, aiding in material identification and composition analysis. FTIR is commonly used in fields such as chemistry, biology, and material science, with applications ranging from material identification and quality control to environmental monitoring and pharmaceutical analysis. Its key advantages include speed, sensitivity, and non-destructive analysis, making it an indispensable tool for researchers in the nanotechnology field.

2.2.2. X-ray diffraction (DRX)

Crystalline structure of NPs can be derived from X-ray diffraction patterns. X-ray diffraction (XRD) is utilized to analyze the atomic and molecular arrangement within crystals through the examination of how incident X-rays are diffracted. This phenomenon occurs due to the constructive interference between matter and X-rays. Constructive interference is observed when the waves reflected by successive crystal planes are in phase, indicating that their phase difference is a multiple of the incident X-ray wavelength (λ). To observe a diffraction peak, the optical path difference traveled by the radiation between these planes (2d sin θ) must align with Bragg's law, where d represents the distance between crystal planes and θ is the diffraction angle [72]. Figure I.3 presents an illustrative diagram depicting the process of X-ray diffraction within a crystalline structure.

$$2d\ \sin(\theta) = n\,\lambda \qquad (I-1)$$

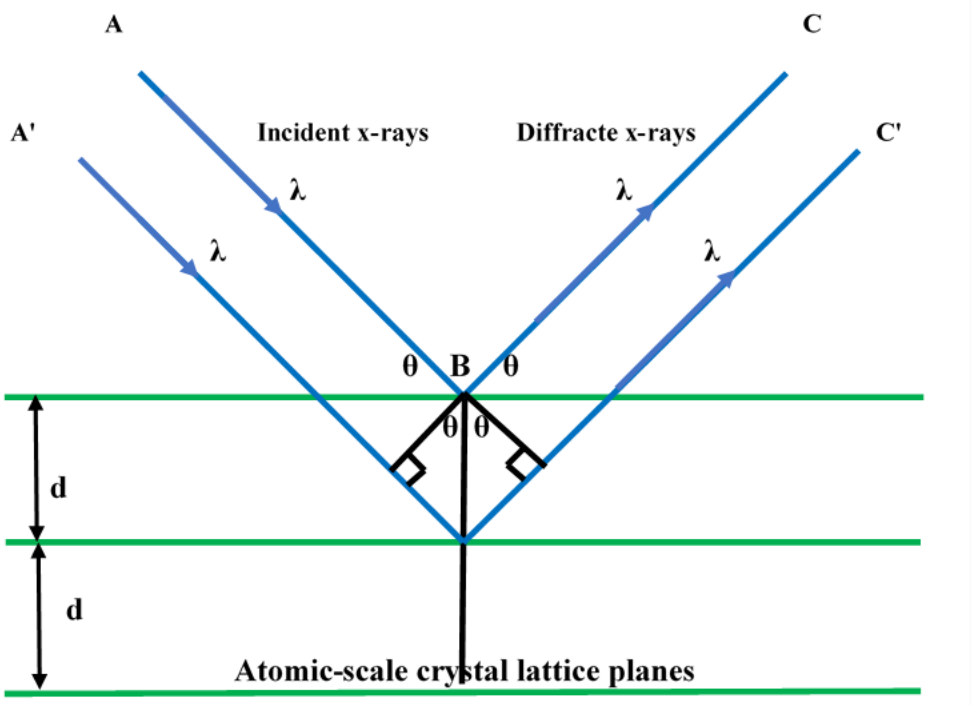

Figure I.2 : Diagram illustrating X-ray diffraction in a crystal [72].

The analysis of X-ray diffraction spectra enables us to ascertain the size of the crystal. By measuring the full width at half maximum of peaks in a spectrum, the wavelength of the X-rays emitted by the source (λ), and the diffraction angle (θ) at which they appear, we can calculate the grain size (D) using the following Scherrer formula :

$$D(nm) = \frac{k\ \lambda}{\beta\ cos(\theta)} \qquad (I-2)$$

X-rays directed towards the sample are generated using a copper anode (Kα=1.540593 nm). The analysis covers angles ranging from 2θ = 10° to 80° with an increment of 0.100° and an integration time of 1 second. Detection is conducted using a Dectris Mythen 1K detector, which is a one-dimensional detector with an active length of 3.22°. Subsequently, the diffractograms are processed using the PANalytical ICSD Database. The lattice parameters (a, b, and c), c/a ratio, dislocation density (δ), internal micro-strain, volume of the NPs, and the number of unit cells present (n) can determinedand calculated using following well-knowns formulas [13, 73-80]:

a) The lattice parameters (a, b, and c)

$$a = b\ (\text{Å}) = \frac{\lambda}{\sqrt{3}\sin(\theta_{100})} \qquad (I-3)$$

$$c\ (\text{Å}) = \frac{\lambda}{\sin(\theta_{002})} \qquad (I-4)$$

b) Dislocation density £ 10^{15} (line/m^2)

$$£\ \left(10^{15}\frac{\text{line}}{m^2}\right) = \frac{1}{D^2} \qquad (I-5)$$

c) d-spacing (Å)

$$\text{d} - \text{spacing}\ (\text{Å}) = \frac{\text{n}\,\lambda}{2\sin\theta} \qquad (I-6)$$

d) Volume of the NPs V (nm3)

$$\text{V}\ (\text{nm}^3) = (\frac{4}{3})\pi(\frac{D}{2})^2 \qquad (I-7)$$

e) Volume of the unit cell *v* (nm^3)

$$v\ (\text{nm}^3) = 0.866\ a^2\ c \qquad (I-8)$$

f) n^o of unit cell present in NPs

$$\text{n}^o = \frac{V}{v} \qquad (I-10)$$

g) Distortion parameter μ

$$\mu = \frac{a^2}{3c^2} + 0.25 \qquad (I-11)$$

h) Bond length L (A˚)

$$\text{L}\ (\text{A}^\circ) = \sqrt{0.3\ a^2\ + (0.5-\mu)^2 c^2} \qquad (I-12)$$

i) Internal micro-strain ε 10^{-3}

$$\varepsilon\ (10^{-3}) = \frac{\beta\cos(\theta)}{4} \qquad (I-13)$$

j) Uniform strain e_{zz} 10^{-3}

$$\text{e}_{zz}\ (10^{-3})\frac{c-c_0}{c_0} \qquad (I-14)$$

k) Strain σ (GPa)

$$\sigma\ (\text{GPa}) = \left[2\text{C}_{13} - \frac{\text{C}_{33}(\text{C}_{11}+\text{C}_{12})}{\text{C}_{13}}\right]\text{e}_{zz} \qquad (I-15)$$

Where, C33(210 GPa) , C11(210 GPa), C12(120 GPa), and C13 (105 GPa) are the elastic stiffness constants.

The comparison of X-ray diffraction (XRD) data provides insights into the type of constraint, either extensive or compact, acting on the cell structure. When the 2θ value deviates from the reference value, it indicates whether the cell is in an expanded or compressed state. For instance, when the

2θ value is lower than the reference, it signifies an expanded cell, whereas a higher value suggests a stressed network. This fluctuation in the 2θ value correlates with alterations in granule size [81]. Furthermore, the decrease in particle size leads to a notable increase in the surface-to-volume ratio. This augmentation offers more active sites for dye adsorption, thereby amplifying the photocatalytic activity [82, 83]. Additionally, the escalation in dislocation density creates intermediate sub-band energy states that serve as electron traps, prolonging charge recombination and extending carrier lifetime [84]. Simultaneously, the lattice expansion signifies the existence of intrinsic defects, such as oxygen vacancies, which further enhance charge separation. Collectively, the combination of size reduction, heightened crystalline defects, and lattice expansion yields NPs with augmented photocatalytic efficacy for dye degradation [85, 86].

2.3. Morphological properties:

transmission electron microscopy (TEM) and Scanning electron microscopy (SEM) are primarily employed for the examination of morphological attributes.

2.3.1. Scanning Electron Microscopy (SEM) and EDAX

SEM is a sophisticated imaging technique employed to capture high-resolution images of a sample's surface, revealing its intricate topography. By directing a focused electron beam onto the sample, SEM exploits electron-matter interactions to produce diverse signals, including secondary electrons, backscattered electrons, and X-rays. These signals are then detected and converted into digital images, enabling visualization of both surface morphology and composition. SEM offers superior imaging capabilities compared to optical microscopes, boasting nanometer-scale resolution and a broad depth of field, which facilitates detailed examination of rough surfaces. Furthermore, SEM allows for the analysis of the elemental composition of the sample surface. The equipment used, such as the Thermo Scientific TM Quattro SEM, integrates advanced imaging and analytical functionalities, including an environmental mode (ESEM) for studying materials under natural conditions. Additionally, energy-dispersive X-ray analysis (EDX) spectra provide insights into the chemical composition and atomic percentage of NPs, with X-ray emission triggered by the electron beam impact aiding in EDX analysis. This method offers a lateral resolution of approximately 1 micron and can detect elements present in atomic concentrations exceeding 1%.

In summary, SEM serves as a versatile tool for acquiring detailed surface images and compositional data, with applications spanning various scientific and industrial fields [13, 87].

2.3.2. Transmission Electron Microscopy (TEM)

TEM is a fundamental technique utilized to investigate the internal microstructural features of materials. In TEM, an electron beam passes through a specimen, and the resulting image is projected onto a fluorescent screen or photographic film, facilitating the observation of internal microstructural details. The contrast in TEM images is generated by variations in beam scattering or diffraction among different elements of the microstructure or defects. To ensure effective transmission of the incident beam, specimens must be prepared as very thin foils. TEM enables magnifications of up to 1,000,000×, allowing the visualization of minute details, such as a single column of atoms. This technique finds applications across diverse fields, including cancer research, virology, materials science, nanotechnology, and semiconductor research. Additionally, TEM is valuable for studying dislocations and other microstructural features in materials, offering insights into their properties and behavior. Through TEM, researchers gain unique insights into the atomic and molecular-scale structure of materials, contributing significantly to scientific advancements and technological innovations [87]. Figure I.4 illustrates a bar chart depicting the effective resolution ranges for two microscopic techniques explored in this chapter, as well as the unaided human eye.

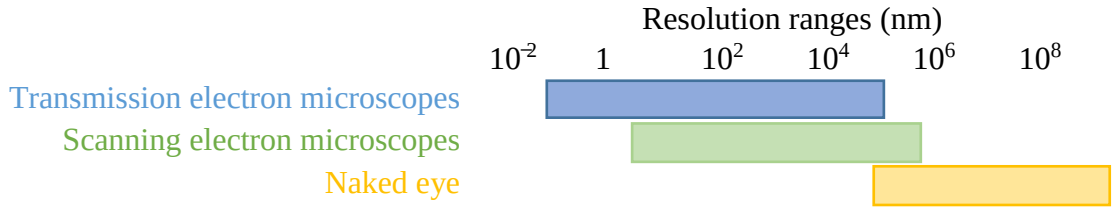

Figure I.3 Bar chart depicting the effective resolution ranges for two microscopic techniques explored in this chapter, as well as the unaided human eye [87].

2.4. Thermal properties:

Thermogravimetric analysis (TGA) serves as a valuable technique for assessing material behavior in response to temperature variations. By monitoring the material's weight loss with increasing temperature, TGA enables the identification of critical points where significant weight changes occur. This method provides essential insights into factors such as solvent residues, absorbed contents, and degradation temperatures. the instrument used for TGA in our work is the METTLER

TOLEDO's Simultaneous Thermal Analysis Device (TGA/DSC): TGA/DSC, capable of tracking mass changes and thermal flow across a broad temperature range from 25 to 1600°C. With the ability to conduct analyses in controlled environments using air, nitrogen, or argon, this device offers flexibility in experimental conditions. Key specifications include adjustable heater rates from 0.1 to 100°C/min and a balance with a measurement range of 5g, complemented by various cream options for precise sample handling.

3. Various Applications of Nanoparticles

NPs exhibit a broad spectrum of applications spanning various fields such as electronics, optoelectronics, industry, energy, nanomedicine, environment and more, following detailed:

3.1. Applications of Nanoparticles in the Industry and Energy

NPs have become integral components in numerous industries, profoundly transforming both processes and products. Several pivotal industrial applications of NPs stand out, shaping the landscape of modern manufacturing and production. Some key examples of industrial applications of NPs include:

3.1.1. Application in petroleum field:

Magnetic NPs exhibit unique characteristics such as size-dependent chemical and physical properties, as well as responsiveness to magnetic fields, rendering them versatile assets for various applications in petroleum engineering. Zhou et al., investigated the burgeoning role of MNPs in diverse processes within the petroleum industry. One such application is in Drilling and Completion Improvement, where MNPs can be integrated into drilling fluids to enhance their rheological properties, thereby promoting improved wellbore stability and reduced fluid loss during drilling operations. Additionally, MNPs can facilitate selective plugging of undesirable formations during well completion processes. Moreover, Magnetic Separation emerges as another key area, where MNPs can be affixed to undesired components present in crude oil, such as asphaltenes, and subsequently separated using an external magnetic field. This facilitates the production of cleaner and more valuable crude oil. Furthermore, MNPs find utility in Reservoir Sensing and Imaging, wherein they can be introduced into reservoirs and monitored using magnetic resonance imaging (MRI) techniques to gain insights into fluid flow patterns and distribution within the reservoir. Lastly, MNPs play a role in Enhanced Oil Recovery (EOR) by serving as

targeted carriers for delivering specific chemicals, such as surfactants, to enhance oil recovery by mobilizing trapped oil within the reservoir [88]. Additionally, Borisov et al., was examined the potential of incorporating NPs into invert emulsion drilling fluids to enhance their efficacy during oil and gas well drilling operations. Traditional drilling fluids often encounter filtration challenges, leading to mud loss and potential instability of the wellbore. The study investigated the utilization of calcium-based NPs as additives in invert emulsion drilling fluids to address these issues. These NPs serve as fluid loss agents, thereby enhancing the filtration characteristics of the drilling fluid. Field trials were conducted to assess the performance of these drilling fluids, with CNP-based invert emulsion fluid utilized in a 20 cubic meter volume. A comparison with conventional fluids revealed a notable reduction in total mud losses, averaging approximately 27% with the CNP-based drilling fluid. This reduction aligns closely with the outcomes observed in laboratory experiments [89].

3.1.2. Applications in electronics:

In recent years, there has been a notable surge in interest surrounding the advancement of printed electronics, primarily due to their potential to offer alternatives to conventional silicon-based methods. Printed electronics present appealing prospects for low-cost, large-area electronic applications, particularly in the realm of flexible displays and sensors. The integration of NPs into functional inks, including metallic NPs, organic electronic molecules, carbon nanotubes (CNTs), and ceramic NPs, has positioned printed electronics as a promising avenue for mass production of novel electronic devices. This transition holds significant implications [90, 91]. Chaudhary, et Mehta, explored the potential application of selenium (Se) NPs in various technological fields. Such, Electronics, whereas components in transistors, solar cells, and light-emitting diodes (LEDs) due to their semiconducting properties. Also, Sensors, where Their unique properties make them suitable for developing sensors for detecting gases, biomolecules, and environmental pollutants [92]. Jiang et al. investigated a novel method for self-assembling monodisperse Ag NPs onto substrates using a volatile organic solvent, specifically chloroform, and a syringe pump to regulate the assembly rate. This approach capitalizes on the use of a volatile solvent, facilitating rapid solvent evaporation and accelerated assembly compared to slower drying techniques. The employment of a syringe pump allows precise control over the assembly rate, enhancing the surface morphology of the resulting coatings. Subsequent heat treatment under mild conditions (200 °C for

15 min) induces sintering of the NPs, leading to the formation of a conductive network with an average size of approximately 4.5 nm. The resulting Ag NP coatings demonstrate commendable electrical conductivity, ranging from 1 to 3 x 10^4 S cm^{-1}, making them suitable for a range of electronic applications. The study also highlights the potential utility of these conductive coatings in electronic components, serving as conductive thin films for electrodes and electrical interconnects. Moreover, the versatility of the method extends to flexible electronics, offering the possibility of generating conductive patterns on flexible substrates for applications in this domain [93].

3.1.3. Uses in pigments:

The NPs are increasingly being used in pigments, especially with recent advancements in synthesis methods that allow for the low-cost production of NPs TiO_2 and ZnO. These materials offer significant optical benefits in pigments due to their high refractive index, which enables strong optical effects and vibrant color depth. Furthermore, their wide energy bandgap makes them well-suited for use in inorganic UV-absorbing pigments, which have been widely adopted in polymers, consumer goods, and surface treatments. A notable advantage of NPs in this application is their ability to provide UV protection without significantly impacting visible light transmission, particularly when their size is below approximately 50 nm. This nearly transparent additive effectively protects surfaces from both UV damage and corrosion [94].

3.1.4. Application in carbon fillers in tires:

Carbon fillers have become integral components in the manufacturing of tires. The advent of industrially produced polymers in the early 20th century spurred a swift evolution in additives and fillers used in various applications. This led to significant enhancements in strength, abrasion resistance, particularly in tire manufacturing, and rheological properties. Consequently, there was a surge in the mass production of nanoparticulate carbon and chemically functionalized nano-carbon particles to meet the growing demands of the industry [94, 95].

3.1.5. Uses in solar cells' technology:

NPs are pivotal in augmenting the efficiency and functionality of solar cells, constituting a vital aspect of solar technology advancements. The primary functions of a solar cell entail the generation

of charge carriers through the absorption of light by a material and the subsequent separation of these carriers to conductive materials for transmitting electricity. The majority of these carriers are generated near the surface of the material. Upon the absorption of light by a semiconductor, electron-hole pairs are generated, significantly enhancing conductivity. To prevent their recombination, these pairs must reach the p-n junction where an electric field separates the charges. Metal oxide semiconductors have garnered attention due to their environmental friendliness, affordability, and high stability. In recent years, they have found applications in photovoltaic systems, serving as photoelectrodes in dye solar cells (DSCs) and contributing to the development of metal oxide p-n junctions. The remarkable flexibility and feasibility of these materials, coupled with their modest cost and scalability, render metal oxides highly promising in next-generation photovoltaics. With their broad bandgap energy range and tunability, various metal oxides show potential as effective photo-harvesters, only select metal oxides have been extensively investigated as photon absorbers. These oxides, when employed in photovoltaic applications, serve multiple purposes, including as light absorbers, transparent electrodes, transport layers, and specialized materials with unique properties and functionalities [96, 97]. Below are several significant applications of NPs in solar technology gleaned from the literature review conducted**,** Bubenhofer et al. proposed an innovative approach to synthesize PbS-TiO_2 heterojunction NPs in a single step, aiming at their potential utilization in solar cell technology. They introduced a one-step aerosol synthesis method employing reducing flame spray pyrolysis. This technique enables the simultaneous generation of PbS NPs affixed to the surface of TiO_2 NPs. The researchers suggested the plausible application of these NPs in solar cells, attributing their suitability to the combined attributes of light absorption and charge separation. Specifically, PbS NPs were noted for their efficient light absorption, while the heterojunction formed between PbS and TiO_2 was highlighted for its facilitation of charge separation, which is crucial for the effective operation of solar cells [98]. Additionally, Salehi et al., conducted a study to assess the potential application of aluminum nanofluid in the cooling of solar cells with the aim of enhancing their performance. As the operating temperature of solar cells rises, their efficiency typically decreases. In this study, the researchers investigated the efficacy of utilizing nanofluid, a liquid containing suspended NPs, as a coolant for solar cells, as opposed to conventional coolants such as water. Specifically, they focused on a nanofluid formulation comprising Al NPs dispersed within a base fluid, which is likely water or another coolant. The inclusion of Al NPs in the base fluid was found to augment its thermal

conductivity, thereby facilitating more effective heat dissipation from the solar cell. Comparative analysis revealed that solar cells cooled with Al nanofluid exhibited a notable enhancement in efficiency compared to those cooled with water [99].

3.1.6. Uses in batteries:

NPs contribute to enhancing the effectiveness and longevity of energy storage devices, including batteries and supercapacitors, by bolstering energy density and charging rates. Specifically, ZnO NPs exhibit promise in these areas [100]. Also, Sarkar et al. examined the potential of high-entropy oxides (HEOs) as an innovative material for reversible energy storage. With the increasing need for renewable energy sources, there's a demand for efficient and dependable energy storage solutions. HEOs stand out as a new material class with distinctive characteristics resulting from their composition, which includes multiple metallic elements in their crystal structure sach, (Co, Mg, Ni, Zn) O and (Co, Cu, Mg, Ni, Zn) O were directly synthesized in a nanocrystalline form. The study delved into the electrochemical properties of HEOs, indicating their suitability for energy storage applications. This research underscores the promise of HEOs as a viable material for future energy storage devices. Their distinct attributes and adaptability for specific purposes signify significant advancements in this critical field [96, 101].

3.2. Applications in the Medical Field:

Extensive research endeavors are dedicated to utilizing NPs for pharmaceutical and biomedical purposes, presenting a promising frontier in healthcare. Mellid-Carballal et al. investigated the potential of viral protein (ViP) NPs in pharmaceutical applications, examining available ViP NP products and ongoing research initiatives to expand their utility [102]. Meanwhile, Mun et al. explored silica NPs as effective drug carriers and diagnostic aids, addressing synthesis methods and potential applications while acknowledging associated challenges [103]. Ibrahim et al. categorized pharmaceutical NPs into distinct classes, emphasizing their diverse roles [104]. Zafar et al. delved into biosynthesized NPs' applications, particularly in drug delivery, pathogen detection, and tissue engineering [105]. Zhang et al. highlighted nanotechnology's significance in drug delivery and tissue engineering, contributing to innovative pharmaceutical products [106]. Aljabali et al. developed tailored solutions for selective drug delivery, employing NPs designed for targeted binding to receptors. Despite these advancements, ensuring NP biocompatibility and

safety remains paramount, requiring meticulous material selection [107]. Additionally, Dhir et al. conducted a comprehensive review of methods for synthesizing metal NPs and their pharmaceutical applications, encompassing recent patents to illustrate the field's rapid evolution [108].

3.3. Nanoparticles Environmental Applications :

NPs have been employed in both detecting and remedying environmental pollutants, including heavy metals and hazardous chemicals. And in wastewater treatment to effectively eliminate organic and inorganic contaminants.

3.3.1. Application of Nanoparticles in Contaminated Soil Remediation:

Karthick et al. provided insights into the mechanisms involved in removing petroleum oil contaminants from soil using chemical surfactant systems, which encompass surfactant solution, surfactant foam, and NP-stabilized surfactant foams [109]. Palansooriya et al., further examined laboratory-based research conducted over the past decade on similar systems for soil decontamination [110]. Additionally, Galdames et al. highlighted zero-valent iron as an effective remediation agent for environmental issues, particularly in soil and groundwater. They summarized the main types of zero-valent iron NPs and their remediation capacities, along with pilot and large-scale studies conducted on various nanomaterials for remediation purposes [111]. Moreover, Huang et al. developed ligand-coated dense NPs (Ligand DNPs) to sequester heavy metal ions deeper into soil and sediments, offering a promising in-situ remediation approach [111].

In another study, Han et al. focused on immobilizing 50 ppm arsenic using nanoscale zero-valent iron (nZVI) and sulfide-modified nanoscale zero-valent iron (SnZVI) in soil over a period of 168 days while assessing their effects on earthworm survival during remediation. They observed a significant reduction in leachable arsenic levels by 93% and 68% after 7 days of treatment with 0.3% nZVI and SnZVI, respectively. The efficacy of arsenic immobilization increased with higher NPs dosages and longer treatment durations. SnZVI demonstrated superior performance compared to nZVI when normalized by their respective surface areas. Utilizing an artificial neural network, the researchers successfully predicted the arsenic immobilization trend over time. Additionally, they found that the survival rate of earthworms decreased from 60% to 10% in untreated arsenic-contaminated soil treated with 0.3% nZVI but increased to 73% with 0.3% SnZVI treatment,

indicating a reduction in nZVI toxicity through sulfidation. Furthermore, both types of NPs mitigated the bioaccumulation of arsenic in E. fetida, suggesting their potential for sustainable soil arsenic remediation [112].

Moreover, Liu et al. discussed the stabilization mechanisms of NP-stabilized surfactant foams (NP-SF) and the factors influencing foam stability [113]. Additionally, Jehan et al. and He et al. evaluated the effectiveness of various materials, including parthenium weed biochar (PBC) and iron-doped ZnO NPs (Fe-ZnO), in adsorbing heavy metals and reducing their uptake by wheat in contaminated soil, demonstrating positive effects on metal immobilization and plant health [114, 115].

3.3.2. Application of Nanoparticles in wastewater treatment:

NPs play a crucial role in the realm of wastewater treatment, offering efficient means for water purification. These nanomaterials possess distinct attributes such as heightened reactivity, functionalization capabilities, a substantial specific surface area, and size-dependent properties, rendering them well-suited for addressing wastewater challenges [116]. The primary objectives of nanotechnology-driven water treatment methods encompass enhanced desalination of sea and brackish water, safe recycling of wastewater, water disinfection, and decontamination endeavors [117]. These pursuits entail the removal of pollutants via biosorption and nanoadsorption mechanisms, detection of contaminants through nanosensors, and the utilization of diverse membrane technologies like reverse osmosis, nanofiltration, photocatalysis, and among others [13, 118, 119]. Nanostructures exhibit unique optical, electrical, and magnetic characteristics compared to bulk materials, owing to their expansive surface area and elevated surface energy. This distinctiveness at the nanoscale imparts a wide array of potential applications in the field of wastewater treatment [13, 117]. The following delineates key applications of NPs in this context, as revealed by extant research findings:

a) Nano-sorbents and Adsorption Technology

Filtration stands as a fundamental step in both water purification and wastewater treatment processes, employing a filter media or membrane to separate solid particles from liquid. Nanofiltration (NF), a pressure-driven membrane separation method, is gaining prominence in these fields due to its unique charge-based repulsion property and high permeation rate, offering a more energy-efficient alternative. The membranes utilized in NF possess specific properties that

facilitate transport through the solution diffusion mechanism, aided by size exclusion characteristics. Furthermore, certain NF membranes feature a fixed surface charge that selectively binds contaminants in the liquid, effectively rejecting solutes due to their small pore sizes. Notably, NF membranes permit the passage of monovalent ions while retaining multivalent ions, a process critical for water softening. The rejection mechanisms in NF vary, with size exclusion predominating for uncharged species, while ionic species are rejected through both size exclusion and electrostatic interaction [120-122]. This water softening process using NF is depicted in Figure I-2.

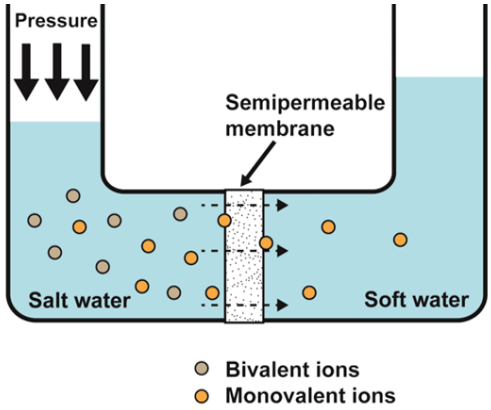

Figure I.4: Schematic depiction of the nanofiltration process for water softening [120].

Additionally, Adsorption stands out as a prominent method for the removal of heavy metals from wastewater. This process involves the accumulation of liquid solute, known as the adsorbate, onto the surface of a solid material, termed the adsorbent, thereby forming a thin atomic or molecular film. Various absorbents have undergone extensive study for their efficacy in treating heavy metals from wastewater, with commonly utilized ones including zeolites, clay minerals, and activated carbons[123]. The application of nanotechnology in adsorption processes has gained traction due to its efficiency in wastewater treatment, attributed to the large surface area and operational flexibility offered by NPs. Moreover, the reversible nature of NPs renders them particularly promising for wastewater treatment as they can be regenerated. Adsorption offers numerous advantages such as high efficiency, ease of operation, and minimal maintenance requirements. Nano-sized metal oxides, notably manganese oxides, cerium oxides (CeO_2), titanium oxides, aluminum oxides, magnesium oxides, and ferric oxides, have shown considerable potential for heavy metal removal in aqueous systems [124]. The synthesis techniques for these adsorbents have advanced over time, with the emergence of more innovative and cost-effective methods. The mechanism underlying heavy metal removal by adsorbents is often likened to that of Lewis acids

and bases. Furthermore, nano-absorbents are noted for their high specific sorption capacity, attributable to the abundance of sorption sites at their surface [117, 125].

b) Nanotechnology Disinfection

Nanotechnology offers a promising avenue for disinfecting wastewater, leveraging the unique properties of NPs to effectively target a broad spectrum of contaminants, including pathogenic bacteria. Compared to traditional disinfectants, NPs present advantages such as minimal production of toxic by-products. The antibacterial mechanism of Ag NPs involves the generation of reactive oxygen species (ROS), along with interactions with cell surface structures and macromolecules. Notably, Ag NPs exhibit effectiveness against both gram-positive and gram-negative bacteria. Recent research explores synergistic approaches, such as combining Ag NPs with magnetic counterparts, to enhance disinfection efficacy and facilitate recovery processes. Magnetic NPs, exemplified by magnetite, contribute to microbial disinfection through ROS release and ion adsorption mechanisms, facilitated by their inherent magnetic properties. Moreover, their magnetic nature enables easy separation from aqueous solutions, enhancing their applicability in wastewater treatment [126]. Ag NPs, renowned for their high specific surface area and potent antimicrobial attributes, stand out as a particularly promising option for wastewater disinfection. Despite their efficacy, the release of Ag NPs into the environment raises concerns regarding their impact on indigenous microbial populations [127], where, Sengupta et al. conducted research centered on the synthesis of Ag NPs utilizing extracts from neem leaves and banana peels. They explored the application of these NPs as antimicrobial agents for degrading contaminants in wastewater treatment processes [128].

c) Photocatalysis

Photocatalysis technology has attracted considerable attention for its potential in treating water contaminated with hazardous aromatic compounds. Semiconductors such as TiO_2 and ZnO are widely employed as photocatalysts, with ZnO gaining prominence in recent years. In photocatalysis, incident light energizes electrons (e^-) in semiconductor materials, prompting them to transition to a conduction band while creating positively charged holes (h^+) in the valence band. This occurs when the energy of incident photons matches or exceeds the band gap energy. Subsequently, the electron migrates to the surface, where they participate in reduction and oxidation reactions crucial for altering the valence states of various contaminants [129-131]. However, a drawback of photocatalysis lies in the high-energy input required due to the wide band

energy gap. Consequently, there is growing interest in developing photocatalysts with more suitable and efficient band gaps. Recent research has explored catalysts such as bio-based catalysts, C_3N_4, and ZnO, which have demonstrated promising band energy gaps. Additionally, magnetic NPs have emerged as popular alternatives, exhibiting enhanced photocatalytic capabilities, where the various materials, including Fe_2O_3/Fe_3O_4, pure metals like Fe and Co, and spinel-type ferromagnets such as $MgFe_2O_4$, $MnFe_2O_4$, and $CoFe_2O_4$, can be employed in synthesizing magnetic NPs for photocatalytic applications [132].

Moreover, Sengupta et al. proposed an environmentally friendly and cost-effective method for synthesizing Ag NPs and explored their potential application in eliminating hazardous dyes from wastewater [128]. As the utilization of nanotechnology in wastewater treatment aims to decrease expenses, there has been a rise in research endeavors focusing on sustainable NP production methods. Several studies have indicated that the recycling of NPs could offer cost reductions compared to using newly synthesized NPs. Mpongwana et al., assessed the economic implications of these recent advancements in nanotechnology for wastewater treatment [124]. Recently, in our research, described in the experimental section, we investigated the photocatalytic properties of ZnO NPs produced using the gliding arc plasma method. Our findings demonstrate a notable efficacy in degrading both cationic and anionic pollutants in aqueous settings. This discovery paves the way for a novel approach to synthesizing photocatalysts based on metal oxides that are efficient, rapid, and cost-effective for decomposing organic pollutants [13].

Conclusion:

NPs represent a cutting-edge area of research with vast potential for societal advancement in fields such as medicine, energy, the environment, information technology, and aerospace science. The synthesis methods discussed, including physical, chemical, and bio-assisted approaches, offer diverse ways to produce NPs with tailored properties. Notably, cold plasma synthesis emerges as a promising approach due to its low-temperature operation, energy efficiency, and environmental compatibility. Consequently, this method yields high-quality NPs with a relatively straightforward setup. Characterization techniques like transmission electron microscopy (TEM) and scanning electron microscopy (SEM) play pivotal roles in analyzing the structure and composition of NPs. The applications of NPs in nanomedicine, water filtration, and materials science underscore their versatility and impact across various sectors. As nanotechnology continues to evolve, NPs are

poised to drive innovation, revolutionize technologies, and open new frontiers in scientific exploration.

Additionally, it is important to note that the field of nanotechnology is still in its early stages of development. There is still much that we do not know about NPs, including their long-term health and environmental effects. Further research is needed to address these concerns and to develop new and innovative applications for NPs.

References of Chapter I

1. Dhand, C., et al., Methods and strategies for the synthesis of diverse nanoparticles and their applications: a comprehensive overview. Rsc Advances, 2015. 5(127): p. 105003-105037.
2. Youssef, F.S., et al., Green synthesis and Biomedical Applications of Zinc Oxide Nanoparticles. Review. Egyptian Journal of Veterinary Sciences, 2024. 55(1): p. 287-311.
3. Khan, M.A., et al., Interface study of hybrid CuO nanoparticles embedded ZnO nanowires heterojunction synthesized by controlled vapor deposition approach for optoelectronic devices. Optical Materials, 2021. 117: p. 111132.
4. Anugrahwidya, R., N. Yudasari, and D. Tahir, Optical and structural investigation of synthesis ZnO/Ag Nanoparticles prepared by laser ablation in liquid. Materials science in semiconductor processing, 2020. 105: p. 104712.
5. Ristić, M., et al., Sol–gel synthesis and characterization of nanocrystalline ZnO powders. 2005. 397(1-2): p. L1-L4.
6. Lee, S.D., et al., Synthesis and photocatalytic property of ZnO nanoparticles prepared by spray-pyrolysis method. 2012. 32: p. 320-326.
7. Atchudan, R., et al., Facile synthesis of zinc oxide nanoparticles decorated graphene oxide composite via simple solvothermal route and their photocatalytic activity on methylene blue degradation. Journal of Photochemistry and Photobiology B: Biology, 2016. 162: p. 500-510.
8. Ni, Y.-h., et al., Hydrothermal preparation and optical properties of ZnO nanorods. Materials Science and Engineering: B, 2005. 121(1-2): p. 42-47.
9. Matinise, N., et al., ZnO nanoparticles via Moringa oleifera green synthesis: Physical properties & mechanism of formation. Applied Surface Science, 2017. 406: p. 339-347.
10. Vidya, C., et al., Hazard free green synthesis of ZnO nano-photo-catalyst using Artocarpus Heterophyllus leaf extract for the degradation of Congo red dye in water treatment applications. Journal of environmental chemical engineering, 2017. 5(4): p. 3172-3180.
11. PJ, J.C., et al., Overview on toxicity of nanoparticles, it's mechanism, models used in toxicity studies and disposal methods–A review. Biocatalysis and Agricultural Biotechnology, 2021. 36: p. 102117.
12. Ali, S., et al., Nanomaterials synthesis by next-generation plasma technology, in Plasma at the Nanoscale. 2022, Elsevier. p. 373-385.
13. Messai, R., et al., GAD Plasma-Assisted Synthesis of ZnO Nanoparticles and Their Photocatalytic Activity. Materials Research Express, 2024.

14. Smaoui, S., et al., Zinc oxide nanoparticles in meat packaging: A systematic review of recent literature. Food Packaging and Shelf Life, 2023. 36: p. 101045.
15. Vyas, S., et al., Comparative study of As-deposited ZnO thin films by thermal evaporation, pulsed laser deposition and RF sputtering methods for electronic and optoelectronic applications. Journal of Electronic Materials, 2015. 44: p. 3401-3407.
16. Bouchat, V., et al., On some applications of nanoparticles synthesized in the gas phase by magnetron discharges. 2013.
17. Veith, G.M., et al., Magnetron sputtering of gold nanoparticles onto WO3 and activated carbon. Catalysis today, 2007. 122(3-4): p. 248-253.
18. Hatakeyama, Y., K. Onishi, and K. Nishikawa, Effects of sputtering conditions on formation of gold nanoparticles in sputter deposition technique. RSC advances, 2011. 1(9): p. 1815-1821.
19. Gaffet, E., et al., Some recent developments in mechanical activation and mechanosynthesis. Journal of materials chemistry, 1999. 9(1): p. 305-314.
20. Calka, A. and D. Wexler, Mechanical milling assisted by electrical discharge. Nature, 2002. 419(6903): p. 147-151.
21. Suñol, J.-J. and L. Escoda, Novel Materials Synthesis by Mechanical Alloying/Milling. 2022, MDPI. p. 6973.
22. Palaniandy, S. and N.H. Jamil, Influence of milling conditions on the mechanochemical synthesis of CaTiO3 nanoparticles. Journal of Alloys and Compounds, 2009. 476(1-2): p. 894-902.
23. Şimşek, T., et al., Band gap engineering of ZnO nanocrystallites prepared via ball-milling. Politeknik Dergisi, 2020. 25(1): p. 89-94.
24. Singh, J., et al., Influence of different milling media on structural, morphological and optical properties of the ZnO nanoparticles synthesized by ball milling process. Materials Science in Semiconductor Processing, 2019. 98: p. 29-38.
25. Kuppusamy, P., et al., Biosynthesis of metallic nanoparticles using plant derivatives and their new avenues in pharmacological applications–An updated report. Saudi Pharmaceutical Journal, 2016. 24(4): p. 473-484.
26. Akhtar, M.S., J. Panwar, and Y.-S. Yun, Biogenic synthesis of metallic nanoparticles by plant extracts. ACS Sustainable Chemistry & Engineering, 2013. 1(6): p. 591-602.
27. Patil, J., et al., Formulation and Evaluation of Verdant Tablets Containing Saponin-Coalesced Silver Nanoparticles Got from Fenugreek Seed Extract. Chemistry Proceedings, 2021. 8(1): p. 56.
28. Kumar, H., et al., Fruit extract mediated green synthesis of metallic nanoparticles: A new avenue in pomology applications. International journal of molecular sciences, 2020. 21(22): p. 8458.
29. Thi, T.U.D., et al., Green synthesis of ZnO nanoparticles using orange fruit peel extract for antibacterial activities. RSC advances, 2020. 10(40): p. 23899-23907.
30. Ismail, S.M.M., et al., Characterization of green synthesized of ZnO nanoparticles by using pinus brutia leaves extracts. Journal of Molecular Structure, 2023. 1280: p. 135063.
31. MESSAI, R., H. BELLAHOUEL, and S.E. DERKOUCHE, Synthèse verte des nanoparticules de ZnO par l'extrait des feuilles de phœnix dactylifera. l. 2020.
32. Kobylinska, N., et al., 'Hairy'root extracts as source for 'green'synthesis of silver nanoparticles and medical applications. RSC advances, 2020. 10(65): p. 39434-39446.
33. Al-Radadi, N.S., Facile one-step green synthesis of gold nanoparticles (AuNp) using licorice root extract: Antimicrobial and anticancer study against HepG2 cell line. Arabian Journal of Chemistry, 2021. 14(2): p. 102956.

34. Noruzi, M., et al., Rapid green synthesis of gold nanoparticles using Rosa hybrida petal extract at room temperature. Spectrochimica Acta Part A: Molecular and Biomolecular Spectroscopy, 2011. 79(5): p. 1461-1465.
35. Munir, H., et al., Plant-mediated green synthesis of nanoparticles, in Advances in green synthesis: Avenues and sustainability. 2021, Springer. p. 75-89.
36. Van Giau, V., S.S.A. An, and J. Hulme, Recent advances in the treatment of pathogenic infections using antibiotics and nano-drug delivery vehicles. Drug design, development and therapy, 2019: p. 327-343.
37. Torres-Chavolla, E., R.J. Ranasinghe, and E.C. Alocilja, Characterization and functionalization of biogenic gold nanoparticles for biosensing enhancement. IEEE transactions on nanotechnology, 2010. 9(5): p. 533-538.
38. Chauhan, A., et al., Fungus-mediated biological synthesis of gold nanoparticles: potential in detection of liver cancer. International journal of nanomedicine, 2011: p. 2305-2319.
39. Durán, N., G. Nakazato, and A.B. Seabra, Antimicrobial activity of biogenic silver nanoparticles, and silver chloride nanoparticles: an overview and comments. Applied microbiology and biotechnology, 2016. 100: p. 6555-6570.
40. Guilger-Casagrande, M. and R.d. Lima, Synthesis of silver nanoparticles mediated by fungi: a review. Frontiers in bioengineering and biotechnology, 2019. 7: p. 287.
41. Goswami, N., R. Saha, and S.K. Pal, Protein-assisted synthesis route of metal nanoparticles: exploration of key chemistry of the biomolecule. Journal of Nanoparticle Research, 2011. 13: p. 5485-5495.
42. Pérez-Page, M., et al., Template-based syntheses for shape controlled nanostructures. Advances in colloid and interface science, 2016. 234: p. 51-79.
43. Gaur, J., et al., Current trends: Zinc oxide nanoparticles preparation via chemical and green method for the photocatalytic degradation of various organic dyes. Hybrid Advances, 2023: p. 100128.
44. Zhang, Z.-B., et al., Nanonization of megestrol acetate by liquid precipitation. Industrial & engineering chemistry research, 2009. 48(18): p. 8493-8499.
45. Bayal, N. and P. Jeevanandam, Synthesis of CuO@ NiO core-shell nanoparticles by homogeneous precipitation method. Journal of alloys and compounds, 2012. 537: p. 232-241.
46. Nazari, M., et al., Synthesis and characterization of maghemite nanopowders by chemical precipitation method. Journal of Nanostructure in Chemistry, 2014. 4: p. 1-5.
47. Souza, R.C.d., et al., Antibacterial activity of zinc oxide nanoparticles synthesized by solochemical process. Brazilian Journal of Chemical Engineering, 2019. 36: p. 885-893.
48. Nayar, P., et al., Comparative study of phase transformation of Al2O3 nanoparticles prepared by chemical precipitation and sol-gel auto combustion methods. Materials Today: Proceedings, 2020. 26: p. 122-125.
49. Eskandari, M.J. and I. Hasanzadeh, Size-controlled synthesis of Fe3O4 magnetic nanoparticles via an alternating magnetic field and ultrasonic-assisted chemical co-precipitation. Materials Science and Engineering: B, 2021. 266: p. 115050.
50. Jain, M., M. Yadav, and S. Chaudhry, Copper oxide nanoparticles for the removal of divalent nickel ions from aqueous solution. Toxin Reviews, 2021. 40(4): p. 872-885.
51. Thakur, S., S. Neogi, and A.K. Ray, Morphology-controlled synthesis of ZnO nanostructures for caffeine degradation and Escherichia coli inactivation in water. Catalysts, 2021. 11(1): p. 63.

52. Jamkhande, P.G., et al., Metal nanoparticles synthesis: An overview on methods of preparation, advantages and disadvantages, and applications. Journal of drug delivery science and technology, 2019. 53: p. 101174.
53. Mitra, A. and G. De, Sol-gel synthesis of metal nanoparticle incorporated oxide films on glass, in Glass Nanocomposites. 2016, Elsevier. p. 145-163.
54. Vishwakarma, A. and S.P. Singh, Synthesis of zinc oxide nanoparticle by sol-gel method and study its characterization. Int J Res Appl Sci Eng Technol, 2020. 8(4): p. 1625-7.
55. Parashar, M., V.K. Shukla, and R. Singh, Metal oxides nanoparticles via sol–gel method: a review on synthesis, characterization and applications. Journal of Materials Science: Materials in Electronics, 2020. 31: p. 3729-3749.
56. Arya, S., et al., influence of processing parameters to control morphology and optical properties of Sol-Gel synthesized ZnO nanoparticles. ECS Journal of Solid State Science and Technology, 2021. 10(2): p. 023002.
57. Ismail, A., et al., The influence of calcination temperature on structural and antimicrobial characteristics of zinc oxide nanoparticles synthesized by Sol–Gel method. Journal of Molecular Structure, 2019. 1196: p. 332-337.
58. Seong, G. and J.C. Rendón-Angeles, Hydrothermal Synthesis of Nanoparticles. 2023, MDPI-Multidisciplinary Digital Publishing Institute.
59. Alam, M.S., et al., Forced convective heat transfer coefficient measurement of low concentration nanorods ZnO–ethylene glycol nanofluids in laminar flow. Nanomaterials, 2022. 12(9): p. 1568.
60. Watanabe, A., et al., Fabrication of liquid scintillators loaded with 6-phenylhexanoic acid-modified ZrO2 nanoparticles for observation of neutrinoless double beta decay. Nanomaterials, 2021. 11(5): p. 1124.
61. Chen, D., X. Jiao, and G. Cheng, Hydrothermal synthesis of zinc oxide powders with different morphologies. Solid State Communications, 1999. 113(6): p. 363-366.
62. Baruwati, B., D.K. Kumar, and S.V. Manorama, Hydrothermal synthesis of highly crystalline ZnO nanoparticles: a competitive sensor for LPG and EtOH. Sensors and Actuators B: Chemical, 2006. 119(2): p. 676-682.
63. Kaur, A., et al., Supported bimetallic nanoparticles as anode catalysts for direct methanol fuel cells: A review. International Journal of Hydrogen Energy, 2021. 46(29): p. 15820-15849.
64. Ali, S., et al., Noble metals based bimetallic and trimetallic nanoparticles: controlled synthesis, antimicrobial and anticancer applications. Critical Reviews in Analytical Chemistry, 2021. 51(5): p. 454-481.
65. Nyabadza, A., et al., A review of physical, chemical and biological synthesis methods of bimetallic nanoparticles and applications in sensing, water treatment, biomedicine, catalysis and hydrogen storage. Advances in Colloid and Interface Science, 2023: p. 103010.
66. Muralidharan, G., et al., Cladding alloys for fluoride salt compatibility final report. Oak Ridge National Laboratory: Oak Ridge, TN, USA, 2011.
67. Tavakoli, A., M. Sohrabi, and A. Kargari, A review of methods for synthesis of nanostructured metals with emphasis on iron compounds. chemical papers, 2007. 61(3): p. 151-170.
68. Sharma, G., et al., Novel development of nanoparticles to bimetallic nanoparticles and their composites: A review. Journal of King Saud University-Science, 2019. 31(2): p. 257-269.
69. Kaushik, N.K., et al., Plasma and nanomaterials: Fabrication and biomedical applications. Nanomaterials, 2019. 9(1): p. 98.

70. Bounedjar, N., et al., Non thermal plasma synthesis of ZnO nanoparticles and their corrosion inhibition activity on XC70 mild steel pipeline in 1 M HCl acidic medium. Materials Chemistry and Physics, 2024. 311: p. 128555.
71. Fritzsche, H. and J.J.P.P. Tauc, New York,) p, Amorphous and liquid semiconductors. 1974. 254.
72. Christov, C., Biomolecular spectroscopy: advances from integrating experiments and theory. 2013.
73. Langford, J.I. and A. Wilson, Scherrer after sixty years: a survey and some new results in the determination of crystallite size. Journal of applied crystallography, 1978. 11(2): p. 102-113.
74. Benyamina, I., et al., New Bi2O3-ZnO composite deposited on glass wool. Effect of the synthesis method on photocatalytic efficiency under visible light. Applied Surface Science, 2019. 483: p. 859-869.
75. Saravanakkumar, D., et al., Synthesis and characterization of CuO/ZnO/CNTs thin films on copper substrate and its photocatalytic applications. OpenNano, 2019. 4: p. 100025.
76. Batool, S., et al., Green synthesized ZnO-Fe2O3-Co3O4 nanocomposite for antioxidant, microbial disinfection and degradation of pollutants from wastewater. Biochemical Systematics and Ecology, 2022. 105: p. 104535.
77. Kumar, G.A., M.R. Reddy, and K.N. Reddy. Structural and Optical properties of ZnO thin films grown on various substrates by RF magnetron sputtering. in IOP Conference Series: Materials Science and Engineering. 2015. IOP Publishing.
78. Godavarti, U., V. Mote, and M. Dasari, Role of cobalt doping on the electrical conductivity of ZnO nanoparticles. Journal of Asian Ceramic Societies, 2017. 5(4): p. 391-396.
79. Chithra, M.J., K. Pushpanathan, and M. Loganathan, Structural and optical properties of Co-doped ZnO nanoparticles synthesized by precipitation method. Materials and Manufacturing Processes, 2014. 29(7): p. 771-779.
80. Majeed, M.H., et al., Influence of annealing process on structural, optical and electronic properties of nano-structured ZnO films synthesized by hydrothermal technique: Supported by DFT study. Materials Science and Engineering: B, 2022. 282: p. 115793.
81. Ferreira, N.S., et al., Visible-light-responsive photocatalytic activity significantly enhanced by active [V Zn+ VO+] defects in self-assembled ZnO nanoparticles. Inorganic Chemistry, 2021. 60(7): p. 4475-4496.
82. Dodd, A., et al., Effect of particle size on the photocatalytic activity of nanoparticulate zinc oxide. Journal of Nanoparticle Research, 2006. 8: p. 43-51.
83. Kusiak-Nejman, E., et al., Size-dependent effects of ZnO nanoparticles on the photocatalytic degradation of phenol in a water solution. Applied Surface Science, 2021. 541: p. 148416.
84. Giamello, E., M. Chiesa, and M.C. Paganini, Point defects in electron paramagnetic resonance. Defects at Oxide Surfaces, 2015: p. 303-326.
85. Gunkel, F., et al., Oxygen vacancies: The (in) visible friend of oxide electronics. Applied physics letters, 2020. 116(12).
86. Hassaan, M.A., et al., Principles of photocatalysts and their different applications: a review. Topics in Current Chemistry, 2023. 381(6): p. 31.
87. Callister, W.D., et al., Materials science and engineering: an introduction. Vol. 7. 2007: John wiley & sons New York.
88. Zhou, K., et al., Application of magnetic nanoparticles in petroleum industry: A review. Journal of Petroleum Science and Engineering, 2020. 188: p. 106943.

89. Borisov, A.S., M. Husein, and G. Hareland, A field application of nanoparticle-based invert emulsion drilling fluids. Journal of Nanoparticle Research, 2015. 17: p. 1-13.
90. Kosmala, A., et al., Synthesis of silver nano particles and fabrication of aqueous Ag inks for inkjet printing. Materials Chemistry and Physics, 2011. 129(3): p. 1075-1080.
91. Khan, I., K. Saeed, and I. Khan, Nanoparticles: Properties, applications and toxicities. Arabian journal of chemistry, 2019. 12(7): p. 908-931.
92. Chaudhary, S. and S. Mehta, Selenium nanomaterials: applications in electronics, catalysis and sensors. Journal of nanoscience and nanotechnology, 2014. 14(2): p. 1658-1674.
93. Jiang, C., L. Li, and P.W. Pong, Controlled convective self-assembly of silver nanoparticles in volatile organic solvent and its application in electronics. RSC advances, 2015. 5(120): p. 98747-98756.
94. Stark, W.J., et al., Industrial applications of nanoparticles. Chemical Society Reviews, 2015. 44(16): p. 5793-5805.
95. Felix, D.G. and G. SivaKumar, Nano particles in automobile tires. IOSR J. Mech. Civ. Eng, 2014. 11: p. 7-11.
96. Chavali, M.S. and M.P. Nikolova, Metal oxide nanoparticles and their applications in nanotechnology. SN applied sciences, 2019. 1(6): p. 607.
97. Jose, R., V. Thavasi, and S. Ramakrishna, Metal oxides for dye-sensitized solar cells. Journal of the American Ceramic Society, 2009. 92(2): p. 289-301.
98. Bubenhofer, S.B., et al., Large-scale synthesis of PbS–TiO2 heterojunction nanoparticles in a single step for solar cell application. The Journal of Physical Chemistry C, 2012. 116(30): p. 16264-16270.
99. Salehi, R., et al., Study on the performance of solar cells cooled with heatsink and nanofluid added with aluminum nanoparticle. International Journal of Thermofluids, 2023. 20: p. 100445.
100. Singh, R., et al., AC Pandey Biological approach of zinc oxide nanoparticles formation and its characterization., 2011, 2. DOI: https://doi. org/10.5185/amlett. indias. 204: p. 313-317.
101. Sarkar, A., et al., High entropy oxides for reversible energy storage. Nature communications, 2018. 9(1): p. 3400.
102. Mellid-Carballal, R., et al., Viral protein-based nanoparticles (part 2): Pharmaceutical applications. European Journal of Pharmaceutical Sciences, 2023: p. 106558.
103. Mun, E. and B. Zhaisanbayeva, Silica Nanoparticles for Biomedical Application: Challenges and Opportunities. Eurasian Journal of Applied Biotechnology, 2020(1).
104. Ibrahim, M.A. and A.A. Abdellatif, Applications of nanopharmaceuticals in delivery and targeting. Nanopharmaceuticals: Principles and Applications Vol. 1, 2021: p. 73-114.
105. Zafar, N., et al., Pharmaceutical and biomedical applications of green synthesized metal and metal oxide nanoparticles. Current Pharmaceutical Design, 2020. 26(45): p. 5844-5865.
106. Zhang, D., et al., Green synthesis of metallic nanoparticles and their potential applications to treat cancer. Frontiers in chemistry, 2020. 8.
107. Aljabali, A.A. and M.A. Obeid, Inorganic-organic nanomaterials for therapeutics and molecular imaging applications. Nanoscience & Nanotechnology-Asia, 2020. 10(6): p. 748-765.
108. Dhir, S., et al., An Overview of Metallic Nanoparticles: Classification, Synthesis, Applications, and their Patents. Recent Patents on Nanotechnology, 2023.
109. Karthick, A., B. Roy, and P. Chattopadhyay, A review on the application of chemical surfactant and surfactant foam for remediation of petroleum oil contaminated soil. Journal of environmental management, 2019. 243: p. 187-205.

110. Palansooriya, K.N., et al., Soil amendments for immobilization of potentially toxic elements in contaminated soils: A critical review. Environment international, 2020. 134: p. 105046.
111. Galdames, A., et al., Zero-valent iron nanoparticles for soil and groundwater remediation. International Journal of Environmental Research and Public Health, 2020. 17(16): p. 5817.
112. Han, Z., et al., Emerging investigator series: immobilization of arsenic in soil by nanoscale zerovalent iron: role of sulfidation and application of machine learning. Environmental Science: Nano, 2021. 8(3): p. 619-633.
113. Liu, J., et al., Applications of functional nanoparticle–stabilized surfactant foam in petroleum-contaminated soil remediation. Journal of Hazardous Materials, 2023. 443: p. 130267.
114. Jehan, S., et al., Comparative efficacy of Parthenium hysterophorus (L.) derived biochar and iron doped zinc oxide nanoparticle on heavy metals (HMs) mobility and its uptake by Triticum aestivum (L.) in chromite mining contaminated soils. International Journal of Phytoremediation, 2023. 25(14): p. 1890-1900.
115. He, L., et al., Remediation of heavy metal contaminated soils by biochar: Mechanisms, potential risks and applications in China. Environmental pollution, 2019. 252: p. 846-855.
116. Thangavelu, L. and G.R. Veeraragavan, A survey on nanotechnology-based bioremediation of wastewater. Bioinorganic chemistry and applications, 2022. 2022.
117. Rathod, S., et al., Exploring synthesis and applications of green nanoparticles and the role of nanotechnology in wastewater treatment. Biotechnology Reports, 2024: p. e00830.
118. Kumar, S., et al., Nanotechnology-based water treatment strategies. Journal of nanoscience and nanotechnology, 2014. 14(2): p. 1838-1858.
119. Kim, M., et al., Green-synthesis of anisotropic peptone-silver nanoparticles and its potential application as anti-bacterial agent. Polymers, 2019. 11(2): p. 271.
120. Bora, T. and J. Dutta, Applications of nanotechnology in wastewater treatment—a review. Journal of nanoscience and nanotechnology, 2014. 14(1): p. 613-626.
121. Bellona, C., et al., Comparing nanofiltration and reverse osmosis for drinking water augmentation. Journal-American Water Works Association, 2008. 100(9): p. 102-116.
122. Yangali-Quintanilla, V., et al., Proposing nanofiltration as acceptable barrier for organic contaminants in water reuse. Journal of Membrane Science, 2010. 362(1-2): p. 334-345.
123. Burakov, A.E., et al., Adsorption of heavy metals on conventional and nanostructured materials for wastewater treatment purposes: A review. Ecotoxicology and environmental safety, 2018. 148: p. 702-712.
124. Mpongwana, N. and S. Rathilal, A review of the techno-economic feasibility of nanoparticle application for wastewater treatment. Water, 2022. 14(10): p. 1550.
125. Muharrem, I. and O.K. Ince, An overview of adsorption technique for heavy metal removal from water/wastewater: a critical review. International Journal of Pure and Applied Sciences, 2017. 3(2): p. 10-19.
126. Najafpoor, A., et al., Effect of magnetic nanoparticles and silver-loaded magnetic nanoparticles on advanced wastewater treatment and disinfection. Journal of Molecular Liquids, 2020. 303: p. 112640.
127. Amini, Z.P., Using nanomembrane to heavy metal removal from wastewater: A mini-review. Advances in Applied NanoBio-Technologies, 2022. 3(1): p. 7-13.

128. Sengupta, A. and A. Sarkar, Synthesis and characterization of nanoparticles from neem leaves and banana peels: a green prospect for dye degradation in wastewater. Ecotoxicology, 2022. 31(4): p. 537-548.
129. Gao, X. and X. Meng, Photocatalysis for heavy metal treatment: A review. Processes, 2021. 9(10): p. 1729.
130. Sharma, R. Nanotechnology: an approach for water purification-review. in IOP Conference Series: Materials Science and Engineering. 2021. IOP Publishing.
131. Simeonidis, K., et al., Implementing nanoparticles for competitive drinking water purification. Environmental Chemistry Letters, 2019. 17: p. 705-719.
132. Simonsen, G., M. Strand, and G. Øye, Potential applications of magnetic nanoparticles within separation in the petroleum industry. Journal of Petroleum Science and Engineering, 2018. 165: p. 488-495.

Chapter II

Overview of cold plasma: Definition, Chemical species generated and Applications

Chapter II: Overview of cold plasma

Definition, Chemical species generated and Applications

In 1879, William Crookes laid the groundwork for plasma science by conducting experiments that involved ionizing gas within an electrical discharge tube using high voltage applied through a voltage coil. This ionized gas, which he termed "radiant matter," formed the basis of early understanding in the field. Nearly fifty years later, in 1927 [1], Irvin Langmuir introduced the term "plasma," marking a significant development in the terminology and conceptualization of this phenomenon [2].

In the 1950s and 1960s, cold plasma was used in the development of new types of lasers and plasma displays. In the 1970s, cold plasma was used to develop new methods for etching and depositing thin films. In the 1980s, cold plasma was used to develop new methods for surface modification and cleaning [3].

In the 1990s, cold plasma began to be used for a variety of medical applications, including wound healing, cancer treatment, and blood coagulation. In the 2000s, cold plasma was used to develop new methods for NPs synthesis, and air and water purification. Today, cold plasma is used in a wide variety of applications [4].

This chapter provides a comprehensive exploration of cold plasma, a unique state of matter with diverse applications across various industries. It begins by defining plasma as a neutral ionized gas composed of positive ions, electrons, and neutral particles, highlighting its significance as a fundamental state of matter alongside solids, liquids, and gases. The chapter elucidates the transition from gas to plasma, emphasizing the ionization process that leads to the formation of free electrons and positive ions. Furthermore, it distinguishes between hot thermal plasma, generated at high temperatures, and cold plasma, which operates at significantly lower temperatures through methods like dielectric barrier discharge (DBD), GAD plasma and jet plasma. The discussion extends to the chemical species generated within cold plasma, emphasizing their role in electrochemical reactions and the impact of different operating gases on material properties. Moreover, it discusses the numerous applications of plasma in domains such as medicine, environmental protection, food Industry, material science and energy. Overall, the chapter sets the

stage for a detailed exploration of the characteristics and applications of cold plasma technology. Understanding the plasma, characteristics, and applications is crucial for realizing their full potential across multiple fields.

1. Definition of Plasma

Matter exists in four primary states: solid, liquid, gas, and plasma. As energy applied to atoms increases, the thermal motion within solids intensifies, overcoming interactions like ionic bonds and transitioning to liquids. Likewise, liquid atoms absorb sufficient energy to surpass surrounding forces, transforming into gas atoms. The translational energy of gas atoms is notably higher than that of liquids and solids. With increased energy, electrons overcome electrostatic potential barriers, leading to ionization-producing free electrons and positive ions. Plasma, a neutral ionized gas, comprises positive ions, electrons, and neutral particles, forming a substantial part of the observable mass in the universe. Plasma occurs naturally in phenomena like lightning or can be artificially induced by subjecting gas to a strong electrical field. It is categorized into two types: hot thermal plasma, generated at high temperatures, and cold plasma [5, 6].

Hot thermal plasma, typically reaching thousands of degrees Celsius, is produced through methods like electric arcs or lasers. It is applied in welding, cutting, surface treatment, and material production, including ceramics and refractory metals [5].

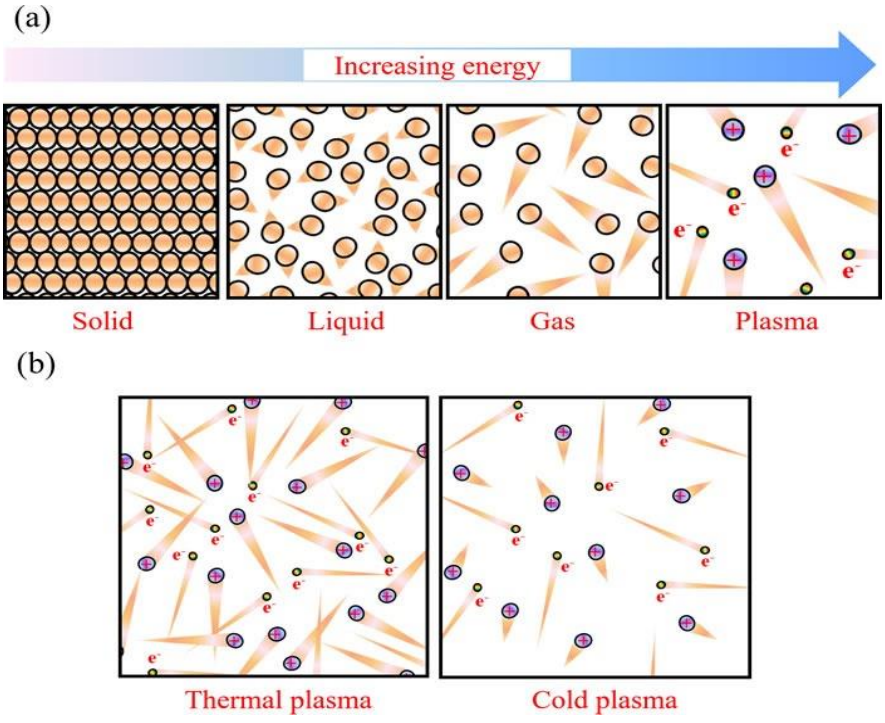

Figure II.1: Physical Description of Plasmas.

(a) Schematic representation showing the four fundamental states of matter. The triangular tails indicate the intensity of thermal motion in the particles. (b) Diagrammatic illustration of thermal plasma and cold plasma. Brown spheres represent neutral atoms, violet spheres represent positively charged ions, and iridescent spheres represent electrons [6].

Conversely, cold or NTP is created at temperatures much lower than the gas's thermal equilibrium. Various methods achieve this, such as high-frequency electric fields, microwaves, or lasers, taking different forms like DBD, jet plasma (JP) [6], microwave plasma, and GAD plasma ...etc. NTPs have diverse applications, including surface cleaning, air and water purification, and medical uses. They play a crucial role in semiconductor production and nanomaterial synthesis [5]. The following figure showcases Physical Description of Plasmas.

2. Chemical species generated within Cold Plasma:

Plasma serves as the origin of electrochemical reactions, governed by factors typical of any electrochemical process, including (i) the characteristics of the active electrodes and their interaction with the surrounding medium, (ii) the nature and composition of the medium, (iii) the specific properties of the target molecules, and (iv) the electrical energy imparted to the electrochemical reactor [7, 8], figure II.2, showed the plasma reactive species generated using different operating gases in different interaction phases. In a recent investigation aiming to enhance gelatin-based film using cold plasma, various feed gases yielded distinct effects on the film properties. Specifically, argon induced an increase in surface roughness, while, oxygen gas plasma resulted in a reduction in film permeability post-treatment. Conversely, nitrogen and air plasma were observed to enhance the film's antimicrobial activity [9]. This underscores the significant impact of the variety of reactive species generated during plasma treatment on the alterations it can induce in biological systems. Hence, comprehensive investigations into the selection of gases and their combinations are imperative to tailor plasma chemistry for prospective applications [10].

For practical utilization, cost-effective plasma production entails the utilization of atmospheric air [11]. Due to its abundance in oxygen and nitrogen, plasma generated in atmospheric air predominantly consists of active species such as reactive oxygen–nitrogen species (RONS), which play crucial roles in redox reactions [8, 12]. Common reactive mixtures found in atmospheric air plasma include $NO_3, NO_2, O_2^-, O, .OH, N_2O, HO_2, N, N_2^-, NO, O_2, O_3$ and H_2O_2 [7, 11, 13-15]. Additionally, when plasma comes into contact with moisture, reactive species such as NO_3, NO_2,

O_3 and H_2O_2 are generated [7, 8, 11, 13-15] . These species, known as long-lived reactive species, exhibit prolonged shelf life in the liquid phase compared to other short-lived reactive species [7, 16]. A study conducted by Attri et al. further demonstrated that combining gases enhanced processing efficiency by increasing the presence of crucial reactive species in plasma, consequently reducing the microbial load in the target material, combining various working gases offers the advantage of generating predetermined reactive species [7, 8, 17]. Additionally, Takamatsu et al. investigated the characteristics of different gas plasmas (including air, oxygen, carbon dioxide, nitrogen, helium, and argon) incorporated into liquid. It was observed that oxygen and carbon dioxide plasma exhibited abundant production of singlet oxygen, whereas nitrogen, helium, and argon plasma resulted in higher production of $\cdot OH$ radicals [8, 13, 18]. In cold plasma, reactive oxygen, Hydroxyl radical and nitrogen species are widely recognized as the predominant reactive components.

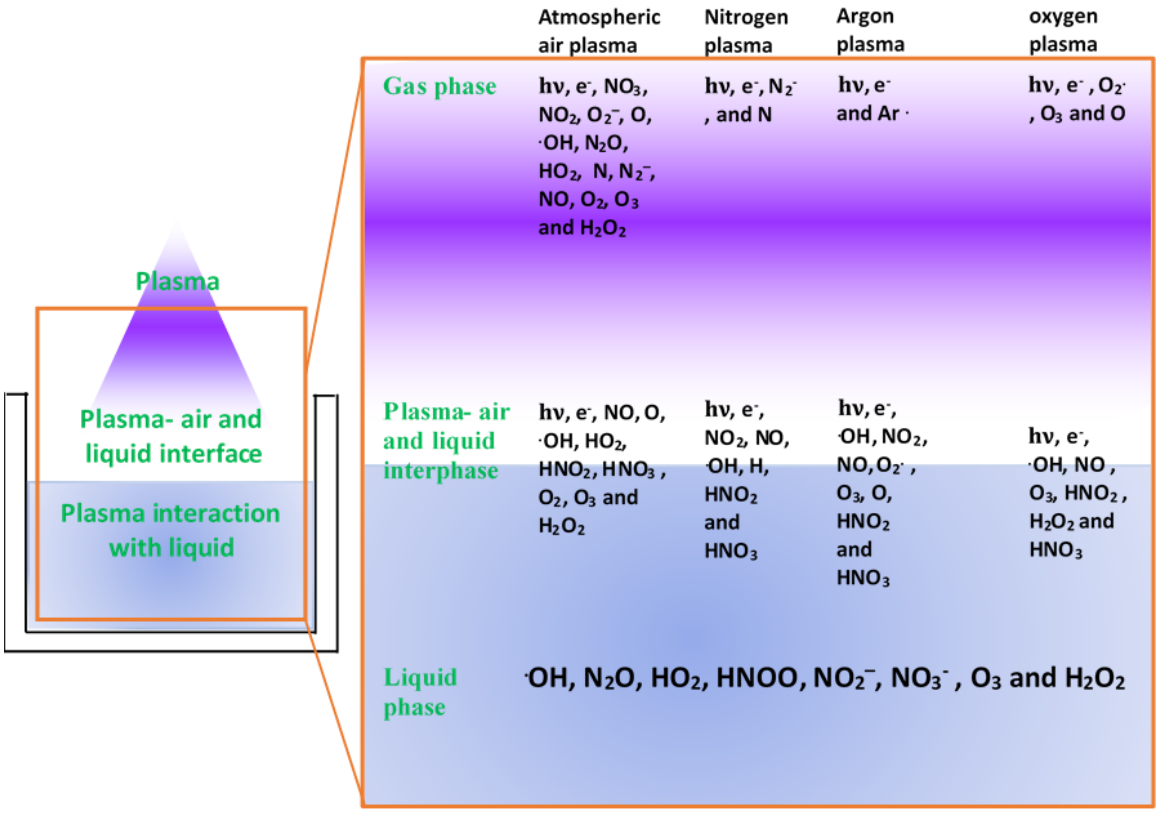

Figure II.2: The plasma reactive species generated using different operating gases.

2.1. Hydroxyl radical:

The hydroxyl radical exhibits high reactivity, characterized by a short lifespan of approximately 10^{-9} seconds and a heightened oxidation potential of 2.8 eV [19]. The presence of moisture or water plays a pivotal role in the generation of hydroxyl radicals within plasma environments. Key functions of hydroxyl radicals (·OH) encompass hydrogen atom abstraction, electrophilic addition, and transfer. Numerous reactions contribute to the generation of ·OH radicals in plasma, including the following [7, 11, 19]:

$$H_2O + e^- \rightarrow H^{\bullet} + {}^{\bullet}OH + e^- \qquad (II.1)$$

$$H_2O + h\nu \rightarrow H + {}^{\bullet}OH + e^- \qquad (II.2)$$

$$O_2 + e^- \rightarrow 2O^{\bullet} + e^- \qquad (II.3)$$

$$H_2O + O \rightarrow 2{}^{\bullet}OH \qquad (II.4)$$

2.2. Reactive oxygen species:

ROS, an acronym for reactive oxygen species, encompasses a variety of molecular entities including free radicals, ions, excited molecules, and atoms derived from molecular oxygen. These species are prevalent and dominant across a wide range of gas plasma environments, exhibiting an extended lifespan in comparison to other reactive species in the gaseous phase. Moreover, the lower dissociation energy of oxygen molecules (5.2 eV per molecule) renders them more readily available in plasma gas than other reactive species. Within the category of ROS [13], both radical and nonradical oxygen derivatives are included. Radical species comprise peroxyl (ROO·), hydroxyl (·OH) radicals, and the superoxide anion ($O_2{}^{\cdot -}$), while nonradical species encompass ozone, the hydroxide ion (OH^-), singlet oxygen, and hydrogen peroxide [7, 11, 13, 19].

$$O_2 + e^- + H^+ \rightarrow H_2O{\bullet}^- \rightarrow H^+ + O_2{\bullet}^- \qquad (II.5)$$

$$H_2O{\bullet}^- + e^- + H^+ \rightarrow H_2O_2 \qquad (II.6)$$

$$\bullet OH + e^- + H^+ \rightarrow H_2O \qquad (II.7)$$

2.3. Reactive nitrogen species (RNS):

Reactive nitrogen species (RNS) are a diverse array of compounds formed within plasma through the conversion of nitric oxide. These species include NO, NO_2, $ONOO^-$, HNO_2, and HNO_3. NO is generated from the energization or ionization of nitrogen gas and participates in reactions with oxygen species like O_2, O_3, and O_2^- to yield various other RNS. Despite possessing antioxidant properties, NO also contributes to nitrosative damage by producing reactive intermediates that

oxidize biomolecules. Nitrogen dioxide (NO_2) results from NO reactions with atomic and molecular oxygen, and in dry air plasma, NO_2 forms from interactions between ozone (O_3) and $NO\cdot$ Additionally, NO_2 reacts with O_3 to produce nitrate (NO_3). Peroxynitrite ($ONOO^-$) forms from NO and superoxide, acting as a potent oxidant that decomposes into radicals, causing oxidative damage. Nitric acid (HNO_3) and nitrous acid (HNO_2) are produced when plasma interacts with liquids, contributing to its germicidal effects. Various factors such as gas composition, humidity levels, and pH influence the generation and stability of RNS [7, 8, 11, 13-15, 17, 19].

$$N + O_2 \rightarrow NO + O \quad (II.8)$$

$$N_2 + e^- \rightarrow N + N + e^- \quad (II.9)$$

$$NO + O_3 \rightarrow NO_2 + O_2 \quad (II.10)$$

$$N_2 + O \rightarrow NO + N \quad (II.11)$$

$$NO + O_2 \rightarrow 2NO_2 \quad (II.12)$$

$$N + O_3 \rightarrow NO + O_2 \quad (II.13)$$

$$N + \bullet OH \rightarrow NO + H \quad (II.14)$$

$$NO_2 + \bullet OH \rightarrow HNO_3 \quad (II.15)$$

$$NO + \bullet OH \rightarrow HNO_2 \quad (II.16)$$

$$NO_2 + N \rightarrow N_2O + O \quad (II.17)$$

$$NO_2 + O_3 \rightarrow NO_3 + O_2 \quad (II.18)$$

$$O_2 + e^- + NO \rightarrow ONOO^- \quad (II.19)$$

$$H_2O_2 + NO_2 \rightarrow HNO_3 + \bullet OH \quad (II.20)$$

$$H_2O_2 + NO \rightarrow HNO_2 + \bullet OH \quad (II.21)$$

2.4. Photon emission:

Photon emission occurs during the atomic and molecular transitions of excited species, resulting in the release of photons across varying wavelengths, a phenomenon primarily contingent upon the constituent atoms and molecules. The emitted photons span a spectrum from ultraviolet (UV) radiation to infrared (IR) radiation, with the specific range dictated by the type of feed gas employed for plasma generation. Particularly in low-pressure environments, plasma generation facilitates the production of vacuum ultraviolet radiation (VUV), typically below 275 nm, known for its germicidal effects on microorganisms and its capacity to induce bond cleavage in biomolecules. Moreover, owing to the elevated energy levels of these photons, typically falling

within the range of 6–20 eV, they are efficacious in the disruption of chemical bonds, as well as in processes such as photoionization and photolysis of liquids. An additional noteworthy characteristic distinguishing UV radiation from other reactive species is its ability to penetrate several millimeters into treated substances. This property allows UV radiation to induce the dissociation of long-lived reactive species like hydrogen peroxide, ozone, and nitric and nitrous acids within the liquid phase into other reactive species [7, 8, 14, 17, 20], such:

$$H_2O_2 + h\nu \rightarrow O_2 + \cdot OH \qquad (II.22)$$

$$O_3 + h\nu \rightarrow O_2 + O \qquad (II.23)$$

3. Applications of Cold Plasma

Cold plasma, also known as NTP, has unique properties that allow its use in a wide range of applications across industries. This is an overview of the major applications of cold plasma technology. Figure II.3 showcases several of its applications across diverse fields.

3.1. Environmental protection:

Cold plasma technology has emerged as a promising avenue for environmental conservation, particularly in the remediation of air, water and soil pollutants. Recent advancements in cold plasma technology have underscored its environmental compatibility, high efficacy in removing contaminants, and energy efficiency in various treatment processes, including those pertaining to air, water and soil purification [21].

3.1.1. Air pollutant treatment:

Cold plasma technology presents a promising avenue for air pollutant treatment, especially concerning the removal of volatile organic compounds (VOCs) and other air pollutants. Through the generation of highly reactive species, cold plasma has the capability to break down and oxidize pollutants, thereby facilitating their removal from the air. However, the efficiency of cold plasma technology hinges on various factors, such as the type of gas utilized, the electrical conductivity of the air, and the temperature and humidity of the ambient environment. To fully harness the potential of cold plasma technology for air pollutant treatment, further research and development efforts are imperative. These endeavors should aim to optimize the performance of cold plasma systems while addressing challenges such as capital investment and process running costs. By advancing our understanding and refining the application of cold plasma technology, we can enhance its

effectiveness in mitigating air pollution and contribute to environmental conservation efforts. Research indicates that cold plasma exhibits efficacy in treating hazardous gases and pollutants present in the atmosphere. Moreover, studies have elucidated the effectiveness of cold atmospheric plasma treatment in reducing the survival of microorganisms and disinfecting inanimate surfaces [22-24].

Figure II.3: Illustration depicting the application of cold plasma across various fields.

3.1.2. Waste treatment:

Addressing this issue is particularly challenging due to the complex composition of textile wastewater, which includes various dyes, textile auxiliaries, and other chemicals associated with textile production [21, 25]. However, Textile wastewater presents a significant environmental challenge due to its highly toxic nature, resulting in substantial ecological damage [26]. Tecer et al. developed an atmospheric pressure plasma (ACP) reactor for the reduction of various reactive

azo dyes present in textile wastewater, treating a volume of at least 30 liters. Following a 90-minute treatment, the chemical oxygen demand (COD) of the ACP-treated wastewater was reduced by 99%, and its color became transparent. Moreover, the treated wastewater was successfully recycled in subsequent dyeing processes. Notably, the fabric dyed using the recycled wastewater exhibited similar quality characteristics, including color, levelness, and speed performance, when compared to fabric dyed using osmosis water [27]. Nippatla and Philip attempted to use underwater parallel-multi-tube atmospheric pressure plasma to decrease textile dye dissolved in textile wastewater and discovered that almost 70% of dyes could be degraded within 10-min plasma treatment. The increased dye degradation with decreased O_3, H_2O_2, and NO_3^- suggests that these active species participate in the dye decomposition. This result provides a competitive technology for conventional decomposition of textile dyes [26]. Furthermore, Pandiyaraj et al. (2021) demonstrated that the addition of Cu-TiO_2 NPs to dye wastewater could synergistically improve the degradation effect. The photocatalytic activity of Cu-TiO_2 NPs resulted in the formation of oxygen vacancies upon plasma stimulation. Subsequently, electrons from the plasma interacted with oxidized Ti^{4+}, leading to the formation of unstable Ti^{3+} species on the surface of Cu-TiO_2 NPs. This process facilitated the generation of more reactive species, thereby enhancing the capability of dye degradation through a synergistic effect between NPs and plasma [28]. Similarly, certain chemicals can be utilized in conjunction with NTP to enhance dye removal efficiency or degradation. Iervolino et al. observed that the addition of hydrogen peroxide led to a significant improvement in azo dye removal efficiency, increasing from 60% to 80% within a mere 2.5 min. This enhancement was attributed to the increased release of hydroxyl radicals from hydrogen peroxide during the process [29].

3.1.3. Soil treatment:

Soil remediation using cold plasma has emerged as a promising approach, demonstrating effectiveness in treating various types of organic pollutants [21]. Cold plasma exhibits rapid reaction rates and generates a multitude of chemically reactive species, leading to a wide and uniform discharge that enhances reaction efficiency [21]. Recent advancements have focused on developing coaxial DBD reactors to generate direct plasma microdischarges within soil pores [24, 30]. Studies have shown the efficacy of cold plasma in degrading pollutants such as, persistent organic pollutants (POPs), non-aqueous phase liquids (NAPLs), and diesel fuel like

dichlorodiphenyl-trichloroethane (DDT) and polychlorinated biphenyls (PCBs) [31-34], Furthermore, research is expanding to include other contaminants such as antibiotics and pesticides [21, 35-37]. A comparison between ozone treatment and DBD plasma for pyrene-contaminated soil revealed a significant difference in removal rates (i.e., <50% and 95%, respectively) [38]. Additionally, studies employing corona plasma for soil decontamination have shown enhanced degradation efficiency with increased needle numbers. Combining corona discharge with catalysts has further improved degradation rates, with some catalysts reducing pollutant concentrations to below detection limits [19, 39-44]. Peurrung et al. introduced an in-situ instrumentation setup designed for comprehensive processing, considering the capability of corona discharge to address a broad spectrum of organic contaminants [45]. The GAD represents a transitional form of atmospheric pressure discharge, as identified in prior research [21, 46]. GAD has been recognized as highly effective in various environmental applications, particularly in remediation efforts. Like other types of plasma discharge, GAD offers the advantage of easy scalability owing to its straightforward equipment requirements, as well as its flexible and controllable operations. It has demonstrated notable efficiency in removing organic contaminants. Recently, researchers have investigated the utilization of cold gliding arc plasma in combination with a fluidized bed for soil remediation, achieving impressive efficiency rates (up to 95% removal within 25 min under optimal conditions) [21, 47].

3.2. Food Industry:

Cold plasma technology is employed in the food industry to enhance antimicrobial activity, modify structures, and decontaminate surfaces [48]. Its application extends to decontaminating low-moisture foods [49, 50], such as, almonds [51, 52], spices [53-57], starch [58], dried walnut kernels [59, 60], peanuts [48, 61], pistachios [61], hazelnuts [48, 61], and wheat flour [62]. Numerous studies have highlighted that the effectiveness microbial inactivation in these foods using cold plasma depends significantly on the electrical and operational parameters applied. Increasing power, voltage, frequency, and treatment time leads to enhanced microbial log reductions, where the continuous plasma treatment proves more effective than pulsed treatment [54]. It was also noted that microwave-driven plasma exhibits higher antimicrobial activity compared to radiofrequency plasma [53], and air plasma outperforms nitrogen plasma. Additionally, reducing the distance between the food and plasma source improves efficacy [58]. Where the different ionized gases like

sulfur hexafluoride produce varied antimicrobial effects due to their unique chemical properties [61]. In summary, optimizing electrical settings, treatment time, plasma generation method, gas selection, and sample placement is crucial to maximize microbial log reductions. Cold plasma technology proves efficient and environmentally friendly for preserving low-moisture foods, contributing to improved food safety [48-52, 57-59].

3.3. Agriculture:

Several studies demonstrate that plant pathogens are responsible for economic losses, generally estimated between 20 and 30% on average. For example, these losses amount to 30.0% for rice, 21.5% for wheat, and 22.5% for corn, but they can sometimes exceed 40%, as is the case for corn with a rate of 41.1% [63], if these agents are not properly controlled [64]. Moreover, their number has increased over the past 100 years [64, 65]. Globalization also facilitates faster spreading of pathogens, notably with the growing emergence of quarantined diseases [50]. At the same time, the number of resistant pathogens is constantly increasing, while the arsenal of available pesticides is diminishing. These realities, coupled with global warming and the creation of more favorable conditions for pathogens, should lead to an increase in the incidence rate of diseases. This could prompt producers to resort more to chemicals, which, in turn, could increase the presence of pesticide residues in food products [64]. The climate emergency has become increasingly apparent in recent years, marked by frequent droughts and erratic rainfall patterns. The past decade has been identified as the warmest on record [66]. This shift in global climate conditions poses challenges for both plant cultivation and disease management. The rise in CO_2 levels and temperatures may contribute to the emergence of new diseases as plant susceptibility to specific pathogens could potentially change [64, 66-68].

In recent times, cold plasma technologies have been increasingly utilized in agriculture for a variety of purposes. These include purifying seeds and crops meant for planting or storage, accelerating seed germination and plant growth, reducing pathogen presence, generating nitrogen-based fertilizers, rehabilitating soil, sterilizing processing equipment, and mitigating ethylene to slow down aging [69, 70]. Additionally, treating water with a plasma discharge, such as a cold plasma jet, enhances its properties beneficial to plants. PAW has shown significant effects on seed germination, seedling development [66, 71-73], can indirectly influence agricultural processes through the utilization of plasma-activated water (PAW) [74-77], and can enhance crop yields

when used for irrigation during growth stages[67, 78, 79]. This is primarily achieved by the nitrogen fixation serves as a noteworthy nitrogen source for plants through the production of nitric oxide, nitrite, nitrate, dinitrogen trioxide, dinitrogen pentoxide, and ammonia [80, 81]. These forms of nitrogen are easily absorbed by plants as they are mobile and soluble in soil, making them suitable fertilizers [82]. However, nitrogen-fixed water tends to be acidic (pH 2–3) due to dissolved nitrogen oxides and hydrogen peroxide, which can harm certain crops [72, 83]. One solution for neutralization involves immersing Mg, Al, or Zn in water, as demonstrated by Lamichhane et al. [76].

3.4. Medicine and Healthcare:

The ability of cold atmospheric plasma to inactivate bacteria recently gained more relevance because modern society has been facing several serious healthcare challenges. Amongst these are:

3.4.1. Wound Healing:

Cold plasma can disinfect wounds, stimulate cell proliferation and blood vessel growth. It accelerates chronic wound healing for ulcers, burns, infections …etc [84, 85].

3.4.2. Cancer Treatment:

Cold plasma holds significant promise in the field of cancer treatment. A notable application involves inducing apoptosis to destroy cancer cells and reduce tumors [86, 87], ultimately leading to their demise. Cold plasma also triggers immunogenic cell death, enhancing the removal of cancer cells. This process includes releasing tumor-associated antigens and facilitating antigen processing [6, 87, 88], providing opportunities for synergistic combinations with immunotherapy regimens. Cold plasma emerges as a promising novel therapy for various cancers [86], including melanoma, glioblastoma [87], pancreatic, breast, liver, and others. While the use of cold plasma in cancer treatment is actively researched, additional studies are needed to fully comprehend its potential and mechanisms of action [5]. Nonetheless, existing research highlights its promising role in modifying cancer cell characteristics, fostering immune responses, and overcoming drug resistance [5, 68, 86-89].

3.4.3. Blood coagulation:

NTP stimulates blood coagulation, promptly stopping bleeding. The use of this technique in managing bleeding and facilitating faster surgical healing is becoming more important. Research suggests that NTP may induce blood coagulation by transforming fibrinogen into fibrin, hence promoting rapid clot formation in whole blood and the activation of coagulation factors [85, 90, 91].

3.4.4. Sterilization:

Sterilization is one of the oldest and most mentioned medicinal uses of plasma. It is crucial for preventing the spread of pathogens in healthcare environments. Plasma provides a chemical-free alternative to traditional procedures such as autoclaving and chemical disinfection due to its outstanding antibacterial properties. It may be used on surfaces, equipment, and wounds in medical facilities. The plasma treatment effectively eliminates germs, viruses, and fungus, making it very easy and efficient [85, 89, 91, 92].

3.4.5. Dentistry:

One of the key advantages of plasma is that its discharge can be relatively easily applied to irregular surfaces and hard-to-reach areas in the oral cavity. Plasma can be used for root canal disinfection, tooth whitening, composite restoration for cavities. It allows less invasive dental treatments, and generated from sufficiently small devices can also be applied directly inside the dental canal. Moreover, unlike liquid antimicrobials, plasma can be applied precisely to specific sites in the oral cavity without causing any unpleasant side effects. Furthermore, bacterial strains commonly found in dental biofilms are developing increased resistance. Failure to remove dental biofilm can lead to serious diseases like aspiration pneumonia, endocarditis, and other systemic disorders. Therefore, plasma represents a promising technology for effective yet targeted dental biofilm removal to improve oral health [1].

3.4.6. Cosmetology:

Cold plasma skin treatment, also known as plasma skin resurfacing, is effective in reducing skin imperfections like acne, wrinkles, scars, and pigmentation by stimulating collagen and elastin production and regenerating skin cells, resulting in improved skin elasticity and a youthful appearance. It is safe for all skin types, making it a promising option for individuals with diverse skin concerns [1, 85, 93].

3.4.7. Biofilm Removal:

Cold plasma is a promising technology for removing biofilms on surgical tools and medical devices, reducing hospital-acquired infections. It can also prevent biofilm formation in the food industry and medical sectors, making it a promising technology for maintaining hygienic conditions. Cold plasma's antifouling ability and inactivation of bacterial biofilms have been investigated, making it a significant advancement in infection control and maintaining hygienic conditions in healthcare and food industries [1, 79, 84, 93-95].

3.5. Energy:

Cold plasma technology has diverse applications in energy sectors such as combustion, hydrogen production, and renewable energy. The non-equilibrium conditions induced by plasma enable distinctive chemical reactions that are beneficial for enhancing energy processes:

3.5.1. Plasma-assisted combustion:

Plasma-assisted combustion, a method using cold plasma to improve combustion efficiency in engines like gas turbines, triggers faster and more thorough combustion of fuel/air mixtures, resulting in increased power output and reduced emissions. This technology has potential applications in internal combustion engines, gas turbines, and aerospace engines, improving flame stability, ignition, and overall combustion efficiency while reducing emissions. However, further research is needed to fully understand the mechanisms and refine the technology for practical implementation [32, 96].

3.5.2. Plasma-assisted solar cell:

Plasma-assisted manipulation of solar cells involves the utilization of plasmas to conduct surface treatments at reduced temperatures, thereby augmenting cell efficiency and performance. This method facilitates the fabrication of solar cells through an integrated process that amalgamates plasma and vacuum, thereby enhancing device efficacy. Tsai et al. investigated the application of a DBD plasma jet to treat NiO_x hole transport layers within perovskite solar cells. Operating at low temperatures and atmospheric pressure, the plasma jet enabled the treatment of thermally sensitive layers without inducing damage. This treatment induced oxygen vacancies and Ni^{3+} states on the NiO_x surface, thereby enhancing its conductivity. X-ray and ultraviolet photoelectron spectroscopy

analyses demonstrated that the plasma treatment shifted NiO_x bands closer to the perovskite valence band, subsequently improving hole extraction efficiency. Additionally, the treatment reduced charge transfer resistance and enhanced hole mobility. The low-temperature DBD jet provides a straightforward approach for modifying interfacial layers in perovskite solar cells without compromising other components. Furthermore, plasma-induced defects in NiOx energy levels bolstered conductivity and hole extraction, thereby enhancing cell performance[97]. Hvojnik et al. examined the impact of atmospheric cold plasma cleaning of fluorine-doped tin oxide (FTO) substrates on the quality of TiO_2 electron transport layers in printed carbon-based perovskite solar cells. The study revealed that plasma treatment notably decreased organic species on the FTO surface and mitigated the occurrence of defects and pinholes in the blocking layer. Consequently, carbon-based perovskite solar cells (C-PSCs) employing plasma-treated FTO substrates achieved an efficiency of 4.4%, comparable to the 4.5% efficiency attained with chemically cleaned FTO [98].

3.5.3. Hydrogen production:

Cold plasma technology enables the conversion of natural gas into hydrogen through plasma reforming, offering a promising alternative to traditional methods like steam reforming. The resulting syngas, comprising mainly H_2 and CO, used as a substitute for natural gas. Further research is ongoing to fully understand the mechanisms involved and optimize plasma reforming for practical applications [99, 100].

3.5.4. Plasma-assisted methane conversion:

Facilitates the breakdown of methane bonds under mild operational conditions, yielding syngas ($CO + H_2$) or other valuable intermediates. These intermediates can then undergo additional catalytic processes to produce higher-value products [101-103].

3.6. Material science:

Cold plasma technology has been applied in the field of materials science for the production of various nanomaterials and surface modification:

3.6.1. Surface modification:

The realm of materials surface modification through 'cold', low-pressure plasma treatment has seen significant growth since systematic research began in the 1960s. Recent years have witnessed particularly rapid expansion, notably in the adaptation of polymer surfaces for industrial purposes such as enhancing paint adhesion and bonding in composites[104]. Extensive plasma research delves into the impact of high-energy ions on material surfaces [105-107] , encompassing phenomena like sputtering, implantation, and secondary electron emission. These effects play pivotal roles in surface modification, as well as in initiating and sustaining plasma. In low-pressure plasma applications like surface coating, the presence of high-energy precursors is favored for optimal film adhesion, while alterations in surface roughness influence substrate wetting properties. Chemical sputtering occurs when plasma species react with the substrate, generating molecules and radicals. Plasma chemistry is intricate, involving numerous species and chemical reactions driven by accelerated electrons, resulting in chemically active, low-temperature plasmas [108]. Denes and Manolache underscore the enduring interest in controlled plasma surface modification and its potential for advancing technologies [109]. Other notable contributions include Turmanova et al.'s exploration of surface grafting polymerization of vinyl monomers on poly(tetrafluoroethylene) films using plasma [110], and Smet et al.'s demonstration of plasma treatment's potential to enhance the antifouling properties of Polydimethylsiloxane, rendering it more suitable for various biomedical applications [111].

3.6.2. Synthesis of Nanomaterial:

Various types of cold plasma have been employed for synthesizing fine powders with tailored properties, such as high purity or controlled particle size. These include the microwave plasma, JP, DBD, and GAD plasma.

d) Plasma Jet:

Is extensively employed in nanomaterial synthesis. The rapid heating of gas by the arc column and its expansion after the confinement nozzle leads to the formation of a stream of hot gas, which is crucial for the synthesis of NPs. Plasma can be generated using various techniques such as AC (pulse) plasma jet, radio frequency (RF), inductive or capacitive coupling, alternating current (AC), or pulsed power. Precursors can either be transported through the tube or placed directly in contact with the plasma outside the tube.

Figure II.4, provides a comprehensive depiction of the configuration of a plasma jet reactor, where it consists of an internal stainless-steel needle electrode upstream, securely sealed into a quartz tube, and a downstream external ring copper electrode situated on the exterior of the tube. Manipulating the distance between the high-voltage and ground electrodes enables control over the concentration of generated species. This phenomenon is attributed to the augmented accumulation of charge on the inner surface of the capillary tube as the electrode distance increases, thereby facilitating the ionization process. Additionally, key parameters for generating a plasma jet include: the distance D_{E-E} between the high voltage and ground electrodes, the distance D_{E-O} between the ground electrode and the orifice, and the distance D_{O-Ts} from the orifice to the liquid-air interface [112, 113].

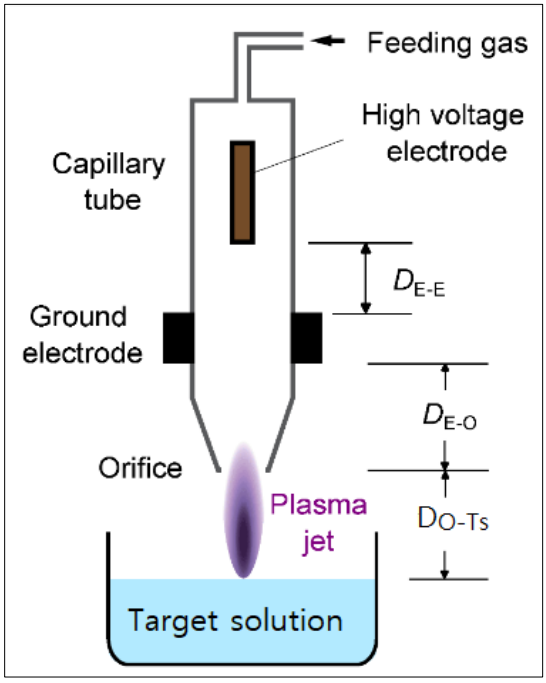

Figure II.4: Depiction of the configuration of a plasma jet reactor [112, 113].

These systems are capable of producing a wide range of metals, metal oxides, and semiconductor nanostructures. For instance, Anantha et al. achieved the synthesis of ZnO with flower-like and rod morphologies, with an average diameter of 60 nm, using an atmospheric pressure, low-temperature AC (pulse) plasma jet [114]. Similarly, Cho et al. synthesized W-x wt% Cu (x = 5, 10, and 20 wt%) nanocomposites by injecting a blend of micro-powders of tungsten trioxide (WO_3) and CuO into an inductively coupled radiofrequency (RF) thermal plasma. Moreover, they fabricated Ni-W nanostructures using a similar approach, constituting a nonconventional alloy system and serving

as excellent electrode candidates for highly integrated microcircuit applications [115]. Additionally, Bapat et al. produced single-crystal silicon NPs with diameters ranging from 20 to 80 nm using a constricted, filamentary capacitively coupled low-pressure plasma [116]. Khan et al. report the interaction of argon and helium plasma jets with the particle aerosol, produced by ns laser ablation of an Ag target and subsequently their transport for deposition on a distant substrate. The plasma jet facilitates the transport of the particle aerosol under the upshot of plasma ionic wind, caused by the high electric field in the plasma, Ag NPs were formed within the diameter range of 5–50 nm [117].

e) Dielectric Barrier Discharge (DBD)

Figure II.5, illustrates typical planar (plate-to-plate) configurations of DBD, known for their simplicity and scalability for high-volume production. In DBD Atmospheric Cold Plasma (ACP), a dielectric barrier layer, such as glass, thin enamel, alumina, ceramic materials, or silica glass, or polymer layers, blocks the discharge, covering one or both electrodes or suspended between them to prevent spark or arc discharge. The efficacy of this system heavily relies on various process parameters, such as, exposure duration, packaging material, substrate type, and device setup [118, 119]. However, at very high frequencies, the dielectric's ability to limit current may diminish. DBD devices are characterized by their simplicity, stability, reliability, and cost-effectiveness [119, 120]. It's important to differentiate between volumetric DBD and surface DBD; in the latter, electrodes are asymmetrically positioned, separated by the dielectric, with no additional volumetric air gap, causing discharge to occur at the barrier's surface. Coaxial DBDs, on the other hand, feature discharge gaps between cylindrical electrodes and dielectrics in an annular configuration, offering greater gas volume treatment and reactive species production. The discharge in annular DBDs is reported to be less homogeneous and stable compared to planar DBDs. Despite recent advances in other DBD configurations, planar and annular DBDs remain the most common. DBD demonstrates high efficiencies in short-term treatments of less than 1 minute, especially when utilizing ambient air instead of noble gases like helium or argon, reducing operational costs. The electrical energy in DBD systems is primarily transferred to electrons, keeping the surrounding gas close to ambient temperature. Moreover, non-equilibrium plasma DBDs can operate at elevated pressures, making them suitable for various industrial applications [119, 121].

DBD is well-suited for generating large volumes of non-equilibrium diffuse plasma at atmospheric pressure. Extensive research has improved our understanding and optimization of DBD systems [122-126]. DBDs utilize a dielectric material like glass or alumina covering at least one electrode. These electrodes are powered by high AC voltages in the kilovolt range at frequencies in the kilohertz range. The dielectric barrier enables diffuse plasma generation.

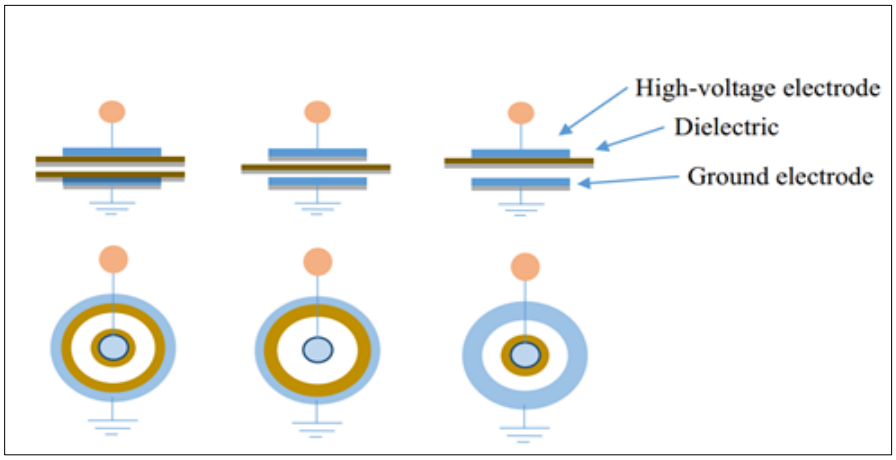

Figure II.5: Typical basic configurations of DBD ACP reactor [119].

The wide expansive plasma volumes from DBDs have enabled various applications including ozone generation, material surface modification, and flow control actuators. In summary, DBD can produce extensive non-thermal atmospheric plasmas through dielectric covered electrodes supplied with high AC voltages and frequencies, leading to diverse applications [84]. Regarding its application in the synthesis of nanomaterials, a recent example is provided here, a recent study by M. Tsumaki et al. utilized a Helium atmospheric pressure DBD to fabricate controlled sub-micrometer spheroidzed ZnO particles with an average diameter of 100 nm to 150 nm. In this process, micro-droplets of zinc acetate solution are exposed to atmospheric-pressure non-equilibrium plasma within a DBD. This results in plasma-ionized species reducing the metallic salt, leading to the formation of a distinctive ZnO nanocomposite structure comprising crystalline wurtzite NPs embedded in an amorphous matrix [127]. Additionally, Altaf et al. relied on a DBD to reduce Ag^{+} ions at the plasma-liquid interface into Ag NP under statistically optimized conditions for biological and photocatalytic applications. The efficiency and reactivity of Ag NP were enhanced by statistically optimizing reaction parameters using a Box model prepared under optimized conditions. They obtained particles ranging from 19 to 37 nanometers [128].

f) Microwave plasma:

The microwave plasma reactor setup, illustrated in Figure II. 6, is designed for the synthesis of NPs and incorporates two particle collection methods. The reactor features a reaction tube constructed from quartz glass, which traverses the cavity where plasma is initiated. Volatile and water-free precursors, such as chlorides, carbonyls, metal-alkoxides, or metalalkyls, are vaporized external to the reaction tube and blended with a carrier gas. These components are introduced as gases into the system just before the plasma zone, where chemical reactions in the gas-phase lead to NP formation. This reactor is particularly suitable for synthesizing metal oxide NPs [129].

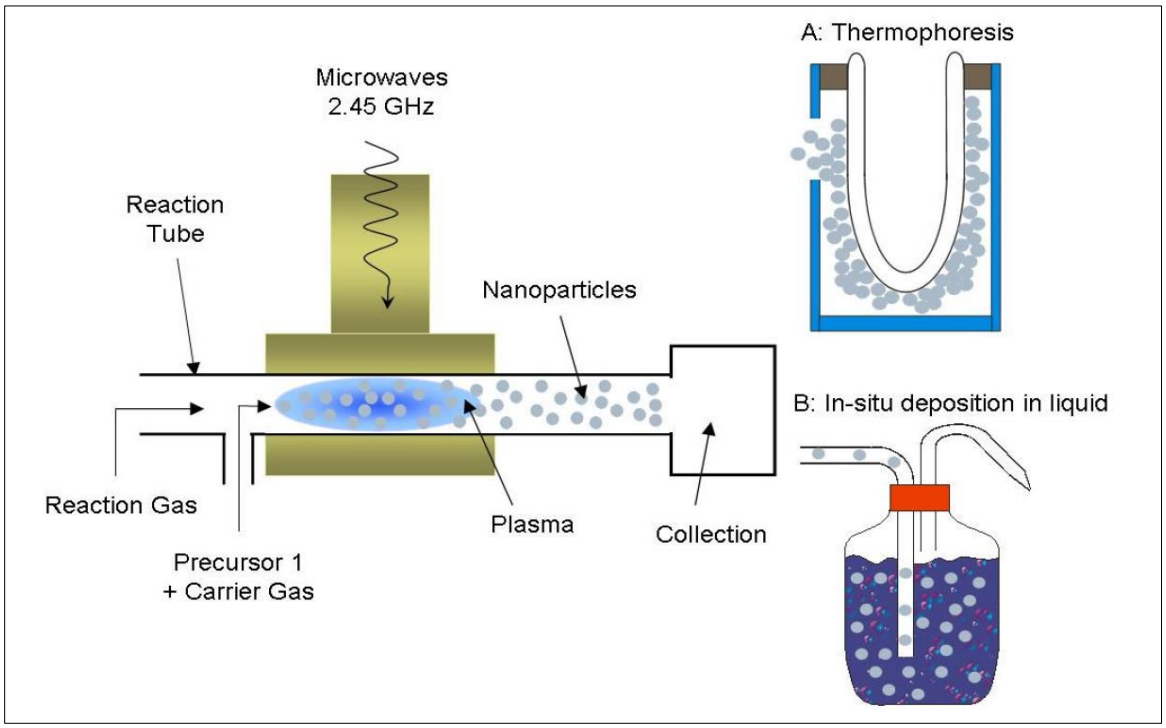

Figure II.6: Schematic representation of the microwave plasma synthesis principle for NPs, illustrating two powder collection methods: (A) thermophoresis and (B) in-situ deposition in liquids [129].

The use of microwave plasma for the synthesis of nanomaterials has been a topic of interest in recent years. Several studies have demonstrated the efficient synthesis of various nanomaterials using microwave plasma technology. In this technique, the process of particle formation in gas phases is facilitated by the ionization and dissociation of compounds, alongside particle charging within the plasma. Instead, NP formation in plasmas appears to resemble a chemical clustering process, influenced by the reactions of specific chemical species, which vary across different material systems. By tailoring synthesis conditions [130]. For example, B. Lee et al, explored how varying microwave input power and water vapor levels impacts the structure of ZnO nanowires

cultivated through an atmospheric-pressure microwave plasma system. Their study revealed that manipulating plasma temperature and the concentration of OH radicals enabled precise control over the aspect ratio of ZnO nanowires. Consequently, they achieved a diverse range of aspect ratios spanning from 10 to 340, thereby demonstrating the ability to produce ZnO nanowires with customizable structures. [131]. D. S. Y. Jayathilake and colleagues present a study on the microwave-assisted fabrication of highly conducting materials, including Al-doped ZnO (AZO), Ga-doped ZnO (GZO), and Al, Ga codoped ZnO (AGZO), offering cost-effective alternatives to indium tin oxide (ITO) for transparent conducting applications. Despite a significantly shorter microwave post-synthesis heat treatment duration of only 90 seconds compared to the conventional radiant heat treatment lasting 3 hours, the resistivity values obtained for the pellets were comparable. The resulting films exhibited impressive characteristics, including a visible transmittance of up to 90% and a resistivity of 5.7 × 10–3 Ω·cm, which positions them as competitive alternatives to the high-cost ITO films currently available [132]. B-J Lee and colleagues successfully synthesized ZnO NPs utilizing a microwave plasma torch system operating at atmospheric pressure. In this process, Zn powder was introduced into the microwave plasma region where it underwent melting and vaporization. The resulting ZnO nanowires, characterized by a diameter of 109.5 ± 8.0 nm and a length ranging from 5 to 6 μm, were efficiently produced utilizing inexpensive compressed air as the microwave plasma gas [133].

g) Gliding arc discharge plasma (GAD)

The utilization of GAD plasma for the synthesis of diverse nanomaterials has been extensively investigated across various studies, encompassing C NPs, C nanosheets, C nanotubes, ZnO Nano Powder, and TiO_2 NPs [11, 98, 134-138]. The GAD apparatus depicted in Figure II.7, is inspired by various configurations outlined in literature for NPs synthetases and treating contaminated liquids. Operating on the principle of generating a NTP plume at atmospheric pressure, the setup comprises several key components. These include a compressed air saturator to ensure adequate water content in the air stream, an inlet nozzle to regulate plasma gas flow and interaction with electrodes, and diverging electrodes with a well specified gap, responsible for generating the electric arc and defining the plasma plume volume. The apparatus is powered by a high-voltage transformer, facilitating the initiation and sustenance of the arc. The resulting plasma plume, sweeping along the electrode gap, generates active species. Optimization of GAD performance

entails considerations such as nozzle diameter, inter-electrode distance, plasma gas composition (air saturated with water), gas flow rate, and power input, which have been established based on previous studies to ensure consistent operation and effective plasma generation [11, 134, 136, 139-147].

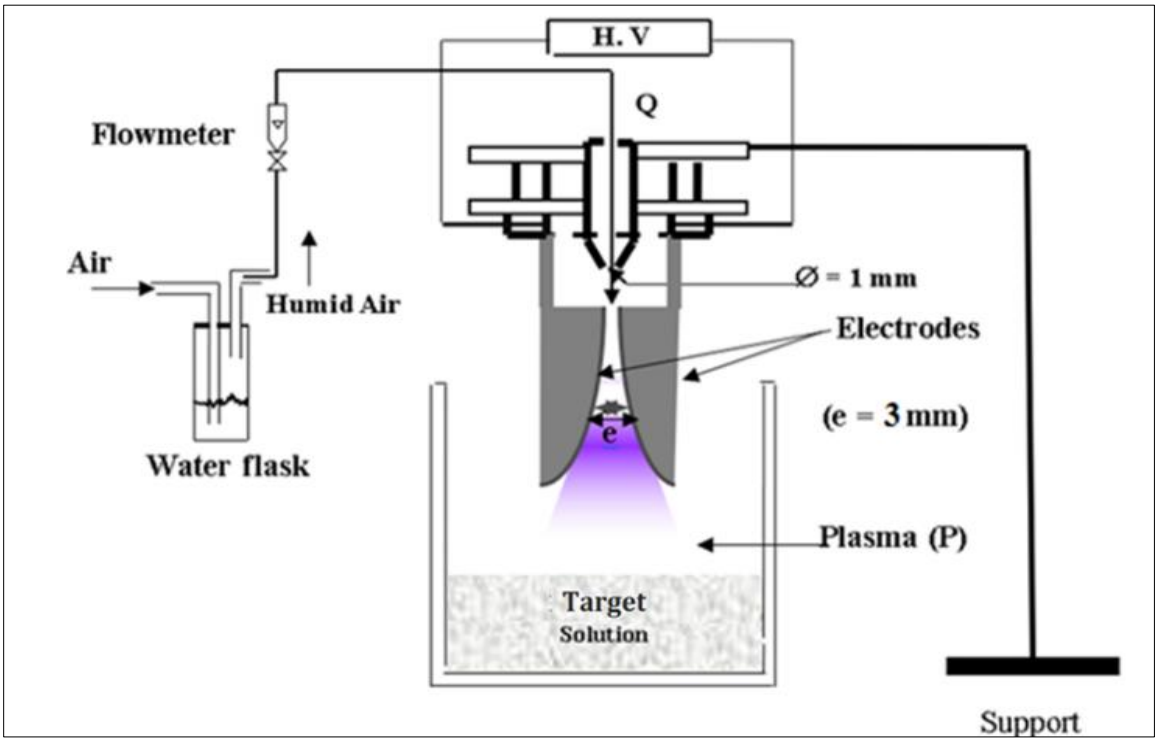

Figure II.7: Configuration of GAD plasma reactor used for NP synthesis [11].

Wang et al. pioneered a novel NTP process employing magnetically stabilized GAD for the continuous synthesis of carbon Nano-onions (CNOs), achieving a consistent diameter range of 70–200 nm through propane decomposition [135]. Moreover, Ma et al. explored the synthesis of carbon nanosheets in a gliding arc reactor, revealing a thickness of less than 3 nm through graphite exfoliation, presenting superior uniformity and thinness compared to toluene dissociation [98]. In addition, our team investigated the physicochemical properties of ZnO NPs synthesized via GAD plasma, showcasing their potential for nanomaterial synthesis and application in photocatalysis [11], and the corrosion inhibition of XC70 mild steel pipelines in a harsh 1 M HCl acidic environment [148]. Acayanka et al. delved into the synthesis of TiO_2 NPs and nanorods utilizing GAD plasma, characterizing them and highlighting their potential as photocatalysts, with nanorods exhibiting lengths of 50-100 nm and diameters of 5-15 nm [137]. Similarly, a novel TiO_2/SnO_2 nanocomposite was synthesized through GAD plasma at atmospheric pressure. A precursor

comprising $TiCl_3$ and $SnCl_2$ mixtures underwent plasma-induced oxidation, resulting in SnO2 microstructures (10-40 µm) enveloped with TiO_2 nanorods (6-8 nm diameter) [136]. Additionally, Tiya-Djowe et al. engineered α-FeOOH nanostructures featuring hollow spheres reminiscent of sea urchins, boasting enhanced catalytic properties, with particle diameters ranging from 200 to 300 nm [149]. Likewise, Tatchemo et al. successfully synthesized MnO_2 nanorods, showcasing their efficacy in degrading the azo dye Amaranth Red. Rapid conversion of potassium permanganate ($KMnO_4$) into α-MnO_2 nanorods yielded structures with diameters ranging between 50-100 nm and lengths between 1-2 µm via this method [138].

Numerous types of plasma remain unexplored within the scope of this discussion, which I shall enumerate without further elucidation. These encompass atmospheric pressure glow discharge torch (APGD-t) [150, 151], floating electrode dielectric barrier discharge (FE-DBD) [152, 153], hollow cathode micro-discharge air plasma jet [154], nanosecond plasma gun [155] microwave plasma torch [156], and plasma brush [86, 157]…etc.

Conclusion:

The unique properties of cold plasma make it a valuable tool with diverse applications across multiple industries. Its generation involves subjecting a gas to an intense electrical field, leading to ionization and the formation of plasma, distinct from the higher temperature thermal plasma. Cold plasma offers several advantages, notably its cleanliness and cost-effectiveness, rendering it suitable for various applications. Among its forms, GAD plasma stands out for its advantages, particularly in NP synthesis.

This chapter has provided an overview of cold plasma, covering its historical background, different types, applications, and safety considerations. Cold plasma technology exhibits versatility, presenting numerous potential applications, especially in the realm of nanotechnology. Ongoing research in cold plasma promises further advancements and innovations, expanding its utility in diverse fields.

The rapid growth of cold plasma technology foretells its significant impact across industries, poised to drive developments in medical treatments, material science, energy solutions, and environmental technologies. As this technology evolves, it holds the potential to revolutionize various sectors, shaping the landscape of future technological advancements.

References of Chapter II

1. Braný, D., et al., Cold atmospheric plasma: A powerful tool for modern medicine. International journal of molecular sciences, 2020. 21(8): p. 2932.
2. Langmuir, I., Oscillations in ionized gases. Proceedings of the National Academy of Sciences, 1928. 14(8): p. 627-637.
3. Dufour, T., From basics to frontiers: A comprehensive review of plasma-modified and plasma-synthesized polymer films. Polymers, 2023. 15(17): p. 3607.
4. Kim, S. and C.-H. Kim, Applications of plasma-activated liquid in the medical field. Biomedicines, 2021. 9(11): p. 1700.
5. Murillo, D., et al., Exploring the Use of Cold Atmospheric Plasma to Overcome Drug Resistance in Cancer. Biomedicines, 2023. 11(1): p. 208.
6. Yan, D., J.H. Sherman, and M. Keidar, Cold atmospheric plasma, a novel promising anti-cancer treatment modality. Oncotarget, 2017. 8(9): p. 15977.
7. Brisset, J.-L., et al., Chemical reactivity of discharges and temporal post-discharges in plasma treatment of aqueous media: examples of gliding discharge treated solutions. Industrial & Engineering Chemistry Research, 2008. 47(16): p. 5761-5781.
8. Dharini, M., S. Jaspin, and R. Mahendran, Cold plasma reactive species: Generation, properties, and interaction with food biomolecules. Food Chemistry, 2023. 405: p. 134746.
9. Ledari, S.A., J.M. Milani, and F.S. Lanbar, Improving gelatin-based emulsion films with cold plasma using different gases. Food Science & Nutrition, 2020. 8(12): p. 6487-6496.
10. Whitehead, J.C., The chemistry of cold plasma, in Cold plasma in food and agriculture. 2016, Elsevier. p. 53-81.
11. Messai, R., et al., GAD Plasma-Assisted Synthesis of ZnO Nanoparticles and Their Photocatalytic Activity. Materials Research Express, 2024.
12. Rehman, M.U., et al., Comparison of free radicals formation induced by cold atmospheric plasma, ultrasound, and ionizing radiation. Archives of biochemistry and biophysics, 2016. 605: p. 19-25.
13. Ozcan, A. and M. Ogun, Biochemistry of reactive oxygen and nitrogen species. Basic principles and clinical significance of oxidative stress, 2015. 3: p. 37-58.
14. Burlica, R., M.J. Kirkpatrick, and B.R. Locke, Formation of reactive species in gliding arc discharges with liquid water. Journal of electrostatics, 2006. 64(1): p. 35-43.
15. Ferhat, M.F., M.R. Ghezzar, and A. Addou, Hydrodynamics and mass transfer investigations in a biphasic plasma reactor. International Journal of Chemical Reactor Engineering, 2021. 19(4): p. 369-381.
16. Privat-Maldonado, A., et al., Reduction of human glioblastoma spheroids using cold atmospheric plasma: The combined effect of short-and long-lived reactive species. Cancers, 2018. 10(11): p. 394.
17. Attri, P., et al., Influence of reactive species on the modification of biomolecules generated from the soft plasma. Scientific reports, 2015. 5(1): p. 8221.
18. Takamatsu, T., et al., Investigation of reactive species using various gas plasmas. Rsc Advances, 2014. 4(75): p. 39901-39905.
19. Phaniendra, A., D.B. Jestadi, and L. Periyasamy, Free radicals: properties, sources, targets, and their implication in various diseases. Indian journal of clinical biochemistry, 2015. 30: p. 11-26.

20. Suenaga, Y., et al., Influence of controlling plasma gas species and temperature on reactive species and bactericidal effect of the plasma. Applied Sciences, 2021. 11(24): p. 11674.
21. Aggelopoulos, C.A., Recent advances of cold plasma technology for water and soil remediation: A critical review. Chemical Engineering Journal, 2022. 428: p. 131657.
22. Urashima, K., Review of Plasma Technologies for Contribution of Environmental Purification. IEEE Open Journal of Nanotechnology, 2022. 3: p. 159-165.
23. Kaiser, M., et al., Bifocal plasma source for treatment of gaseous pollutants. Surface and Coatings Technology, 2003. 174: p. 498-502.
24. Aggelopoulos, C. and C. Tsakiroglou, A new perspective towards in-situ cold plasma remediation of polluted sites: Direct generation of micro-discharges within contaminated medium. Chemosphere, 2021. 266: p. 128969.
25. Arslan-Alaton, I. and I. Alaton, Degradation of xenobiotics originating from the textile preparation, dyeing, and finishing industry using ozonation and advanced oxidation. Ecotoxicology and Environmental Safety, 2007. 68(1): p. 98-107.
26. Nippatla, N. and L. Philip, Electrocoagulation-floatation assisted pulsed power plasma technology for the complete mineralization of potentially toxic dyes and real textile wastewater. Process Safety and Environmental Protection, 2019. 125: p. 143-156.
27. Tecer, L.H., et al., Investigation of the treatment of textile wastewater with cold atmospheric plasma reactor (profoks) and reuse of recycled water in reactive dyeing process of cotton. Journal of Natural Fibers, 2022. 19(6): p. 2382-2389.
28. Pandiyaraj, K.N., et al., Dye wastewater degradation by the synergetic effect of an atmospheric pressure plasma treatment and the photocatalytic activity of plasma-functionalized Cu–TiO2 nanoparticles. Journal of Hazardous Materials, 2021. 405: p. 124264.
29. Iervolino, G., V. Vaiano, and V. Palma, Enhanced azo dye removal in aqueous solution by H2O2 assisted non-thermal plasma technology. Environmental Technology & Innovation, 2020. 19: p. 100969.
30. Hatzisymeon, M., et al., Highly energy-efficient degradation of antibiotics in soil: Extensive cold plasma discharges generation in soil pores driven by high voltage nanopulses. Science of The Total Environment, 2021. 786: p. 147420.
31. Aggelopoulos, C., et al., Parametric analysis of the operation of a non-thermal plasma reactor for the remediation of NAPL-polluted soils. Chemical Engineering Journal, 2016. 301: p. 353-361.
32. Zhao, J., et al., Remediation of diesel fuel polluted soil using dielectric barrier discharge plasma. Chemical Engineering Journal, 2021. 417: p. 128143.
33. Aggelopoulos, C., et al., Non-aqueous phase liquid-contaminated soil remediation by ex situ dielectric barrier discharge plasma. International journal of environmental science and technology, 2015. 12: p. 1011-1020.
34. Aggelopoulos, C., et al., Dielectric barrier discharge plasma used as a means for the remediation of soils contaminated by non-aqueous phase liquids. Chemical Engineering Journal, 2015. 270: p. 428-436.
35. Aggelopoulos, C., D. Tataraki, and G. Rassias, Degradation of atrazine in soil by dielectric barrier discharge plasma–potential singlet oxygen mediation. Chemical Engineering Journal, 2018. 347: p. 682-694.
36. Aggelopoulos, C., et al., Remediation of ciprofloxacin-contaminated soil by nanosecond pulsed dielectric barrier discharge plasma: Influencing factors and degradation mechanisms. Chemical Engineering Journal, 2020. 393: p. 124768.
37. Wang, T., et al., Glyphosate contaminated soil remediation by atmospheric pressure dielectric barrier discharge plasma and its residual toxicity evaluation. Journal of Hazardous Materials, 2016. 320: p. 539-546.
38. Mu, R., et al., Remediation of pyrene-contaminated soil by active species generated from flat-plate dielectric barrier discharge. Chemical Engineering Journal, 2016. 296: p. 356-365.

39. Zhan, J., et al., Remediation of soil contaminated by fluorene using needle-plate pulsed corona discharge plasma. Chemical Engineering Journal, 2018. 334: p. 2124-2133.
40. Zhan, J., et al., Remediation of perfluorooctanoic acid (PFOA) polluted soil using pulsed corona discharge plasma. Journal of hazardous materials, 2020. 387: p. 121688.
41. Wang, T.C., et al., Degradation of pentachlorophenol in soil by pulsed corona discharge plasma. Journal of hazardous materials, 2010. 180(1-3): p. 436-441.
42. Wang, T.C., et al., Depth dependence of p-nitrophenol removal in soil by pulsed discharge plasma. Chemical Engineering Journal, 2014. 239: p. 178-184.
43. Li, R., et al., Evaluation of pulsed corona discharge plasma for the treatment of petroleum-contaminated soil. Environmental Science and Pollution Research, 2017. 24: p. 1450-1458.
44. Wang, T.C., et al., Evaluation of the potential of soil remediation by direct multi-channel pulsed corona discharge in soil. Journal of hazardous materials, 2014. 264: p. 169-175.
45. Peurrung, L.M. and A.J. Peurrung, The in situ corona for treatment of organic contaminants in soils. Journal of Physics D: Applied Physics, 1997. 30(3): p. 432.
46. Martin-del-Campo, J., S. Coulombe, and J. Kopyscinski, Influence of operating parameters on plasma-assisted dry reforming of methane in a rotating gliding arc reactor. Plasma Chemistry and Plasma Processing, 2020. 40(4): p. 857-881.
47. Du, C., et al., Remediation of Phenanthrene-Contaminated Soil Using Non-thermal Plasma Fluidized Bed. Plasma Remediation Technology for Environmental Protection, 2017: p. 7-20.
48. Sen, Y., B. Onal-Ulusoy, and M. Mutlu, Aspergillus decontamination in hazelnuts: Evaluation of atmospheric and low-pressure plasma technology. Innovative Food Science & Emerging Technologies, 2019. 54: p. 235-242.
49. Rao, W., et al., The application of cold plasma technology in low-moisture foods. Food Engineering Reviews, 2023. 15(1): p. 86-112.
50. Domonkos, M., et al., Applications of cold atmospheric pressure plasma technology in medicine, agriculture and food industry. Applied Sciences, 2021. 11(11): p. 4809.
51. Deng, S., et al., Inactivation of Escherichia coli on almonds using nonthermal plasma. Journal of food science, 2007. 72(2): p. M62-M66.
52. Niemira, B.A., Cold plasma reduction of Salmonella and Escherichia coli O157: H7 on almonds using ambient pressure gases. Journal of Food Science, 2012. 77(3): p. M171-M175.
53. Darvish, H., et al., Effect of low-pressure cold plasma processing on decontamination and quality attributes of Saffron (Crocus sativus L.). Food Science & Nutrition, 2022. 10(6): p. 2082-2090.
54. Charoux, C.M., et al., Effect of non-thermal plasma technology on microbial inactivation and total phenolic content of a model liquid food system and black pepper grains. Lwt, 2020. 118: p. 108716.
55. Hemmati, V., et al., Cold atmospheric-pressure plasma treatment of turmeric powder: microbial load, essential oil profile, bioactivity and microstructure analyses. International Journal of Food Science & Technology, 2021. 56(5): p. 2224-2232.
56. Hertwig, C., et al., Decontamination of whole black pepper using different cold atmospheric pressure plasma applications. Food Control, 2015. 55: p. 221-229.
57. Durek, J., et al., Pilot-scale generation of plasma processed air and its influence on microbial count, microbial diversity, and selected quality parameters of dried herbs. Innovative Food Science & Emerging Technologies, 2022. 75: p. 102890.
58. Beyrer, M., et al., Cold atmospheric plasma inactivation of microbial spores compared on reference surfaces and powder particles. Food and Bioprocess Technology, 2020. 13: p. 827-837.
59. Ahangari, M., Y. Ramezan, and M.R. Khani, Effect of low pressure cold plasma treatment on microbial decontamination and physicochemical properties of dried walnut kernels (Juglans regia L.). Journal of Food Process Engineering, 2021. 44(1): p. e13593.
60. Amini, M. and M. Ghoranneviss, Effects of cold plasma treatment on antioxidants activity, phenolic contents and shelf life of fresh and dried walnut (Juglans regia L.) cultivars during storage. Lwt, 2016. 73: p. 178-184.

61. Basaran, P., N. Basaran-Akgul, and L. Oksuz, Elimination of Aspergillus parasiticus from nut surface with low pressure cold plasma (LPCP) treatment. Food microbiology, 2008. 25(4): p. 626-632.
62. Chaple, S., et al., Effect of atmospheric cold plasma on the functional properties of whole wheat (Triticum aestivum L.) grain and wheat flour. Innovative Food Science & Emerging Technologies, 2020. 66: p. 102529.
63. Savary, S., et al., The global burden of pathogens and pests on major food crops. Nat Ecol Evol 3: 430–439. 2019.
64. Pańka, D., et al., Can cold plasma be used for boosting plant growth and plant protection in sustainable plant production? Agronomy, 2022. 12(4): p. 841.
65. Wu, B., et al., Current insights into fungal species diversity and perspective on naming the environmental DNA sequences of fungi. Mycology, 2019. 10(3): p. 127-140.
66. Attri, P., et al., Plasma agriculture from laboratory to farm: A review. Processes, 2020. 8(8): p. 1002.
67. Puač, N., M. Gherardi, and M. Shiratani, Plasma agriculture: A rapidly emerging field. Plasma processes and polymers, 2018. 15(2): p. 1700174.
68. Lin, S.-P., et al., Applications of atmospheric cold plasma in agricultural, medical, and bioprocessing industries. Applied Microbiology and Biotechnology, 2022. 106(23): p. 7737-7750.
69. Filimonova, E. and R.K. Amirov, Simulation of ethylene conversion initiated by a streamer corona in an air flow. Plasma Physics Reports, 2001. 27: p. 708-714.
70. Ji, S.-H., et al., Enhancement of vitality and activity of a plant growth-promoting bacteria (PGPB) by atmospheric pressure non-thermal plasma. Scientific reports, 2019. 9(1): p. 1044.
71. Adhikari, B., et al., Cold atmospheric plasma-activated water irrigation induces defense hormone and gene expression in tomato seedlings. Scientific reports, 2019. 9(1): p. 16080.
72. Adhikari, B., et al., Cold plasma seed priming modulates growth, redox homeostasis and stress response by inducing reactive species in tomato (Solanum lycopersicum). Free Radical Biology and Medicine, 2020. 156: p. 57-69.
73. Bradu, C., et al., Reactive nitrogen species in plasma-activated water: Generation, chemistry and application in agriculture. Journal of Physics D: Applied Physics, 2020. 53(22): p. 223001.
74. Attri, P., et al., CAP modifies the structure of a model protein from thermophilic bacteria: Mechanisms of CAP-mediated inactivation. Scientific reports, 2018. 8(1): p. 10218.
75. Hoon Park, J., et al., A comparative study for the inactivation of multidrug resistance bacteria using dielectric barrier discharge and nano-second pulsed plasma. Scientific reports, 2015. 5(1): p. 13849.
76. Lamichhane, P., et al., Low-temperature plasma-assisted nitrogen fixation for corn plant growth and development. International Journal of Molecular Sciences, 2021. 22(10): p. 5360.
77. Shaw, P., et al., Bacterial inactivation by plasma treated water enhanced by reactive nitrogen species. Scientific reports, 2018. 8(1): p. 11268.
78. Thirumdas, R., et al., Plasma activated water (PAW): Chemistry, physico-chemical properties, applications in food and agriculture. Trends in food science & technology, 2018. 77: p. 21-31.
79. Dahle, S., J. Žigon, and R. Fink, Cold plasma for sustainable control of hygienically relevant biofilms. The interaction of plasma distance and exposure time. International Journal of Environmental Health Research, 2023: p. 1-15.
80. Ghimire, B., et al., The role of UV photolysis and molecular transport in the generation of reactive species in a tissue model with a cold atmospheric pressure plasma jet. Applied Physics Letters, 2019. 114(9).
81. Mumtaz, S., et al., Pulsed high-power microwaves do not impair the functions of skin normal and cancer cells in vitro: A short-term biological evaluation. Journal of Advanced Research, 2020. 22: p. 47-55.
82. Van Alphen, S., et al., Sustainable gas conversion by gliding arc plasmas: a new modelling approach for reactor design improvement. Sustainable Energy & Fuels, 2021. 5(6): p. 1786-1800.

83. Judée, F., et al., Plasma-activation of tap water using DBD for agronomy applications: Identification and quantification of long lifetime chemical species and production/consumption mechanisms. Water research, 2018. 133: p. 47-59.
84. Laroussi, M., Cold plasma in medicine and healthcare: The new frontier in low temperature plasma applications. Frontiers in Physics, 2020. 8: p. 74.
85. Moszczyńska, J., K. Roszek, and M. Wiśniewski, Non-thermal plasma application in medicine—Focus on reactive species involvement. International Journal of Molecular Sciences, 2023. 24(16): p. 12667.
86. Faramarzi, F., et al., Cold physical plasma in cancer therapy: mechanisms, signaling, and immunity. Oxidative medicine and cellular longevity, 2021. 2021.
87. Min, T., et al., Therapeutic Effects of Cold Atmospheric Plasma on Solid Tumor. Frontiers in Medicine, 2022. 9: p. 884887.
88. Živanić, M., et al., Current State of Cold Atmospheric Plasma and Cancer-Immunity Cycle: Therapeutic Relevance and Overcoming Clinical Limitations Using Hydrogels. Advanced Science, 2023. 10(8): p. 2205803.
89. Gan, L., et al., Medical applications of nonthermal atmospheric pressure plasma in dermatology. JDDG: Journal der Deutschen Dermatologischen Gesellschaft, 2018. 16(1): p. 7-13.
90. Nagaraj, G., et al., Mechanism of Blood Coagulation by Non-Thermal Atmospheric Pressure Dielectric Barrier Discharge Plasma. Blood, 2007. 110(11): p. 3162.
91. Nomura, Y., et al., Investigation of blood coagulation effect of nonthermal multigas plasma jet in vitro and in vivo. journal of surgical research, 2017. 219: p. 302-309.
92. Pai, K., et al., Investigation of the roles of plasma species generated by surface dielectric barrier discharge. Scientific reports, 2018. 8(1): p. 16674.
93. Busco, G., et al., The emerging potential of cold atmospheric plasma in skin biology. Free Radical Biology and Medicine, 2020. 161: p. 290-304.
94. Matthes, R., et al., Efficiency of biofilm removal by combination of water jet and cold plasma: An in-vitro study. BMC Oral Health, 2022. 22(1): p. 1-16.
95. Hage, M., et al., Cold plasma surface treatments to prevent biofilm formation in food industries and medical sectors. Applied Microbiology and Biotechnology, 2022: p. 1-20.
96. Choi, Y.H. and J. Hwang, Review on Plasma-Assisted Ignition Systems for Internal Combustion Engine Application. Energies, 2023. 16(4): p. 1604.
97. Tsai, J.-H., et al., Low-temperature (< 40 C) atmospheric-pressure dielectric-barrier-discharge-jet treatment on nickel oxide for p–i–n structure perovskite solar cells. ACS omega, 2020. 5(11): p. 6082-6089.
98. Hvojnik, M., et al., The effect of atmospheric cold plasma cleaning of FTO substrates on the quality of TiO2 electron transport layers for printed carbon-based perovskite solar cells. 2021.
99. Hrycak, B., et al., Hydrogen production by the steam reforming of synthetic biogas in atmospheric-pressure microwave (915 MHz) plasma. Scientific Reports, 2023. 13(1): p. 2204.
100. Lee, D.H., et al., Plasma-assisted hydrogen generation: A mechanistic review. Fuel Processing Technology, 2023. 247: p. 107761.
101. Feng, J., et al., Plasma-Assisted Reforming of Methane. Advanced Science, 2022. 9(34): p. 2203221.
102. Wang, Y.-F., et al., Methane steam reforming for producing hydrogen in an atmospheric-pressure microwave plasma reactor. International Journal of Hydrogen Energy, 2010. 35(1): p. 135-140.
103. Li, S., et al., Plasma-Assisted Dry Reforming of CH4: How Small Amounts of O2 Addition Can Drastically Enhance the Oxygenate Production─ Experiments and Insights from Plasma Chemical Kinetics Modeling. ACS Sustainable Chemistry & Engineering, 2023. 11(42): p. 15373-15384.
104. Liston, E., L. Martinu, and M. Wertheimer, Plasma surface modification of polymers for improved adhesion: a critical review. Journal of adhesion science and technology, 1993. 7(10): p. 1091-1127.
105. Federici, G., et al., Plasma-material interactions in current tokamaks and their implications for next step fusion reactors. Nuclear Fusion, 2001. 41(12): p. 1967.

106. Saman, N.M., M.H. Ahmad, and Z. Buntat, Application of cold plasma in nanofillers surface modification for enhancement of insulation characteristics of polymer nanocomposites: a review. IEEE Access, 2021. 9: p. 80906-80930.
107. Wolf, R. and A.C. Sparavigna, Role of plasma surface treatments on wetting and adhesion. Engineering, 2010. 2(06): p. 397.
108. Tabares, F.L. and I. Junkar, Cold plasma systems and their application in surface treatments for medicine. Molecules, 2021. 26(7): p. 1903.
109. Denes, F.S. and S. Manolache, Macromolecular plasma-chemistry: an emerging field of polymer science. Progress in polymer science, 2004. 29(8): p. 815-885.
110. Turmanova, S., et al., Surface grafting polymerization of vinyl monomers on poly (tetrafluoroethylene) films by plasma treatment. Journal of Polymer Research, 2008. 15: p. 309-318.
111. De Smet, N., M. Rymarczyk-Machal, and E. Schacht, Plasma-induced surface modification of polydimethylsiloxane aimed at reducing salt and protein deposition. Journal of Biomaterials Science, Polymer Edition, 2011. 22(18): p. 2457-2473.
112. Ghimire, B., et al., Enhancement of hydrogen peroxide production from an atmospheric pressure argon plasma jet and implications to the antibacterial activity of plasma activated water. Plasma Sources Science and Technology, 2021. 30(3): p. 035009.
113. Wong, K.S., et al., Plasma-activated water: Physicochemical properties, generation techniques, and applications. Processes, 2023. 11(7): p. 2213.
114. Ananth, A., et al., Soft jet plasma-assisted synthesis of Zinc oxide nanomaterials: Morphology controls and antibacterial activity of ZnO. Chemical Engineering Journal, 2017. 322: p. 742-751.
115. Oh, J.-W., et al., In situ synthesis of bimetallic tungsten-copper nanoparticles via reactive radio-frequency (RF) thermal plasma. Nanoscale research letters, 2018. 13: p. 1-7.
116. Bapat, A., et al., Plasma synthesis of single-crystal silicon nanoparticles for novel electronic device applications. Plasma physics and controlled fusion, 2004. 46(12B): p. B97.
117. Khan, T.M., G.A.S. Alves, and A. Iqbal, Processing laser ablated plasmonic nanoparticle aerosols with nonthermal dielectric barrier discharge jets of argon and helium and plasma induced effects. Scientific Reports, 2023. 13(1): p. 77.
118. Suwal, S., et al., Mechanism characterization of bacterial inactivation of atmospheric air plasma gas and activated water using bioluminescence technology. Innovative food science & emerging technologies, 2019. 53: p. 18-25.
119. Feizollahi, E., N. Misra, and M. Roopesh, Factors influencing the antimicrobial efficacy of dielectric barrier discharge (DBD) atmospheric cold plasma (ACP) in food processing applications. Critical Reviews in Food Science and Nutrition, 2021. 61(4): p. 666-689.
120. Misra, N., et al., In-package cold plasma technologies. Journal of Food Engineering, 2019. 244: p. 21-31.
121. Mandal, R., A. Singh, and A.P. Singh, Recent developments in cold plasma decontamination technology in the food industry. Trends in food science & technology, 2018. 80: p. 93-103.
122. Donohoe, K.G., THE DEVELOPMENT AND CHARACTERIZATION OF AN ATMOSPHERIC PRESSURE NONEQUILIBRIUM PLASMA CHEMICAL REACTOR. 1976: California Institute of Technology.
123. Bartnikas, R., Note on discharges in helium under ac conditions. Journal of Physics D: Applied Physics, 1968. 1(5): p. 659.
124. Massines, F., et al., Glow and Townsend dielectric barrier discharge in various atmosphere. Plasma physics and controlled fusion, 2005. 47(12B): p. B577.
125. Pipa, A., et al., Experimental determination of dielectric barrier discharge capacitance. Review of Scientific Instruments, 2012. 83(7).
126. Gao, K., et al., Mode transitions of a helium dielectric barrier discharge from Townsend, normal glow, to abnormal glow with varying voltage rising time. AIP Advances, 2019. 9(11).

127. Tsumaki, M., Y. Shimizu, and T. Ito, Size-controlled sub-micrometer spheroidized ZnO particles synthesis via plasma-induced processing in microdroplets. Materials Letters, 2016. 166: p. 81-84.
128. Altaf, N.U.H., et al., Non-Thermal Plasma Reduction of Ag+ Ions into Silver Nanoparticles in Open Atmosphere under Statistically Optimized Conditions for Biological and Photocatalytic Applications. Materials, 2022. 15(11): p. 3826.
129. Hanemann, T. and D.V. Szabó, Polymer-nanoparticle composites: from synthesis to modern applications. Materials, 2010. 3(6): p. 3468-3517.
130. Szabó, D.V. and S. Schlabach, Microwave plasma synthesis of materials—From physics and chemistry to nanoparticles: A materials scientist's viewpoint. Inorganics, 2014. 2(3): p. 468-507.
131. Lee, B.-J., et al., Structure-controllable synthesis of ZnO nanowires using water vapor in an atmospheric-pressure microwave plasma system. Current Applied Physics, 2021. 28: p. 52-58.
132. Jayathilake, D., et al., Microwave-assisted synthesis and processing of Al-doped, Ga-doped, and Al, Ga codoped ZnO for the pursuit of optimal conductivity for transparent conducting film fabrication. ACS Sustainable Chemistry & Engineering, 2017. 5(6): p. 4820-4829.
133. Lee, B.-J., S.-I. Jo, and G.-H. Jeong, Synthesis of ZnO nanomaterials using low-cost compressed air as microwave plasma gas at atmospheric pressure. Nanomaterials, 2019. 9(7): p. 942.
134. Doudi, D., et al., Eco-friendly synthesis and characterization of ZnO and Mg-Ag-doped ZnO nanoparticles using Phoenix dactylifera L. seeds: exploring biological activity and structural properties. Biomass Conversion and Biorefinery, 2024: p. 1-21.
135. Wang, C., et al., Continuous preparation of carbon nano-onions in a non-thermal plasma process. Materials Letters, 2020. 272: p. 127808.
136. Acayanka, E., et al., Synthesis, characterization and photocatalytic application of TiO2/SnO2 nanocomposite obtained under non-thermal plasma condition at atmospheric pressure. Plasma Chemistry and Plasma Processing, 2016. 36(3): p. 799-811.
137. Acayanka, E., et al., Plasma-assisted synthesis of TiO2 nanorods by gliding arc discharge processing at atmospheric pressure for photocatalytic applications. Plasma Chemistry and Plasma Processing, 2013. 33(4): p. 725-735.
138. Tatchemo, F.B., et al., Gliding arc plasma synthesis of MnO 2 nanorods for the plasma-catalytic bleaching of azoic Amaranth Red dye. Topics in Catalysis, 2017. 60: p. 962-972.
139. Abdelmalek, F., et al., Plasmachemical degradation of azo dyes by humid air plasma: Yellow Supranol 4 GL, Scarlet Red Nylosan F3 GL and industrial waste. Water Research, 2004. 38(9): p. 2339-2347.
140. Tsagou-Sobze, E., et al., Gliding discharge-induced oxidation of a toxic alkaloid. Journal of hazardous materials, 2008. 152(1): p. 446-449.
141. Moussa, D. and J.-L. Brisset, Disposal of spent tributylphosphate by gliding arc plasma. Journal of hazardous materials, 2003. 102(2-3): p. 189-200.
142. Yan, J., et al., Degradation of gas–liquid gliding arc discharge on Acid Orange II. Journal of hazardous materials, 2008. 157(2-3): p. 441-447.
143. Hentit, H., et al., Plasma-catalytic degradation of anthraquinonic acid green 25 in solution by gliding arc discharge plasma in the presence of tin containing aluminophosphate molecular sieves. Journal of Molecular Catalysis A: Chemical, 2014. 390: p. 37-44.
144. Ferhat, M.F., et al., Conception of a novel spray tower plasma-reactor in a spatial post-discharge configuration: Pollutants remote treatment. 2017. 321: p. 661-671.
145. Abdelmalek, F., et al., Gliding Arc Discharge (GAD) assisted catalytic degradation of bisphenol A in solution with ferrous ions. 2008. 63(1): p. 30-37.
146. Ghezzar, M., et al., Enhancement of the bleaching and degradation of textile wastewaters by Gliding arc discharge plasma in the presence of TiO2 catalyst. 2009. 164(2-3): p. 1266-1274.
147. Ghezzar, M., et al., Gliding arc plasma assisted photocatalytic degradation of anthraquinonic acid green 25 in solution with TiO2. Applied Catalysis B: Environmental, 2007. 72(3-4): p. 304-313.

148. Bounedjar, N., et al., Non thermal plasma synthesis of ZnO nanoparticles and their corrosion inhibition activity on XC70 mild steel pipeline in 1 M HCl acidic medium. Materials Chemistry and Physics, 2024. 311: p. 128555.
149. Tiya-Djowe, A., et al., Non-thermal plasma synthesis of sea-urchin like α-FeOOH for the catalytic oxidation of Orange II in aqueous solution. Applied Catalysis B: Environmental, 2015. 176: p. 99-106.
150. Leduc, M., S. Coulombe, and R.L. Leask, Atmospheric pressure plasma jet deposition of patterned polymer films for cell culture applications. IEEE transactions on plasma science, 2009. 37(6): p. 927-933.
151. Coulombe, S., et al., Miniature atmospheric pressure glow discharge torch (APGD-t) for local biomedical applications. Pure and Applied Chemistry, 2006. 78(6): p. 1147-1156.
152. Fridman, G., et al., Floating electrode dielectric barrier discharge plasma in air promoting apoptotic behavior in melanoma skin cancer cell lines. Plasma Chemistry and Plasma Processing, 2007. 27: p. 163-176.
153. Vandamme, M., et al., ROS implication in a new antitumor strategy based on non-thermal plasma. International journal of cancer, 2012. 130(9): p. 2185-2194.
154. Kolb, J.F., et al., Cold atmospheric pressure air plasma jet for medical applications. Applied Physics Letters, 2008. 92(24).
155. Brullé, L., et al., Effects of a non thermal plasma treatment alone or in combination with gemcitabine in a MIA PaCa2-luc orthotopic pancreatic carcinoma model. PloS one, 2012. 7(12): p. e52653.
156. Babaeva, N.Y., et al., Production of active species in an argon microwave plasma torch. Journal of Physics D: Applied Physics, 2018. 51(46): p. 464004.
157. Duan, Y., C. Huang, and Q. Yu, Cold plasma brush generated at atmospheric pressure. Review of scientific instruments, 2007. 78(1).

General Conclusion

General Conclusion

This work emphasizes the importance of research on industrial wastewater treatment processes for environmental and public health preservation. Through an in-depth analysis of the obtained results, it is clear that ZnO NPs synthesized by NTP have significant potential in the field of wastewater treatment.

First, our research has demonstrated that NTP offers an efficient and environmentally friendly synthesis method for producing ZnO NPs. Compared to other synthesis methods, NTP allows for rapid and economical production of NPs while minimizing the use of harmful chemicals. This synthesis approach also presents great flexibility in terms of controlling the properties of the NPs, including their size, shape, and composition.

Furthermore, our studies have revealed that ZnO NPs synthesized by NTP exhibit remarkable performance in the degradation processes of organic compounds present in wastewater. Photocatalysis tests showed a high catalytic activity of the NPs, leading to efficient and rapid degradation of organic pollutants (such, CR, MB, BCB and ASA). This degradation capacity was observed in a range of organic compounds, demonstrating the versatility and applicability of NTP-synthesized NPs in various wastewater treatment applications. Also, under various light source (UV light and sun light).

In addition, our investigations have highlighted the stability and durability of metal oxide NPs synthesized by NTP. Recycling tests showed that the NPs retain their catalytic activity even after multiple cycles of use, suggesting significant potential for long-term use in industrial wastewater treatment application.

Another, utilizing various characterization techniques, the study reveals that prolonged discharge durations result in smaller particle sizes, elevated band gap energies, crystalline defects, and intensified UV-visible absorption peaks.

Additionally, our investigations demonstrate the high effectiveness of combining GAD plasma-synthesized ZnO nanoparticles with NTP treatment for aspirin degradation. This method achieves high degradation efficiency, significant TOC removal, moderate energy consumption, and employs environmentally friendly materials. These findings have important implications for wastewater treatment, presenting a promising solution to mitigate pollution, enhance water quality, and effectively degrade organic compounds in wastewater.

However, despite these promising results, some limitations and challenges need to be considered. For example, further characterization of NTP-synthesized NPs is necessary to fully understand their physicochemical properties and their mechanism of action in the degradation processes of organic compounds. Additionally, further studies on the environmental impact and toxicity of NPs are essential to assess their safety for large-scale use.

In conclusion, metal oxide NPs synthesized by NTP represent a promising avenue for industrial wastewater treatment. Their efficiency, durability, and low environmental impact make them an attractive option for industries seeking sustainable solutions for waste management. However, further research is needed to optimize this technology and ensure its long-term safety and effectiveness.

Future Prospects: On the Use of GAD Plasma for the Production of ZnO NPs

The future prospects and perspectives on using gliding arc plasma in the production of zinc oxide nanoparticles are diverse and promising, including:

Improving Production Efficiency: Extensive research can be conducted to enhance production efficiency in terms of energy and raw materials used, making the process more economical and environmentally friendly.

Controlling Particle Size and Shape: New techniques can be developed to more precisely control the size and shape of zinc oxide nanoparticles, improving their properties and potential applications.

Increasing Productivity: By improving equipment and operating conditions, productivity can be increased to meet the growing demand for nanomaterials in various industries.

New Industrial Applications: Zinc oxide nanoparticles can be used in a wide range of industrial applications, such as protective coatings, electronic devices, cosmetics, and medicine, opening new avenues for commercial use.

Environmental Research: The developed the use of zinc oxide nanoparticles can be explored in water and air treatment applications, due to their catalytic properties, helping to address pressing environmental issues.

Innovations in Health and Medicine: Research can contribute to the development of new medical uses for zinc oxide nanoparticles, such as drug delivery systems and antibacterial treatments, given their unique biological properties.

Integration with Other Technologies: Gliding arc plasma can be integrated with other technologies such as 3D printing or other nanotechnologies to enhance the production and application capabilities of zinc oxide nanoparticles.

Sustainability: Efforts can be made to make the production process more sustainable by reducing waste and using renewable energy sources for plasma reactor operating.

Scientific Achievements

1. Publications, Patents and Conferences

International scientific publications

Publisher: IOPscience

Impact factor: 2.3

International Category: Q3

National Category: A

Published: 10 /01/2024

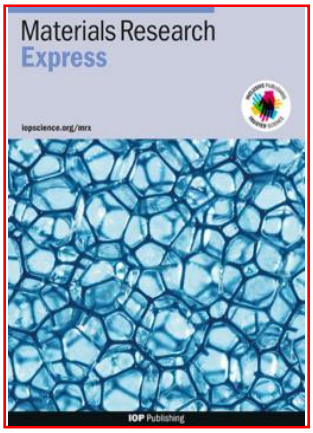

Messai, R., Ferhat, M.F., Belmekki**,** B et al.

"GAD Plasma-Assisted Synthesis of ZnO nanoparticles and Their Photocatalytic Activity," Materials Research Express, 11 015006 (2024).

https://doi.org/10.1088/2053-1591/ad1a82

Publisher: Springer Nature

Impact factor: 5.8

International Category: Q1

National Category: A

Published: 01 /015/2024

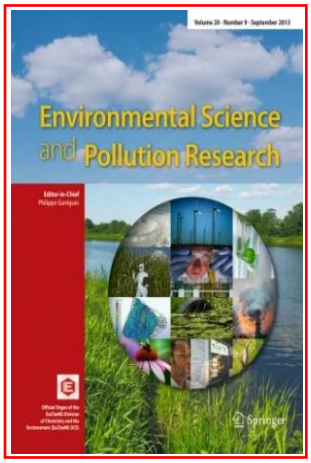

Messai, R., Ferhat, M.F., Serouti, A. et al. **''Rapid synthesis of ZnO nanoparticles via gliding arc discharge: unveiling the impact of discharge time on particle properties and photocatalytic performance**''. Environ Sci Pollut Res 31, 33885–33903 (2024). **https://doi.org/10.1007/s11356-024-33442-3**

Related articles

Publisher: Elsevier Science Sa

Impact factor: 4.6

International Category: Q2

National Category: A

Published: 01/01/2024

Bounedjar, N., Ferhat, M.F., Toukal, L., **Messai, R., "Non-thermal plasma synthesis of ZnO nanoparticles and their corrosion inhibition activity on XC70 mild steel pipeline in 1 M HCl acidic medium".** Materials Chemistry and Physics, 311: p. 128555. (2024). **https://doi.org/10.1016/j.matchemphys.2023.128555**

Publisher: Springer Nature

Impact factor: 5.8

International Category: Q1

National Category: A

Published: 22 June 2024

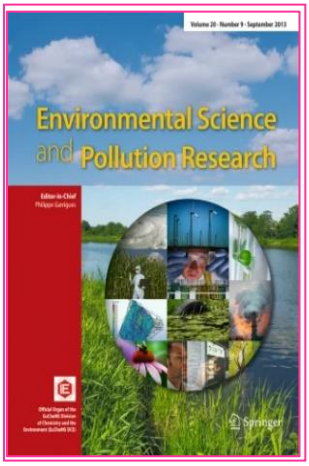

Latra Benkhira, M.F. Ferhat., M.T.O. Khaled., **R. Messai.,** et al. **"Multifunctional assessment of copper-doped ZnO nanoparticles synthesized via gliding arc discharge plasma technique: antioxidant, antibacterial, and photocatalytic performance"**. Environ Sci Pollut Res, p. 1-14 (2024). **https://doi.org/10.1007/s11356-024-34054-7**

Publisher: Springer Nature

Impact factor: 3.5

International Category: Q2

National Category: A

Published: 18 Sept 2024

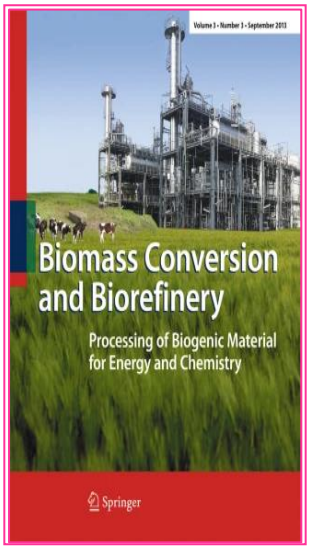

Doudi, D., N. Mahboub, N. Gheraissa, I. Laib, N. Cherrada, **R. Messai** and N. Slimani. **"Eco-friendly synthesis and characterization of ZnO and Mg-Ag-doped ZnO nanoparticles using Phoenix dactylifera L. seeds: exploring biological activity and structural properties"**. Biomass Conversion and Biorefinery: 1-21 (2024). **https://doi.org/10.1007/s13399-024-06115-x**

Patented

N° du Brevet: 12844

N° de Dépôt: 220966

Date de Dépôt : 04/12/22

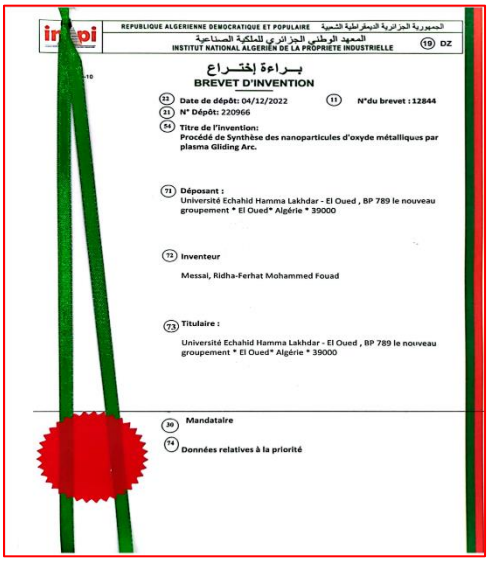

REPUBLIQUE ALGERIENNE DEMOCRATIQUE ET POPULAIRE
الجمهورية الجزائرية الديمقراطية الشعبية
المعهد الوطني الجزائري للملكية الصناعية
INSTITUT NATIONAL ALGERIEN DE LA PROPRIETE INDUSTRIELLE
(19) DZ

براءة إختراع
BREVET D'INVENTION

(22) Date de dépôt: 04/12/2022 (11) N°du brevet : 12844
(21) N° Dépôt: 220966
(54) Titre de l'invention:
Procédé de Synthèse des nanoparticules d'oxyde métalliques par plasma Gliding Arc.

(71) Déposant :
Université Echahid Hamma Lakhdar - El Oued , BP 789 le nouveau groupement * El Oued* Algérie * 39000

(72) Inventeur
Messal, Ridha-Ferhat Mohammed Fouad

(73) Titulaire :
Université Echahid Hamma Lakhdar - El Oued , BP 789 le nouveau groupement * El Oued* Algérie * 39000

(30) Mandataire
(74) Données relatives à la priorité

Procédé de Synthèse des nanoparticules d'oxyde métallique par plasma gliding arc

N° du Brevet: 12843

N° de Dépôt: 220965

Date de Dépôt : 04/12/22

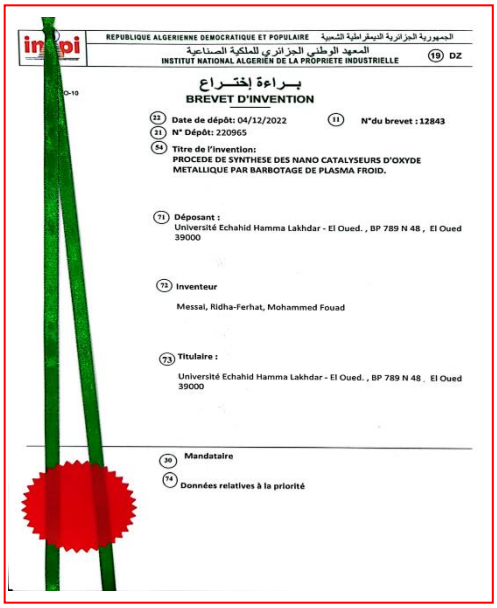

REPUBLIQUE ALGERIENNE DEMOCRATIQUE ET POPULAIRE
الجمهورية الجزائرية الديمقراطية الشعبية
المعهد الوطني الجزائري للملكية الصناعية
INSTITUT NATIONAL ALGERIEN DE LA PROPRIETE INDUSTRIELLE
(19) DZ

براءة إختراع
BREVET D'INVENTION

(22) Date de dépôt: 04/12/2022 (11) N°du brevet : 12843
(21) N° Dépôt: 220965
(54) Titre de l'invention:
PROCEDE DE SYNTHESE DES NANO CATALYSEURS D'OXYDE METALLIQUE PAR BARBOTAGE DE PLASMA FROID.

(71) Déposant :
Université Echahid Hamma Lakhdar - El Oued. , BP 789 N 48 , El Oued 39000

(72) Inventeur
Messal, Ridha-Ferhat, Mohammed Fouad

(73) Titulaire :
Université Echahid Hamma Lakhdar - El Oued. , BP 789 N 48 , El Oued 39000

(30) Mandataire
(74) Données relatives à la priorité

Procédé de Synthèse des nano-catalyseurs d'oxyde métallique par l'injection de bulles de plasma dans leurs sels métalliques

International scientific conferences

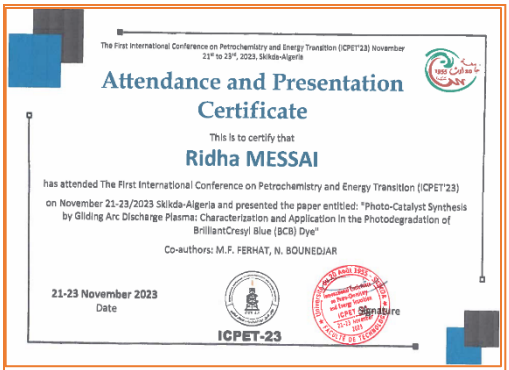
The First International Conference on Petrochemistry and Energy Transition (ICPET'23) November 21st to 23rd, 2023, Skikda-Algeria

Attendance and Presentation Certificate

This is to certify that

Ridha MESSAI

has attended The First International Conference on Petrochemistry and Energy Transition (ICPET'23) on November 21-23/2023 Skikda-Algeria and presented the paper entitled: "Photo-Catalyst Synthesis by Gliding Arc Discharge Plasma: Characterization and Application in the Photodegradation of BrilliantCresyl Blue (BCB) Dye"

Co-authors: M.F. FERHAT, N. BOUNEDJAR

21-23 November 2023
Date

Signature

ICPET-23

Ridha MESSAI, M.F. FERHAT, and N. BOUNEDJAR

"Photo-Catalyst Synthesis by Gliding Arc Discharge Plasma: Characterization and Application in the Photodegradation of Brilliant Cresyl Blue (BCB) Dye" **International Conference on Petro-chemistry And Energy Transition (ICPET 2023) November 21–23, 2023 Skikda-Algeria**

http://oldftech.univ-skikda.dz/icpet23/


People's Democratic Republic of Algeria
Ministry of Higher Education and Scientific Research
University of Echahid Hamma Lakhdar – El-Oued
Faculty of Exact Sciences
Department of Physics

The Second International Conference on Materials, Energy & Environment (MEE'2023)

CERTIFICATE
OF PARTICIPATION

This is to certify that Bounedjar Nourelhouda

Presented an Poster in "The Second International Conference on Materials, Energy & Environment (MEE'2023)" which took place on October 23-24, 2023 in El Oued - Algeria.

Title: Gravimetric Investigation of Zinc Oxide Nanoparticles as Effective Corrosion Inhibitors for XC70 Mild Steel in 1M HCl Acidic Environment

Co-authors: Ferhat mohammed Fouad, Toukal linda, Messai ridha

El Oued - Algeria
October 23-24, 2023

N. Bounedjar, L. Toukal, M. F. Ferhat, **Ridha Messai**

" Gravimetric Investigation of Zinc Oxide Nanoparticles as Effective Corrosion Inhibitors for XC70 Mild Steel in 1M HCl Acidic Environment" **Conference: The Second International Conference on Materials, Energy & Environment (MEE'2023), October 23-24, 2023, at the University of El Oued.**

https://simee2023.sciencesconf.org/

National scientific conferences


People's Democratic Republic of Algeria
Ministry of Higher Education and Scientific Research
University of Echahid Hamma Lakhdar, El-Oued
Faculty of Exacts Sciences

The first national Seminar on Green Chemistry and Natural Products (GCNP'22)

CERTIFICATE OF PARTICIPATION

This Certifies That

Messai Ridha

Presented a oral communication at the First national Seminar on Green Chemistry and Natural Products (GCNP'22), organized from March 14-15, 2022 at the University of Echahid Hamma Lakhdar, El-Oued, entitled:

Etude de la dégradation de l'aspirine par plasma froid (GAD) assisté par les nanoparticules de ZnO biosynthétisé

Co-author (s): Sara Aouadi, Mohammed Fouad Ferhat

GCNP'22 Chairman

Dr. Ammar ZOBEIDI

Ridha MESSAI, Sara Aouadi, Mohammed Fouad Ferhat

" Etude de la dégradation de l'aspirine par plasma froid (GAD) assisté par les nanoparticules de ZnO biosynthétisé" **The First national Seminar on Green Chemistry and Natural Products (GCNP'22), organized from March 14-15, 2022 at the University of Echahid Hamma Lakhdar, El-Oued.**

https://cgcp.sciencesconf.org/

جامعة غليزان
GLIZANE UNIVERSITY

République Algérienne Démocratique et Populaire
Ministère de l'Enseignement Supérieur et de la Recherche Scientifique
Université de Relizane
Faculté des Sciences et Technologies
Département de Chimie
Laboratoire Environnement et Développement Durable (LEDD)

ATTESTATION DE PARTICIPATION

Le président du séminaire atteste que :

MESSAI RIDHA

A présenté une communication Orale intitulée : « CHARACTERIZATION AND PHOTO-CATALYTIC APPLICATION OF ZNO NANOPARTICLES SYNTHESIZED BY NON-THERMAL PLASMA (GLIDING ARC DISCHARGE) ».

Lors du Premier Séminaire National sur les Matériaux pour l'Environnement et Développement Durable (Webinaire) *MEDD'23*, tenu le 09 et 10 Mai 2023 à l'université de Relizane.

Co-auteurs: Latra BENKHIRA , Mohammed Fouad FERHAT

Président du Séminaire | *Chef du Département de Chimie* | *Doyen de la Faculté*

Webinaire MEDD'23 Relizane

Ridha MESSAI, Latra BENKHIRA, Mohammed Fouad FERHAT

" Characterization And Photo-Catalytic Application Of Zno Nanoparticles Synthesized By Non-Thermal Plasma (Gliding Arc Discharge)" **Premier Séminaire National sur les Matériaux pour l'Environnement et Développement Durable (Webinaire) MEDD'23, tenu le 09 et 10 Mai 2023 à l'université de Relizane.**

https://drive.google.com/file/d/1CrAAcyyW1_WvMHrUM_HGiE0qAFVKi6-T/view?usp=drive_link

PEOPLE'S DEMOCRATIC REPUBLIC OF ALGERIA
MINISTRY OF HIGHER EDUCATION AND SCIENTIFIC RESEARCH
University of M'hamed Bougara of Boumerdes
Faculty of Science
Laboratory of Bioinformatics Research, Applied Microbiology, and Biomolecule

NSN'24

National Seminar on Nanomaterials: Synthesis and Applications

NSN'24
5 and 6 June, 2024

CERTIFICATE OF PARTICIPATION

This certificate is awarded to

MESSAI Ridha

for his/her presentation of of Abstract referenced bellow as

Oral in the NSN'24

Title: ZnO Nanoparticle Synthesis via Cold Plasma: Investigation of Structural and Optical Characteristics, and Photodegradation of Methylene Blue dye

Co-author (s): Ferhat Mohamed Fouad, Bounedjar Nourelhouda

President of the Scientific Committee
Scientific Committee Chair of NSN'24
Dr. TOUHAMI Mahdia

President of the Organizing Committee
Organizing Committee Chair of NSN'2024
Dr. BOUKHERROUB Nadia

Ridha MESSAI, M.F. FERHAT, and N. BOUNEDJAR

" ZnO Nanoparticle Synthesis via Cold Plasma: Investigation of Structural and Optical Characteristics, and Photodegradation of Methylene Blue dye" **The National Seminar on Nanomaterials: Synthesis & Application (NSN'24). 5-6 June 2024 at the University of Boumerdes.**

https://nsn2024.univ-boumerdes.dz